Imperial College of Science, Technology and Medicine
Department of Physics

Control of motional states of trapped ions with quantum invariants

Selwyn Güneş Şimşek

Submitted in part fulfilment of the requirements for
the degree of Doctor of Philosophy in Physics of
Imperial College London, March 2022

Abstract

Quantum information processing with trapped ions is a mature field in which single and multiple qubit gates have been demonstrated with exceptionally high process fidelities. As such, there is much interest in designing architectures made up of arrays of ion traps that are able to perform general-purpose quantum computing and manufactured at large scale.

These designs require that ions be shuttled throughout such an architecture as quickly as possible while avoiding decoherence of the internal motional states of the ions. Invariant-based inverse engineering has been proposed as a way to obtain such control procedures, with theoretical and experimental demonstrations. In this thesis, I will explore methods that extend the current results of invariant-based inverse engineering to allow for the precise control of motional states of trapped ions in more than one spatial dimension, which has great applicability to the problem of shuttling trapped ions through these architectures.

First of all, I introduce a novel quantum invariant corresponding to that of a multidimensional motional state and show how it may be used to obtain experimental controls that realise ion shuttling around a corner, with relevant numerical examples. I then discuss how to extend this framework to the control of more than one ion at a time, with a numerical demonstration of separation of two trapped ions. Finally, I outline a method by which one may be able to characterise numerically the effect of noise and anharmonicities in trapping potentials on the motional states of trapped ions.

Copyright declaration

Declaration of authorship

I declare that, except where otherwise referenced, all of the work presented in this thesis is my own, and is based on research carried out during my time at Imperial College London, under the supervision of Florian Mintert.

Chapters 3 and 4 are based on work first presented in, and reuse assets from,

- Selwyn Simsek and Florian Mintert "Quantum control with a multi-dimensional Gaussian quantum invariant" *Quantum* **5**, 409 (2021), [1]

which is published under the Creative Commons Attribution 4.0 International (CC BY 4.0) license.

Chapters 5 and 6 are based on work first presented in, and reuse assets from,

- Selwyn Simsek and Florian Mintert "Quantum invariant-based control of interacting trapped ions" arXiv preprint (2021), submitted to *Physical Review Research*, [2]

which is available on the arXiv under the Creative Commons Attribution 4.0 International (CC BY 4.0) license.

Acknowledgements

I would like to thank my supervisor Florian Mintert, for his help and guidance throughout my PhD. Without him I am sure that the ideas presented here would not have come to fruition. I would also like to thank Modesto Orozco Ruiz, who in only a few short months as a new PhD student has contributed many new insights and with whom I have enjoyed many productive conversations.

I am also grateful for all the interactions I have had with everyone in the Controlled Quantum Dynamics Theory group at Imperial, including (but certainly not limited to) Adam Callison, Sean Garraway, Jake Lishman, Rick Mukherjee, Alex Paige, Omar Raii, Frederic Sauvage, Hongzheng Zhao and Omar Raii.

I would also like to thank all of my collaborators at the Ion Quantum Technology group at the University of Sussex, for their tireless efforts in pushing forwards the frontiers in experimental physics. I am always impressed by the depth of their skill and experience, and am humbled and excited at the prospect of my work being realised in experiment soon.

Finally, I would like to thank my parents, who always encouraged me to follow my academic dreams.

Contents

List of Figures

Chapter 1

Introduction

The concept of a so-called quantum computer, a device which uses coherent manipulations of a quantum mechanical system to carry out useful computational work, has been discussed for many years. Such devices promise to solve certain computational problems quickly that are thought to take exponential time on a classical computer. Since the introduction of the quantum computer as a thought experiment in the 1980s, advances in control of small systems that demonstrate quantum behaviour, as well as the development of sophisticated error-correction techniques, have made it plausible to consider the construction of a quantum computer.

Quantum computers may be constructed out of a variety of candidate physical systems, all of which have different features that make them amenable to the necessary control techniques, such as quantum silicon photonics, superconducting quantum circuits, or trapped ions. A key choice that must be made in any design of a quantum computer is the identification of some part of a physical system with a qubit, which may be thought of as a two-level system that encodes some useful quantum information. Examples of qubits include the hyperfine energy levels of a trapped ion, or a photon existing in a superposition of being in two optical modes.

In order for a quantum computer to be useful, it must be able to process large amounts of quantum information flexibly and in parallel. In particular, one requires the ability to entangle qubits together at will in order to compute useful things, such as the factorisation of a large number or simulating the physical properties of a quantum system. Such requirements are

experimentally demanding in practice.

Proof of concept experiments demonstrating the manipulation of quantum information on physical devices, including the required entangling operations, have been carried out on a variety of physical platforms. However, these involve the manipulation of only a few qubits, whereas useful quantum computers are expected to consist of tens of thousands of qubits at the very least. As a result, the design of a quantum computer must be scalable to higher numbers of qubits, otherwise it would not be practical to build. For example, the manipulation of a wide variety of physical systems involves the application of lasers, each of which must be aligned individually. It is impractical to expect to be able to align tens of thousands of lasers at the same time.

The design of a scalable quantum computer is not straightforward, requiring as it does great attention to the characteristics of the underlying physical system that is being controlled as well as an assessment of the practicality of construction of the device. For some twenty years now, it has been proposed to build a scalable quantum computer using trapped ions. Such a device would consist of a very large microfabricated structure throughout which ions may be trapped using a combination of static and oscillating electric fields, and the qubits are encoded in the internal states of the ions.

The advantage of this architecture is that it requires only small numbers of ions to be trapped together at one time. As a result, a very large number of ions may be maintained throughout the structure all at once, while the operation of the quantum computer involves only coherent manipulation of a small number of ions at a time. Such manipulations have been demonstrated experimentally to very high accuracy. In particular, single qubit manipulations and operations that introduce entanglement between pairs of qubits have been demonstrated with very high accuracy, even in the presence of heating and noise. They may also be carried out using global microwave fields and magnetic field gradients, which removes the need for cumbersome alignment of a large number of lasers.

The fact that the building blocks of a trapped ion quantum computer, which is to say the single and entangling qubit operations, can be performed with ease, is very encouraging for the

prospect of building a scalable quantum computer. However, in addition to the engineering challenges that must be overcome in manufacturing such a device at scale, there remain some outstanding technical challenges. In particular, such designs require trapped ions to be shuttled throughout a large structure in order to generate the types of long-range entanglement necessary to carry out a useful quantum computation. Additionally, one needs to be able to separate ions that are initially trapped together into two distinct traps.

Although trapped ion shuttling and separation have been demonstrated successfully in experiment, one would prefer to be able to perform both operations quickly, robustly, and in a manner that does not excite the motional states of the ions in question. There exist a number of theoretical open questions relating to ion shuttling and separation that must be solved in order to design and build a useful trapped ion quantum computer. In this thesis I will address a number of these questions, with a view to contemporary implementation of ion shuttling and separation in currently existing ion trapping chips. In particular, I demonstrate how to achieve fast ion shuttling in any number of spatial dimensions, as well as progress in the control of more than one trapped ion, with numerical demonstrations.

In Ch. 2, I discuss quantum computing in detail and outline how trapped ion quantum computation is implemented experimentally, with a view to motivating the study of physically relevant problems in the theory of ion shuttling and separation. I will also summarise the state of the art in ion shuttling and separation, the physics of ion traps, and introduce the reader to the notion of invariant-based inverse engineering, in which I proceed to prove a number of results in this thesis.

In Ch. 3, I introduce a new quantum invariant that may be used to control single ions in any number of spatial dimensions. I prove its correctness, show how it may be used to carry out invariant-based inverse engineering, and discuss its properties and how it relates to an already discovered quantum invariant.

In Ch. 4, I employ the invariant derived in Ch. 3 to obtain experimental controls that shuttle an ion around a corner in the plane, which is relevant to the experimental problem of shuttling ions through a junction in a segmented ion trap.

In Ch. 5, I attempt to generalise the results of Ch. 3 to more than one ion. I present another quantum invariant that corresponds to a system of many interacting ions and discuss its features and limitations. I show how it may be employed in a simplified physical scenario to control two ions.

In Ch. 6, I employ an invariant used in Ch. 5 to realise separation of two trapped ions. I discuss the features of the resulting experimental controls and the dynamics of the trapped ions.

In Ch. 7, I discuss the prospect of working with trapping potentials that are not quadratic in position. I outline how to use the invariant of Ch. 3 to implement time-dependent perturbation theory, which allows for a numerical account of noise and higher than quadratic trapping potentials that are naturally present in experimental systems.

Chapter 2

Background Theory

In this chapter, I will introduce the notion of quantum computing, and explore its historical development and applications to the solution of real world problems. I will then discuss the field of quantum computing with trapped ions, with particular reference to proposals to realise scalable quantum computing, and introduce the problems of ion shuttling and separation. I will explore relevant aspects of trapped ion physics in detail, as well as Gaussian states, which play an important role in the analysis of trapped ion motional dynamics. I will also introduce quantum invariants, and discuss how they may be used to realise ion shuttling and separation. I will conclude with an important technical lemma that will be used throughout this thesis.

2.1 Introduction to quantum computing

In recent years, much experimental work has been done on realising a 'quantum computer', a physical device that promises to perform some computational tasks such as simulation of quantum systems much faster than the computers we have today. First proposed by Feynman [3, 4], after several decades of theoretical and experimental work, the concept of a quantum computer has developed from a thought experiment into a series of concrete engineering proposals that can be realised using near-contemporary technology.

A quantum computer uses coherent manipulations of a quantum-mechanical system to realise

computations. There exist many equivalent ways of describing the operation of a quantum computer. A particularly useful one is the so-called *gate model* [4, 5, 6] of quantum computing. In this setting, the physical system at hand is taken to consist of a large number of two-level subsystems, often referred to as qubits [7, 8], which may usefully be thought of as idealised two-level systems. The operation of the computer revolves around performing coherent manipulations on small numbers of qubits, typically one or two qubits at a time. Such manipulations are described by unitary evolution of the states of the qubits, and by performing many such manipulations on the qubits over time, one can create a potentially very large entangled state over all of the qubits. After some such unitary evolution has been realised, the qubits are measured, resulting in a binary string of measurement outcomes, which is the result of the quantum computation.

The ability to carry out such manipulations leads to a computational advantage in certain tasks [9, 10] over that attainable with traditional computers, hereafter to be referred to as classical computers. In particular, the time taken for a quantum computer to solve certain problems scales more favourably with problem size than the corresponding time taken on a classical computer. Various quantum algorithms, designed to be run on quantum computers, have been constructed. At first consisting of problems mostly of theoretical interest [10], Shor's algorithm [11] was eventually discovered, which allows one to factor a number in polynomial time, a feat not thought to be possible with classical computers. This spurred much interest and development in the field of quantum computing. Since then, many other quantum algorithms have been discovered to carry out difficult and interesting tasks, which are too numerous to list here. Examples include Grover's algorithm for unstructured search [12], the hidden subgroup problem [13] as well as a growing family of quantum computational chemistry algorithms [14] that can determine the properties of molecules that are too impractical to determine with a classical computer, with demonstrations on contemporary superconducting quantum computers [15]. The new field of quantum natural language processing [16, 17, 18] exploits various resemblances between diagrammatic categorical quantum mechanics and language grammars to carry out natural language processing on quantum computers. Quantum computers are also thought to be much faster at solving certain tasks in computational linear algebra [19] which

has spurred interest in the use of quantum computers to carry out tasks in machine learning [20, 21, 22].

After the discovery of useful quantum algorithms, the question turned to the practicality of the construction of such a device. For some time, it was believed that the development of quantum computers would not be possible, as one cannot realise unitary evolution of real-world quantum mechanical systems to complete accuracy, due to the effects of experimental imperfection and environmental noise [23]. The argument went that over time, errors would build up in the state of the quantum computer, destroying the result of the quantum computation before it could be measured [23]. The development of quantum error-correcting codes [24, 25, 26] showed that this need not be an obstacle to the construction of a quantum computer. In a quantum system that is subject to noise that can cause errors, quantum information may be protected against certain classes of noise by encoding it inside larger physical systems. One can then perform measurements on the larger physical system in such a way that the measurement preserves the quantum information while the measurement outcomes give information about which error has occured in the underlying physical system, allowing one to carry out a further unitary evolution to recover the state of the system. As such, the presence of noise on individual physical qubits is not necessarily an obstacle to storing coherent quantum information in them.

Subsequently, error-correcting codes were used to develop fault-tolerant quantum computing, in which errors in the implementation of unitary evolution and qubit measurement at the end of the operation are dealt with in a similar manner. The foundational result of the field is the 'threshold theorem' [27, 28], a milestone in the development of quantum computing. The threshold theorem states that, as long as the effects of noise and experimental defects are below a sufficiently low threshold, one can in principle carry out quantum computations to arbitrary accuracy, with only a modest overhead in computational resources. Much work has been done on the development of quantum error-correcting codes [29, 30, 31] and fault tolerant quantum computing [32, 33, 34], including the estimation of what the thresholds are likely to be for real-world experimental systems [35]. Modern error-correcting codes [36, 37] deliver thresholds that exceed 1%, which are certainly attainable in various physical systems.

After quantum computing was shown to be feasible in the presence of noise and imperfections, the question turned to which physical systems would be desirable to build a quantum computer out of. The qualities that a candidate ought to satisfy were laid out by DiVincenzo [38]. One requires a physical system which can be well-isolated from the environment and whose quantum state can be manipulated coherently to a high degree. There exist many different proposals, each with their own advantages and disadvantages. Examples include the superconducting quantum computer [39, 40, 41], the linear optical quantum computer [42, 43, 44] and the neutral atom quantum computer [45, 46]. Impressive developments towards useful quantum computing have been made on many of them [47, 48, 49]. Of particular interest is the concept of the trapped ion quantum computer.

2.2 Trapped ion quantum computing

In this section, I will review the concept, advantages and history of trapped ions in quantum information processing, and outline how scalable quantum computing may be achieved using them.

Ions have trapped for decades now [50, 51], and can be cooled using various approaches including Doppler cooling [52, 53] and sideband cooling [54, 55]. One reason for doing so is that the trapped ion may be very well isolated from its environment in practice, which allows for the internal states of the ion to be addressed coherently. In practice, lifetimes on the order of minutes [56] have been observed. Key applications of trapped ions include the manufacture of atomic clocks [57] as well as mass spectroscopy [58]. However, for present purposes, it is their application to quantum information processing that is most relevant.

The coherent manipulation of the internal states of trapped ions has motivated the proposal of trapped ions for quantum information processing experiments. Concretely, the qubit is identified with a choice of two energy levels within the ion, which may originate from the optical [59, 60, 61] or hyperfine [62, 63, 64] transitions. The qubit is prepared by initialising it in one of the two states that comprise the qubit, which can be done with very high fidelity [65].

By applying appropriately chosen electromagnetic radiation, depending on the choice of qubit, one can realise fast [66] single-qubit gates with high fidelities [67, 65] that often well exceed 99%. A requirement of performing quantum computing with trapped ions is that the state of the qubits must be measured. This may be achieved by making use of the fact that some internal states of the ion fluoresce much more than others. One can perform a measurement on the qubit simply by measuring the fluorescence of the ion [68, 69, 70] which has also been achieved with high fidelity [65].

In order to realise interesting quantum information processing experiments, it is necessary to carry out an entangling gate on the qubits, which entails inducing an interaction between the internal states of two different ions. One may carry this out indirectly with two ions that are trapped together in the same trap. Although the internal states of the ions do not interact with each other, the motional states of the ions are coupled together via the Coulomb interaction. Under the assumption that the two ions are in their joint motional ground state, one may apply appropriately chosen laser light in order to entangle the qubits encoded in the internal states of the two ions [71]. This technique has been successfully implemented experimentally [62, 72] and has motivated the development of related schemes [73] which allow one to entangle more than two ions at a time, with corresponding demonstrations experimentally [74]. These two-qubit gates, much like the single-qubit gates, have been demonstrated to work with very high fidelity, with progress being made towards making them fast [75] and resilient to the effects of errors [76] and heating in the joint motional state of the trapped ions [77, 78].

The ability to carry out all of these operations suffices for the construction of a universal quantum computer, which can realise arbitrary unitary evolution on the collective register of qubits that it maintains. Accordingly, many proof-of-principle experiments demonstrating the efficacy of trapped ions for quantum computing have been demonstrated, including an implementation of a quantum algorithm on five trapped-ion qubits [79].

As outlined, all of the ingredients that are needed to operate a quantum computer have been demonstrated to work very well, culminating in the development of programmable devices that execute a given sequence of quantum gates [80, 81], in effect realising small quantum

computers. From the point of view of the development of quantum computing, the next question to be addressed is that of the construction of very large quantum computers. Although it is hoped that contemporary small quantum computers can compete with traditional computers on certain tasks [82], quantum computers are likely to need more than hundreds of thousands of qubits in order to solve problems that are of industrial interest [83, 84, 85] in reasonable timeframes, which has motivated proposals for *scalable* trapped ion quantum computing.

2.2.1 Scalable trapped ion quantum computing

In this section, I will outline a number of various proposals for scalable quantum computing with trapped ions, and enumerate their advantages and disadvantages as well as engineering challenges that must be surmounted.

A simple approach to performing quantum information processing with a large number of trapped ions involves simply trapping the ions within a single trap [86, 80, 87]. In this scenario, the trapped ions interact with each other via their shared collective motional modes, which is sufficient to implement the aforementioned entangling gates [71, 73]. In order to achieve this, one needs to be able to address the ions individually. There exist a variety of schemes to achieve this. One can deflect the laser that implements a quantum gate to couple to trapped ions individually, as they are well separated in space [88], though this imposes an overhead in terms of additional experimental complexity. Other approaches involve using an AC Stark shift to alter the frequencies of the trapped ions, which is sufficient to allow for the ions to be addressed individually and in pairs [89]. A related approach is the use of magnetic field gradients [90], supplied by current carrying wires that are integrated into the ion trap, to achieve the required frequency shifts. Such techniques have been employed experimentally to construct registers of trapped ions upon which any desired single qubit and entangling operation can be implemented [80], with low levels of crosstalk.

One could therefore attempt to do scalable quantum computing simply by scaling up the numbers of ions that are stored within any one trap. Unfortunately, the schemes used to address the ions break down as the number of ions becomes too high. For example, since

the equilibrium separation distance of ions reduces with the number of trapped ions [91], it becomes harder to resolve the separation between ions, requiring higher and higher magnetic field gradients [90]. There exist also numerous other technical difficulties [92] in manipulating large numbers of ions that are trapped together, which imposes an effective limit on the number of trapped ions that may be used to carry out useful quantum information processing. As a result, approaches to quantum computing with large numbers of trapped ions necessarily involve the use of more than one ion trap, which I will now detail.

In order to surmount the difficulties associated with large numbers of trapped ions, Wineland et. al proposed the concept of the 'quantum charge coupled device' (QCCD) in a now classic paper [93]. A QCCD is a very large two-dimensional structure consisting of electrodes and other experimental apparatus required to manipulate trapped ions is fabricated. During the operation of such a device, ions are trapped in small numbers at trapping zones that are spread throughout the structure. As the ions are never held together in large numbers, the aforementioned scaling issues never arise. In order to induce interactions within pairs of ions that are not trapped together, the ions are continually shuttled around the structure. Ions which are to interact with each other are brought together in the same trap and subsequently driven apart once the necessary two-qubit interaction has been carried out. The difficulties associated with manipulating large numbers of trapped ions in the same trap have been replaced with the engineering challenge of manufacturing a large ion trap structure. A detailed proposal for the construction of a large-scale QCCD using contemporary engineering practices has been proposed [94], as well as an experimental demonstration of the QCCD concept [81] to produce a prototype device. The number of trapped ions scales with the area of the structure, allowing for any number of trapped ions to be maintained with high connectivity [95].

Although in principle there is no limit on the size of a QCCD, in practice one is limited by the fact that the ion traps, typically fabricated on a silicon wafer [96, 97], are limited by the wafer size and cannot be manufactured to arbitrary size. To surmount this obstacle, one would prefer to manufacture a number of QCCD modules with some means of communication between them. One such proposal involves the use of photonic interconnects, in which interactions between ions in different trapping structures are mediated via photons coupled into optical

fibre [98, 99, 100, 101]. The use of photons allows one to consider a wide range of non-local interactions between ions in different traps, as the ions need not be physically close to each other in order to interact. However, the interaction is inherently probabilistic [99] and requires additional optical equipment to implement [98], which may be challenging to manufacture at scale. An additional concern is that the observed entanglement rates are on the order of 1 Hz [102], which is considerably slower than the time taken to execute single-qubit gates [66]. This would greatly increase the clock cycle time, which one would prefer to keep as low as possible compared to the decoherence time [38] in order to increase the number of operations that could be carried out. A simpler approach to connecting QCCD modules [94] involves simply aligning the modules to neighbour each other in space, in such a way that the ions may be shuttled between adjacent trapping structures. The effect of any misalignment of trapping structures imposes an effective potential barrier that any trapped ion must overcome during shuttling. Numerical simulations [94] indicate that the height of this potential barrier is not expected to be prohibitively large in realistic situations.

2.2.2 Ion shuttling and separation

As discussed in Sec. 2.2.1, ions must be shuttled and separated within a QCCD in order to make viable large-scale quantum computing with trapped ions. In this section I will outline the problems of ion shuttling and separation in detail, together with theoretical and experimental progress towards realising them.

Most proposals for a QCCD [93, 94] involve a two-dimensional array of ion traps arranged in a lattice configuration. The traps are connected with so-called X-junctions [93, 103, 104], named after their shape, within which ions are routed [95] in order to travel to different parts of the QCCD. One is therefore interested not only in linear shuttles, in which an ion travels along a straight line, but more complicated motions in which an ion may turn a corner through an X-junction.

Ion shuttling is required to be fast, in order to ensure that the time taken for the QCCD to execute a cycle of the computer is short compared to the decoherence time of the internal states

of the ion [38]. Ions must also be shuttled without excessive excitation of the motional state of the ion. Although ions are best entangled when they are close to their motional ground state, some heating of the motional ground state is tolerated [77]. If the motional states of the trapped ions are excited too highly after shuttling, then not only will the fidelity of entangling gates decrease but the ion may end up lost after successive shuttling operations heat the motional state of the ion excessively. Even such a dramatic error as loss of an ion may be compensated for at the error-correction stage of the computer [105], provided that one has the ability to inject in fresh ions where they have been lost, provided that the rate of ion loss is sufficiently low. One would therefore prefer the motional state of the ion to be heated as little as possible below some acceptable threshold.

The requirement that ion shuttling be done quickly, without exciting the motional mode of the ion after transport, is theoretically and experimentally demanding. Nevertheless, much progress has been made. Ion shuttling has been demonstrated for twenty years now [106] in linear traps, in which ions may be shuttled along a linear axis, with very low ion losses and low observed motional heating, albeit in the limit of large shuttling times. More recently, ions have been shuttled quickly with minimal motional excitations also within a linear trap [107, 108, 81]. Ions of different species have also been shuttled together [81], which is useful as it allows for one species to be employed to sympathetically cool the other [109].

In a QCCD, one has to consider not only linear shuttles of trapped ions, but more complicated motions through X-junctions. Accordingly, much work has been done on demonstrating the transport of ions through various types of microfabricated junction. Ions have been shuttled through a T-junction [110], albeit slowly. Shuttling through junctions in two-dimensional architectures is more challenging due to the presence of a non-vanishing pseudopotential [110] which the ion must overcome during transport. Ions have also been shuttled through a so-called Y-junction [111] consisting of three arms, with the additional technical restriction that the ion is laser-cooled through transport. Performing fast shuttling through a junction remains theoretically and experimentally challenging.

Ions must also be separated quickly during the operation of a QCCD, from being initially at

rest within the same trap to being well-separated within different traps. Although this is more demanding, much progress has been made. Ions have been separated experimentally [106] with more recent efforts focusing on fast ion separation [112, 81]. There is also much interest in designing traps specifically to facilitate fast separation of ions [113, 114].

Although there has been much encouraging progress in the field of ion shuttling and separation, there exist numerous challenges to surmount, in particular those related to dealing with junctions in a QCCD.

2.3 Trapped ion physics

2.3.1 Ion traps

Having introduced ion traps, and their utility for quantum information processing, I will outline here in detail relevant aspects of trapped ion physics, in order to illuminate how the motional dynamics of trapped ions may be controlled in practice, to realise the important tasks of ion shuttling and separation.

In order to trap an ion, it is most convenient to make use of the fact that ions, being charged particles, interact strongly with the electromagnetic field via the Coulomb interaction. By engineering this field carefully, one can ensure that the ion is trapped in a single region. An ion is trapped when it moves in a potential that possesses a potential minimum at which the Hessian of the trapping potential is positive definite. The ion will then experience a restoring force upon experiencing small displacements from the potential minimum, which has the effect of confining the ion to a small region surrounding the potential minimum, which is accordingly often referred to as the centre of the trap.

It follows directly from Maxwell's equations that no charged particle may be trapped by a static electric field [115]. In order to trap ions, it is necessary to consider the imposition of additional electromagnetic fields. There exist two main proposals for achieving this, which I will now address.

First proposed by Dehmelt [116], a Penning trap employs a homogeneous magnetic field, as well as a static electric field supplied by electrodes to provide a potential that can trap ions. Ions [53, 117] as well as other charged particles such as electrons [118] and molecular ions [119] have been trapped in Penning traps for decades, in some cases for months on end [120]. However, there exist various technical disadvantages to doing quantum computing with Penning traps. Some proposed implementations [94] of the QCCD involve the use of carefully engineered magnetic field gradients to drive the entangling gates [63], which is incompatible with the requirement to maintain a homogenous magnetic field in order to trap the ion. As a consequence, Penning traps are not typically considered when considering scalable quantum computing, though proposals do exist [121].

A more convenient alternative involves trapping ions using static and oscillating electric fields. The addition of an oscillating electric field is sufficient to trap charged particles, which is known as a Paul trap [50]. Paul traps are used in the majority of proposals for scalable trapped ion quantum computing [93, 94], in part because it is possible to manufacture Paul traps using conventional microfabrication techniques [122, 123, 96]. Many of the proof-of-principle experiments demonstrating quantum information processing with trapped ions have been realised with Paul traps [62, 74, 124].

2.3.2 Physics of Paul traps

In this section, I will analyse the workings of Paul traps in detail, and derive successive expressions for the effective confining potential that an ion experiences in a Paul trap. I will outline how the trapping potential that an ion experiences may be changed in practice, which must be done to carry out tasks such as ion shuttling and separation.

As stated in Sec. 2.3.1, ions are trapped in Paul traps using a combination of static and oscillating electric fields. Following the presentation of [125], a trapped ion of mass m and charge q in a Paul trap experiences a potential of the form

$$\phi(t, x, y, z) = qV_{DC}(x, y, z) + q\cos(\Omega t)V_{AC}(x, y, z), \tag{2.1}$$

where the quantities $V_{DC}(x, y, z)$ and $\cos(\Omega t)V_{AC}(x, y, z)$ may be thought of as the static and oscillating electric potentials that result from applying some set of voltages to the electrodes that make up a Paul trap.

The ion possesses the corresponding equation of motion

$$m\ddot{\vec{x}} = -q\nabla V_{DC} - q\cos(\Omega t)\nabla V_{AC}. \tag{2.2}$$

The dynamics of ions in the potential $\phi(t, x, y, z)$ may be solved for explicitly in terms of solutions of Mathieu's differential equation [50, 125], from which one can show that ions are trapped in this potential, as long as some conditions relating the quantities V_{DC}, V_{AC} and Ω are met. Nevertheless, it is often cumbersome to work with the potential $\phi(t, x, y, z)$ as it is time-dependent. Assuming that the applied frequency Ω of the oscillating potential is very large, which will often be the case, it is possible to average the dynamics over fast time scales to obtain an *effective* time-independent potential in which the ions move, which will now be shown.

Firstly, the ion trajectory is decomposed into a slow-oscillating component $\vec{x}_S(t)$ and a fast-oscillating component $\vec{x}_D(t)$ [125],

$$\vec{x}(t) = \vec{x}_S(t) + \vec{x}_D(t). \tag{2.3}$$

To obtain an equation of motion, one substitutes Eq. (2.3) into Eq. (2.2) to obtain

$$m\ddot{\vec{x}}_S + m\ddot{\vec{x}}_D = -q\nabla V_{DC}\Big|_{\vec{x}_S+\vec{x}_D} - q\cos(\Omega t)\nabla V_{AC}\Big|_{\vec{x}_S+\vec{x}_D}, \tag{2.4}$$

where the vertical evaluation bars indicate that the quantities ∇V_{DC} and ∇V_{AC} are evaluated at the position $\vec{x}_S + \vec{x}_D$.

Eq. (2.4) is not very illuminating, as it couples together both the slow-oscillating part of the trajectory $\vec{x}_S$ and the fast-oscillating part $\vec{x}_D$ in a complicated way. To make progress, one

assumes further that the fast-oscillating part of the motion $\vec{x}_D$ is small compared to the slow-oscillating part $\vec{x}_S$. This allows one to work to lowest order in the fast-oscillating part of the motion $\vec{x}_D$, which will facilitate many simplifications.

Eq. (2.4) may be simplified by taking Taylor expansions of the quantities ∇V_{DC} and ∇V_{AC} to lowest order in the fast-oscillating part of the motion $\vec{x}_D$ to obtain

$$m\ddot{\vec{x}}_S + m\ddot{\vec{x}}_D = -q\left(\nabla V_{DC}\Big|_{\vec{x}_S} + (\vec{x}_D \cdot \nabla)\nabla V_{DC}\Big|_{\vec{x}_S}\right) - q\cos(\Omega t)\left(\nabla V_{AC}\Big|_{\vec{x}_S} + (\vec{x}_D \cdot \nabla)\nabla V_{AC}\Big|_{\vec{x}_S}\right). \tag{2.5}$$

As Eq. (2.5) contains both small and large terms, one can equate them in order to derive a new equation, which will allow one to solve for the fast-oscillating part of the motion $\vec{x}_D$.

Neglecting small terms of order $\vec{x}_D$ in Eq. (2.5) gives

$$m\ddot{\vec{x}}_S + m\ddot{\vec{x}}_D = -q\nabla V_{DC}\Big|_{\vec{x}_S} - q\cos(\Omega t)\nabla V_{AC}\Big|_{\vec{x}_S}. \tag{2.6}$$

Eq. (2.6) contains both slow and fast oscillating parts, which allows for further simplification. Equating the fast oscillating parts gives

$$m\ddot{\vec{x}}_D = -q\cos(\Omega t)\nabla V_{AC}\Big|_{\vec{x}_S}, \tag{2.7}$$

which can be integrated to obtain

$$\vec{x}_D = \frac{q}{m\Omega^2}\cos(\Omega t)\nabla V_{AC}\Big|_{\vec{x}_S}, \tag{2.8}$$

which is to say that the fast-oscillating part of the dynamics $\vec{x}_D$ has explicitly been solved for.

By substituting the expression in Eq. (2.8) for the fast-oscillating part of the motion $\vec{x}_D$ back into Eq. (2.5), one can obtain an equation of motion involving only the slow-oscillating part of the motion $\vec{x}_S$.

Substituting Eq. (2.8) into Eq. (2.5) gives

$$m\ddot{\vec{x}}_S = -q\nabla V_{DC}\Big|_{\vec{x}_S} - \frac{q^2}{m\Omega^2}\cos(\Omega t)\left(\nabla V_{AC}\Big|_{\vec{x}_S}\cdot\nabla\right)\nabla V_{DC}\Big|_{\vec{x}_S} - \frac{q^2}{m\Omega^2}\cos^2(\Omega t)(\nabla V_{AC}\Big|_{\vec{x}_S}\cdot\nabla)\nabla V_{AC}\Big|_{\vec{x}_S}. \tag{2.9}$$

Although Eq. (2.9) involves only the slow-oscillating part of the dynamics $\vec{x}_S$ as promised, it contains the fast oscillating term $\cos(\Omega t)$. By averaging over fast time scales, an equation of motion involving only slowly varying quantities may be derived.

Concretely, the slow-oscillating part of the dynamics $\vec{x}_S$ does not vary considerably over times $T = \frac{2\pi}{\Omega}$. Averaging Eq. (2.9) over this short time T gives

$$\begin{aligned} m\ddot{\vec{x}}_S &= -q\nabla V_{DC}\Big|_{\vec{x}_S} - \frac{q^2}{2m\Omega^2}(\nabla V_{AC}\Big|_{\vec{x}_S}\cdot\nabla)\nabla V_{AC}\Big|_{\vec{x}_S} \\ &= -\nabla\left(qV_{DC} + \frac{q^2}{4m\Omega^2}\nabla V_{AC}^2\right)\Big|_{\vec{x}_S}. \end{aligned} \tag{2.10}$$

The slow-oscillating part of the motion $\vec{x}_S$ is therefore effectively governed by the potential

$$\phi_{eff} = qV_{DC} + \frac{q^2}{4m\Omega^2}(\nabla V_{AC})^2, \tag{2.11}$$

which is often called the pseudopotential, or the pondermotive potential. This completes the derivation that can be found in full in [125].

Eq. (2.11) determines the pseudopotential ϕ_{eff} in terms of the applied static electric field V_{DC} and the applied oscillating electric field $\cos(\omega t)V_{AC}$. In practice, the motional state of the ion is altered by adjusting the voltages on the trap electrodes, which in turn changes these applied electric fields, resulting in a change in the pseudopotential ϕ_{eff}. Many tasks related to control of trapped ion motional states may therefore be thought of as a search for the appropriate sequences of voltages to apply to the trap electrodes.

The quantity $\vec{x}_D$ is commonly called the micromotion of the ion, which is often neglected altogether. Indeed, as can be seen from inspection of Eq. (2.8), when the quantity ∇V_{AC} vanishes

so does the micromotion $\vec{x}_D$. There exist ways of minimising the effect of the micromotion in experiment [126].

Ions that are trapped at the minimum of the pseudopotential will oscillate small oscillations around the trap minimum. Consequently, they will be affected only by a spatially small region of the pseudopotential ϕ_{eff} surrounding the trap minimum. This allows for the pseudopotential ϕ_{eff} to be replaced by a second-order Taylor expansion in many cases.

The minimum of the pseudopotential ϕ_{eff} coincides with the centre of the trap $\vec{C}$. One can therefore write for the Taylor expansion of the pseudopotential ϕ_{eff}

$$\phi_{eff}(\vec{x}) \approx \phi_{eff}(\vec{C}) + \frac{1}{2}(\vec{x}-\vec{C})^T \nabla\nabla\phi_{eff}\Big|_{\vec{C}} (\vec{x}-\vec{C}), \tag{2.12}$$

which is the potential of a *harmonic* trap, *i.e.* one that is quadratic in position, with trap centre $\vec{C}$. The eigenvectors $\vec{v}_i$ and the positive eigenvalues ω_i^2 of the Hessian of the pseudopotential $\nabla\nabla\phi_{eff}$ denote the principal axes of the trap and the squared trapping frequencies respectively. As a result, the Hessian $\nabla\nabla\phi_{eff}$ of the pseudopotential can be thought of as characterising the curvature of the trap.

As explained in Sec. 2.2.2, there is great interest in shuttling and separation of trapped ions within Paul traps. In practice, these tasks are achieved by modulating the applied static electric field V_{DC} and the applied oscillating electric field $\cos(\omega t)V_{AC}$ over time in some way. This gives rise to a change in the position of the trap centre $\vec{C}$ and the curvature of the trap as characterised by the Hessian of the pseudopotential $\nabla\nabla\phi_{eff}$. Consequently, both the position of the trap centre $\vec{C}$ and the trap curvature $\nabla\nabla\phi_{eff}$ can be thought of as time-dependent quantities, that are ultimately determined by experimental control through the applied static electric field V_{DC} and the applied oscillating electric field $\cos(\omega t)V_{AC}$.

2.4 Phase-space quantum mechanics

Many results in this thesis are proven in the phase-space setting of quantum mechanics, as this is the natural way to deal with Hamiltonians that are quadratic in position and momentum, as well as Gaussian states which are intimately connected with such Hamiltonians. In this section I will introduce various key definitions and results that will be referred to throughout this work, along with a brief history of the use of Gaussian states in computational quantum mechanics.

As demonstrated in Sec. 2.3.2, the motional potentials which trapped ions experience may typically be taken to be time-dependent and quadratic in position, as in Eq. (2.12). It will prove convenient to relabel some quantities. Writing

$$M(t) = \frac{1}{m}\nabla\nabla\phi_{eff}\Big|_{\vec{C}}, \tag{2.13}$$

and

$$\vec{F}(t) = \nabla\nabla\phi_{eff}\Big|_{\vec{C}}\vec{C}, \tag{2.14}$$

the Hamiltonian governing a single ion in the potential given in Eq. (2.12) may be written as

$$H(t) = \sum_i \frac{\hat{p}_i^2}{2m} + \frac{1}{2}m\sum_{ij} M_{ij}(t)\hat{x}_i\hat{x}_j - \sum_i \vec{F}_i(t)\hat{x}_i, \tag{2.15}$$

where m is the mass of the ion and the $\hat{x}_i$ and $\hat{p}_i$ are the position and momentum operators in each of the d spatial dimensions. The quantity $M(t)$ is a real symmetric matrix since it is proportional to the Hessian of the pseudopotential $\nabla\nabla\phi_{eff}\Big|_{\vec{C}}$.

Naturally, $d = 3$ in an experimental setting, though one is free to consider other values. In particular, in linear traps, one usually takes $d = 1$ [127] as the radial modes of motion can often be ignored.

Since the Hamiltonian given in Eq. (2.15) is quadratic both in position and momentum, many simplifications can be made by treating position and momentum on an equal footing. One

introduces the vector of position and momentum operators $\hat{X}$,

$$\hat{X} = \left(\hat{x}_1, \hat{x}_2, ..., \hat{x}_n, \hat{p}_1, \hat{p}_2, ..., \hat{p}_n \right). \tag{2.16}$$

Eq. (2.15) may be rewritten compactly in terms of the phase space operator $\hat{X}$ to get

$$H = \frac{1}{2} \hat{X}^T \Omega \hat{X} + \vec{V} \cdot \hat{X}, \tag{2.17}$$

where

$$\Omega = \begin{bmatrix} mM & \mathbb{O} \\ \mathbb{O} & \frac{1}{m} \mathbb{1} \end{bmatrix}, \tag{2.18}$$

and

$$\vec{V} = \begin{bmatrix} -\vec{F} \\ 0 \end{bmatrix}. \tag{2.19}$$

Eq. (2.17) makes it clear that the Hamiltonian H is a quadratic form in the phase-space operator $\hat{X}$. Such Hamiltonians H have an intimate connection with Gaussian states, which will now be addressed.

2.4.1 Gaussian states

Gaussian states are immensely useful in the analysis of the dynamics of the Hamiltonian given in Eq. (2.17). Under time-evolution, any Gaussian state subject to this Hamiltonian will remain Gaussian [128]. Furthermore, Gaussian states may be characterised in terms of very few parameters, which has facilitated their use in numerical methods to investigate molecular wavepacket dynamics [128, 129, 130, 131, 132, 133], with extensions to more than one spatial dimension [134, 135] and anharmonic potentials [136]. For present purposes, it is useful to note that Gaussian states are characterised entirely in terms of their phase-space expectation X and

covariance matrix Σ [135],

$$X_i = \left\langle \hat{X}_i \right\rangle, \tag{2.20}$$

$$\Sigma_{ij} = \frac{1}{2}\left\langle \hat{X}_i\hat{X}_j + \hat{X}_j\hat{X}_i \right\rangle - \langle X_i \rangle \langle X_j \rangle . \tag{2.21}$$

Gaussian states may be expressed most compactly in terms of their Wigner function [135],

$$W(Z_1, ..., Z_{2n}) = \frac{1}{\sqrt{\pi^n \det \Sigma}} e^{-\frac{1}{2}(Z_i - X_i)\Sigma_{ij}^{-1}(Z_j - X_j)}. \tag{2.22}$$

Having defined the symplectic matrix $\mathcal{S}$ to be

$$\mathcal{S} = \begin{bmatrix} \mathbb{O} & \mathbb{1} \\ -\mathbb{1} & \mathbb{O} \end{bmatrix}, \tag{2.23}$$

the equations of motion for the phase-space expectation X and covariance matrix Σ read

$$\dot{\Sigma} = \mathcal{S}\Omega\Sigma - \Sigma\Omega\mathcal{S}, \tag{2.24}$$

$$\dot{X} = \mathcal{S}\left(\Omega X + \vec{V}\right). \tag{2.25}$$

By integrating Eqs. (2.24) and (2.25), one can efficiently determine the dynamics of a Gaussian state under time-evolution [135], which is useful considering that, in general, determining the dynamics via solution of the time-dependent Schrödinger equation is not easy.

While Eq. (2.24) is an evolution equation for the covariance matrix Σ, Eq. (2.25) is equivalent to Hamilton's equations for a *classical* particle governed by the Hamiltonian given in Eq. (2.17). Consequently, the dynamics of a Gaussian state may be separated into a classical trajectory, given by the phase-space expectation X, and the covariance matrix Σ which contains all relevant quantum mechanical phenomena such as squeezing.

2.5 Quantum invariants

In this section, I will introduce the concept of quantum invariants, together with a brief history of them and some of their properties. I will conclude by detailing their application to the control of motional states of trapped ions.

Quantum invariants were introduced by Lewis [137], in an attempt to analyse the one-dimensional time dependent harmonic oscillator (though motivated by the motion of charged particles in magnetic fields [138] rather than trapped ions). Such systems possess the Hamiltonian

$$H = \frac{p^2}{2} + \frac{1}{2}\omega^2(t)x^2. \tag{2.26}$$

Viewing the Hamiltonian H as defining a *classical* system, one can solve Hamilton's equations to obtain the position $x(t)$ and momentum $p(t)$ of the system. As the frequency $\omega(t)$ is varying in time, the Hamiltonian $H(x(t), p(t))$, considered as a function of the position $x(t)$ and momentum $p(t)$, is not conserved under time evolution. However, if the frequency $\omega(t)$ is slowly varying, then the quantity

$$\frac{H(x(t), p(t))}{\omega(t)} \tag{2.27}$$

is approximately conserved [139, 140]. Such quantities are known as *adiabatic* invariants. A drawback of adiabatic invariants is that they require that all parameters appearing in the Hamiltonian, such as the frequency $\omega(t)$ in Eq. (2.26), to vary slowly, which is not necessarily the case in physical systems that one would like to analyse. They are also inherently classical quantities that do not appear to have quantum counterparts.

In an attempt to expand the applicability of adiabatic invariants to Hamiltonians which are not slowly changing in time, Kruskal [141] outlined how one may derive from a wide class of adiabatic invariants constants of motion that are given by asymptotic expansions that are correct to all orders. Upon application of Kruskal's method to the Hamiltonian given in Eq. (2.26) [142], to some surprise [143] one obtains not an asymptotic expansion but rather an *exact* constant of motion. Furthermore, this construction, which is entirely classical [137], motivates the

definition of a *quantum* invariant, an operator which may be considered to be an exact constant of motion under the quantum dynamics of a time-dependent system [137].

A quantum invariant $\mathcal{I}(t)$ is an operator that satisfies the equation

$$\frac{\mathrm{d}\mathcal{I}(t)}{\mathrm{d}t} = i[\mathcal{I}(t), H(t)], \tag{2.28}$$

and the quantum invariant discovered by Lewis [137] may be written as

$$\mathcal{I}(t) = \frac{1}{2}\left(\frac{\hat{x}^2}{\rho^2} + (\rho\hat{p} - \dot{\rho}\hat{x})^2\right), \tag{2.29}$$

provided that the equation

$$\ddot{\rho} + \omega^2(t)\rho = \frac{1}{\rho^3}, \tag{2.30}$$

often denoted the Ermakov equation [143], is satisfied. It is straightforward to verify directly that the invariant $\mathcal{I}(t)$ given in Eq. (2.29) satisfies the defining equation for a quantum invariant Eq. (2.28) with the Hamiltonian $H(t)$ as defined in Eq. (2.26).

In this work, I will limit myself to the analysis of quantum invariants that are Hermitian. However, non-Hermitian invariants exist and are of use in carrying out various tasks in quantum control theory [144].

Quantum invariants possess many useful and interesting properties that justify their name. It may be shown that the eigenvalues of any invariant $\mathcal{I}$ are constant in time [145]. Furthermore, one can show that the eigenstates of $\mathcal{I}$ can always be chosen in such a way that they solve the time-dependent Schrödinger equation for $H(t)$. I will now detail this proof in detail as it is of prime importance to the use of quantum invariants for quantum control.

2.5.1 Quantum invariants and the Schrödinger equation

Lewis and Riesenfeld [145] were the first to note the important connections between quantum invariants and solutions of the time-dependent Schrödinger equation that ultimately allow for

the use of quantum invariants in control theory. In this section I will reproduce some of their key results contained in [145].

The time-dependent Schrödinger equation reads, in units where $\hbar = 1$,

$$i\frac{\mathrm{d}}{\mathrm{d}t}\left|\psi\right\rangle = H(t)\left|\psi\right\rangle . \tag{2.31}$$

The eigenvalues and eigenstates of the invariant $\mathcal{I}$ have an intimate connection with the Schrödinger equation in Eq. (2.31). Since the invariant $\mathcal{I}$ is Hermitian, they may be taken to satisfy the following relations,

$$\mathcal{I}\left|\lambda,\kappa\right\rangle = \lambda\left|\lambda,\kappa\right\rangle , \tag{2.32}$$

$$\left\langle\lambda',\kappa'|\lambda,\kappa\right\rangle = \delta_{\lambda,\lambda'}\delta_{\kappa,\kappa'}, \tag{2.33}$$

where the eigenvalues λ of the invariant $\mathcal{I}$ are real and the label κ runs over all quantum numbers besides the eigenvalues λ in order to characterise the eigenstates $\left|\lambda,\kappa\right\rangle$ non-degeneratively.

2.5.1.1 Time independence of the eigenvalues of a quantum invariant

The eigenvalues λ are not only real but are also independent of time. One may prove this by demonstrating that the time derivative of the eigenvalues $\frac{\mathrm{d}\lambda}{\mathrm{d}t}$ vanishes. In order to do this, one first needs an expression involving the time derivative of the eigenvalues $\frac{\mathrm{d}\lambda}{\mathrm{d}t}$. Differentiating Eq. (2.32) gives

$$\frac{\mathrm{d}\mathcal{I}}{\mathrm{d}t}\left|\lambda,\kappa\right\rangle + \mathcal{I}\frac{\mathrm{d}}{\mathrm{d}t}\left|\lambda,\kappa\right\rangle = \frac{\mathrm{d}\lambda}{\mathrm{d}t}\left|\lambda,\kappa\right\rangle + \lambda\frac{\mathrm{d}}{\mathrm{d}t}\left|\lambda,\kappa\right\rangle . \tag{2.34}$$

Although Eq.(2.34) contains the time derivative of the eigenvalues $\frac{\mathrm{d}\lambda}{\mathrm{d}t}$, it is not clear how the time derivative of the eigenvalues $\frac{\mathrm{d}\lambda}{\mathrm{d}t}$ depends explicitly on the other quantities involved. By taking an appropriate inner product, one can derive an expression for the time derivative of the eigenvalues $\frac{\mathrm{d}\lambda}{\mathrm{d}t}$. Taking the inner product of Eq. (2.34) with a state $\left|\lambda,\kappa\right\rangle$ gives, after

simplification and cancellations,

$$\frac{\mathrm{d}\lambda}{\mathrm{d}t} = \langle \lambda, \kappa | \frac{\mathrm{d}\mathcal{I}}{\mathrm{d}t} | \lambda, \kappa \rangle \,. \tag{2.35}$$

Eq. (2.35) relates the time derivative of the eigenvalues $\frac{\mathrm{d}\lambda}{\mathrm{d}t}$ to the matrix elements of the time derivative of the invariant $\frac{\mathrm{d}\mathcal{I}}{\mathrm{d}t}$. In order to make progress, it is necessary to derive an additional relation involving the invariant $\mathcal{I}$ and its time derivative $\frac{\mathrm{d}\mathcal{I}}{\mathrm{d}t}$.

Operating on $|\lambda, \kappa\rangle$ with Eq. (2.28) gives, after rearranging, that

$$i\frac{\mathrm{d}\mathcal{I}}{\mathrm{d}t} |\lambda, \kappa\rangle + \mathcal{I}H |\lambda, \kappa\rangle - \lambda H |\lambda, \kappa\rangle = 0. \tag{2.36}$$

Eq. (2.36) involves the time derivative of the invariant $\frac{\mathrm{d}\mathcal{I}}{\mathrm{d}t}$ explicitly. By taking the inner product of Eq. (2.36), one can derive an expression for the matrix elements of the time derivative of the invariant $\frac{\mathrm{d}\mathcal{I}}{\mathrm{d}t}$ that appear on the right hand side of Eq. (2.35).

Taking the inner product of Eq. (2.36) with a state $|\lambda', \kappa'\rangle$ gives,

$$i \langle \lambda', \kappa' | \frac{\mathrm{d}\mathcal{I}}{\mathrm{d}t} | \lambda, \kappa \rangle + (\lambda' - \lambda) \langle \lambda', \kappa' | H | \lambda, \kappa \rangle = 0. \tag{2.37}$$

The matrix element of $\frac{\mathrm{d}\mathcal{I}}{\mathrm{d}t}$ that appears on the left hand side of Eq. (2.37) is of the same form as that appearing on the right hand side of Eq. (2.35). By setting $\lambda = \lambda'$ and $\kappa = \kappa'$, it is possible to equate Eqs. (2.35) and (2.37).

Setting $\lambda = \lambda'$ and $\kappa = \kappa'$ in Eq. (2.37) gives that

$$\langle \lambda, \kappa | \frac{\mathrm{d}\mathcal{I}}{\mathrm{d}t} | \lambda, \kappa \rangle = 0. \tag{2.38}$$

By equating Eqs. (2.35) and (2.38), we see that

$$\frac{\mathrm{d}\lambda}{\mathrm{d}t} = 0, \tag{2.39}$$

which is to say that the eigenvalues λ are indeed constant in time.

2.5.1.2 Eigenstates of a quantum invariant may be chosen to satisfy the Schrödinger equation

Since the invariant $\mathcal{I}$ is a time-dependent operator, and its eigenvalues λ are time-independent, all of the time-dependence of the invariant $\mathcal{I}$ lies in the eigenstates $|\lambda, \kappa\rangle$. The eigenstates $|\lambda, \kappa\rangle$ can be chosen to be solutions of the Schrödinger equation, which will now be proved.

Some of the expressions derived in Sec. 2.5.1.1 will prove useful. Since the eigenvalues λ were eventually shown to be time-independent, it is possible to simplify some of those expressions.

Eq. (2.34) may be simplified to

$$(\lambda - \mathcal{I})\frac{\mathrm{d}}{\mathrm{d}t}|\lambda, \kappa\rangle = \frac{\mathrm{d}\mathcal{I}}{\mathrm{d}t}|\lambda, \kappa\rangle\,. \tag{2.40}$$

Eq. (2.40) may be regarded as an evolution equation for the eigenstates $|\lambda, \kappa\rangle$ that is first-order in time, much like the Schrödinger equation. However, it involves the invariant $\mathcal{I}$, while the Hamiltonian H does not enter directly into Eq. (2.40), as it does in the Schrödinger equation. By manipulating Eq. (2.40) further, it is possible to obtain an equation involving only the Hamiltonian H, which will be of great assistance in exploring the connection between the eigenstates $|\lambda, \kappa\rangle$ and the Schrödinger equation.

Eq. (2.37) relates matrix elements of the time derivative of the invariant $\frac{\mathrm{d}\mathcal{I}}{\mathrm{d}t}$ to matrix elements of the Hamiltonian H. It may be used to eliminate the time derivative of the invariant $\frac{\mathrm{d}\mathcal{I}}{\mathrm{d}t}$ entirely from Eq. (2.40) in favour of H as desired.

In order to do this, one first takes the inner product of Eq. (2.40) with $|\lambda', \kappa'\rangle$ to obtain

$$(\lambda - \lambda')\,\langle\lambda', \kappa'|\frac{\mathrm{d}}{\mathrm{d}t}|\lambda, \kappa\rangle = \langle\lambda', \kappa'|\frac{\mathrm{d}\mathcal{I}}{\mathrm{d}t}|\lambda, \kappa\rangle\,. \tag{2.41}$$

One can then use Eq. (2.37) to eliminate the matrix element $\langle\lambda', \kappa'|\frac{\mathrm{d}\mathcal{I}}{\mathrm{d}t}|\lambda, \kappa\rangle$ in Eq. (2.41) to

obtain a useful equation involving H explicitly,

$$i(\lambda - \lambda') \langle \lambda', \kappa' | \frac{\mathrm{d}}{\mathrm{d}t} | \lambda, \kappa \rangle = (\lambda - \lambda') \langle \lambda', \kappa' | H | \lambda, \kappa \rangle . \tag{2.42}$$

Eq. (2.42) relates the time-derivative of the eigenstates $\frac{\mathrm{d}}{\mathrm{d}t} |\lambda, \kappa\rangle$ to the Hamiltonian H without any reference to the invariant $\mathcal{I}$ as desired. By taking $\lambda \neq \lambda'$, one can simplify Eq. (2.42) further to obtain

$$i \langle \lambda', \kappa' | \frac{\mathrm{d}}{\mathrm{d}t} | \lambda, \kappa \rangle = \langle \lambda', \kappa' | H | \lambda, \kappa \rangle . \tag{2.43}$$

Eq. (2.43) is written in terms of matrix elements, while the Schrödinger equation Eq. (2.31) is the evolution equation of a quantum state. In order to investigate the link between the two, it is helpful to express the Schrödinger equation in terms of matrix elements.

The Schrödinger equation for a state $|\psi\rangle$ reads

$$i \frac{\mathrm{d}}{\mathrm{d}t} |\psi\rangle = H(t) |\psi\rangle . \tag{2.44}$$

By inserting resolutions of the identity into the Schrödinger equation, one obtains an equivalent equation involving matrix elements

$$i \sum_{\lambda', \kappa'} |\lambda', \kappa'\rangle \ \langle \lambda', \kappa' | \frac{\mathrm{d}}{\mathrm{d}t} | \psi \rangle = \sum_{\lambda', \kappa'} |\lambda', \kappa'\rangle \ \langle \lambda', \kappa' | H | \psi \rangle . \tag{2.45}$$

One concludes that if

$$i \langle \lambda', \kappa' | \frac{\mathrm{d}}{\mathrm{d}t} | \psi \rangle = \langle \lambda', \kappa' | H | \psi \rangle . \tag{2.46}$$

for all eigenvalues λ' and all quantum numbers κ', then the Schrödinger equation in Eq. (2.44) is satisfied.

Identifying the eigenstate $|\lambda, \kappa\rangle$ with the state $|\psi\rangle$ gives that Eq. (2.43) is in fact the same as Eq. (2.46). Unfortunately, it does not follow that the eigenstate $|\lambda, \kappa\rangle$ satisfies the Schrödinger equation, as Eq. (2.43) holds only when $\lambda \neq \lambda'$.

In order to show that the eigenstates $|\lambda, \kappa\rangle$ satisfy the Schrödinger equation, it is sufficient to show that they satisfy Eq. (2.46) in the case that $\lambda = \lambda'$, which is to say that

$$i \langle \lambda, \kappa' | \frac{\mathrm{d}}{\mathrm{d}t} | \lambda, \kappa \rangle = \langle \lambda, \kappa' | H | \lambda, \kappa \rangle . \tag{2.47}$$

Eq. (2.47) is not necessarily satisfied by any choice of eigenstates $|\lambda, \kappa\rangle$. There however exists a degree of freedom in choosing the eigenstates $|\lambda, \kappa\rangle$ which has not yet been made use of. The eigenstates $|\lambda, \kappa\rangle$ may be multiplied by any arbitrary phase factor

$$|\lambda, \kappa\rangle \to |\lambda, \kappa\rangle_\alpha = e^{i\alpha_{\lambda,\kappa}(t)} |\lambda, \kappa\rangle , \tag{2.48}$$

to obtain a different set of eigenstates $|\lambda, \kappa\rangle_\alpha$ of the invariant $\mathcal{I}$. This gauge freedom in choosing the phase $\alpha_{\lambda,\kappa}(t)$ of the eigenstates may be employed to demonstrate that, under an appropriate choice of phase $\alpha_{\lambda,\kappa}(t)$, the new eigenstates $|\lambda, \kappa\rangle_\alpha$ satisfy Eq. (2.47).

One starts by observing that since the eigenstates $|\lambda, \kappa\rangle_\alpha$ are indeed eigenstates of $\mathcal{I}$ for any choice of phase $\alpha_{\lambda,\kappa}(t)$, all the results proven so far for the eigenstates $|\lambda, \kappa\rangle$ hold also for the new eigenstates $|\lambda, \kappa\rangle_\alpha$.

The new eigenstates $|\lambda, \kappa\rangle_\alpha$ satisfy Eq. (2.47) provided that the phases $\alpha_{\lambda,\kappa}(t)$ are chosen appropriately. Eq. (2.47) reads, in terms of the new eigenstates $|\lambda, \kappa\rangle_\alpha$,

$$i \langle \lambda, \kappa' |_\alpha \frac{\mathrm{d}}{\mathrm{d}t} | \lambda, \kappa \rangle_\alpha = \langle \lambda, \kappa' |_\alpha H | \lambda, \kappa \rangle_\alpha . \tag{2.49}$$

Substituting the expression in Eq. (2.48) for the new eigenstates $|\lambda, \kappa\rangle_\alpha$ into Eq. (2.49) gives, after rearranging and simplification,

$$\delta_{\kappa\kappa'} \frac{\mathrm{d}\alpha_{\lambda,\kappa}}{\mathrm{d}t} = \langle \lambda, \kappa' | i \frac{\mathrm{d}}{\mathrm{d}t} - H | \lambda, \kappa \rangle . \tag{2.50}$$

As the left hand side of Eq. (2.50) is proportional to the Dirac delta symbol $\delta_{\kappa\kappa'}$, the right hand side must vanish for $\kappa \neq \kappa'$. This is always possible to arrange. Since $i\frac{\mathrm{d}}{\mathrm{d}t} - H$ is a Hermitian

operator [145], one may simply choose the eigenstates $|\lambda, \kappa\rangle$ to diagonalise this operator.

Having done this, the requirement that Eq. (2.50) be satisfied reduces to

$$\frac{\mathrm{d}\alpha_{\lambda,\kappa}}{\mathrm{d}t} = \langle \lambda, \kappa | i\frac{\mathrm{d}}{\mathrm{d}t} - H | \lambda, \kappa \rangle \,. \tag{2.51}$$

Eq. (2.51) is a first order differential equation for the phases $\alpha_{\lambda,\kappa}(t)$. The phases $\alpha_{\lambda,\kappa}(t)$ may always be chosen to satisfy Eq. (2.51), which completes the proof contained in full in [145] that the $|\lambda, \kappa\rangle_\alpha$ satisfy the Schrödinger equation.

The eigenstates $|\lambda, \kappa\rangle_\alpha$ are therefore occasionally referred to as 'transport modes' [127] of the time-dependent Hamiltonian $H(t)$, as any solution of the Schrödinger equation may be built out of them via superposition. As a consequence, if a quantum invariant $\mathcal{I}$ is defined for a time-dependent Hamiltonian $H(t)$, then one may simply diagonalise the invariant $\mathcal{I}$, following the above procedure, as an alternative to solving the time-dependent Schrödinger equation explicitly, which is in general analytically difficult and expensive numerically.

Quantum invariants, in particular the one presented in Eq. (2.29), have found a great variety of applications to different fields, including being used as a theoretical tool to compute topological phases in planar waveguides [146] and minispace quantum cosmologies [147]. They may also be constructed for light beam propagation in nonlinear inhomogeneous media [148]. Quantum invariants have also been constructed for two-level [149, 150] and four-level systems [151]. However, for the current purpose, quantum invariants found a novel application some decades after their discovery to quantum control theory, which I will now turn to.

2.5.2 Invariant-based inverse-engineering

In this section, I will introduce the notion of invariant-based inverse engineering, which allows one to carry out various tasks in quantum control theory, including those related to shuttling and separation of trapped ions.

As explained in Sec. 2.2.2, the problems of ion shuttling and separation require that the motional

states of trapped ions be close to their ground states at the beginning and end of the dynamics. Letting the time T be the duration of the procedure, the initial Hamiltonian $H(0)$ and the final Hamiltonian $H(T)$ may be taken as fixed and determined by the problem at hand. For example, the initial Hamiltonian $H(0)$ and the final Hamiltonian $H(T)$ may represent trapping potentials in distinct locations, in the case of ion shuttling. The problem that this thesis is chiefly concerned with is the derivation of Hamiltonians $H(t)$ where the time t lies between 0 and the duration T that ensure that the ground state of the Hamiltonian of the system at initial time $H(0)$ is driven into the ground state of $H(T)$ a time T later. Such a Hamiltonian $H(t)$ ensures that there is no motional heating of the system at all during transport, and therefore may be regarded as the best possible outcome.

It is possible to generate such Hamiltonians $H(t)$ using a technique based on quantum invariants [152, 127, 153, 150, 154]. First of all, one fixes a choice of initial Hamiltonian $H(0)$ and final Hamiltonian $H(T)$. One then constructs a non-degenerate time-dependent Hermitian operator $\mathcal{I}(t)$ such that $[\mathcal{I}(0), H(0)]$ and $[\mathcal{I}(T), H(T)]$ commute. One then deduces the Hamiltonian $H(t)$ via the requirement that the operator $\mathcal{I}(t)$ is an invariant for the Hamiltonian $H(t)$ *i.e.* by ensuring that Eq. (2.28) is satisfied at all times. Such a choice of $H(t)$ will ensure that $\mathcal{I}$ is a quantum invariant for that Hamiltonian by construction. Furthermore, this Hamiltonian in fact performs ground state to ground state transfer from initial time $t = 0$ to final time $t = T$. Assuming that the population starts in the ground state of $H(0)$ at time $t = 0$, the fact that the ground state of $H(0)$ is non-degenerate and $[\mathcal{I}(0), H(0)]$ implies that the ground state of $H(0)$ is also a non-degenerate eigenstate of $\mathcal{I}(0)$. This non-degenerate eigenstate solves (up to an unimportant time-dependent phase) the Schrödinger equation for $H(t)$, which is to say that the final state of the system after time-evolution is the ground state of $\mathcal{I}(T)$. A similar argument gives that this state must also be an eigenstate of $H(T)$. This approach is commonly denoted 'invariant-based inverse engineering'. For a more complete review of the subject, I refer the reader to [154].

Not many details concerning how one may deduce $H(t)$ from Eq. (2.28) have been given, or indeed it has not even been proved that one ends in the ground state of $H(T)$ as opposed to some higher state. Addressing the first of these issues, the deduction process is highly dependent on

the structure of the physical problem at hand and one cannot make general statements about it without reference to some particular problem. As for the latter, it is often possible to prove that one indeed ends up in the ground state of $H(T)$ with the class of quantum invariants that are discussed in this thesis.

Enough material has already been introduced to give a simple example of invariant-based inverse engineering that will illuminate how the method may be employed. Consider a system governed by the Hamiltonian given in Eq. (2.26). First of all, an initial Hamiltonian $H(0)$ and a final Hamiltonian $H(T)$ must be fixed. Since $H(t)$ is determined by $\omega(t)$, this is equivalent to fixing an initial frequency $\omega(0)$ and a final frequency $\omega(T)$. One then takes Eq. (2.29) to define an operator $\mathcal{I}(t)$, where the scalar function $\rho(t)$ is chosen to satisfy $\dot{\rho}(0) = \ddot{\rho}(0) = \dot{\rho}(T) = \ddot{\rho}(T) = 0$, $\rho(0) = \omega^{-\frac{1}{2}}(0)$ and $\rho(T) = \omega^{-\frac{1}{2}}(T)$. It may be verified that such choices ensure that the operator $\mathcal{I}$ and the Hamiltonian H commute at initial and final times as required.

It remains to ensure that the operator $\mathcal{I}(t)$ is an invariant, which is the case if Eq. (2.30) is satisfied. One can rearrange Eq. (2.30) to obtain the trapping frequency $\omega(t)$ in terms of the scalar quantity ρ,

$$\omega(t) = \sqrt{\frac{1}{\rho^4} - \frac{\ddot{\rho}}{\rho}} \, . \tag{2.52}$$

Using Eq. (2.52) to define the trapping frequency $\omega(t)$ in this way ensures that $\mathcal{I}$ is indeed an invariant for the Hamiltonian H, as Eq. (2.30) is satisfied by construction, and so all the preconditions are met. It is also straightforward to confirm in this case that the population is transferred to the ground state of the final Hamiltonian $H(T)$ as opposed to some excited state. Since the ground state of the initial Hamiltonian $H(0)$ is Gaussian, it remains Gaussian as it is subject to a potential defined through Eq. (2.26) that is quadratic in position. But the only Gaussian eigenstate of $H(T)$ is the ground state as $H(T)$ is the Hamiltonian of a simple harmonic oscillator.

With some modifications, notably the addition of a linear term, the inverse engineering procedure presented here is very similar to that used recently to obtain results in ion shuttling and separation, which will now be addressed.

2.6 Ion shuttling and separation with invariant-based inverse engineering

In this section, I will present recent work that employs invariant-based inverse engineering to perform diverse tasks involving the manipulation of trapped ion motional states, some of which is generalised by the results presented in this thesis.

2.6.1 Ermakov-Lewis invariant

In order to employ invariant-based control, we must certainly have a suitable invariant to use. As noted in Sec. 2.3.2, a trapped ion experiences a potential that is quadratic in position to a good approximation.

Although strictly speaking the dynamics of a trapped ion are three-dimensional, as mentioned in Sec. 2.4 it is valid to consider in linear ion traps only one motional mode of the motion and neglect all others. This is most typically done in the analysis of trapped ions in linear traps, in which the ion is confined to an axis along which it may be shuttled. To model this, one can write down the Hamiltonian

$$H = \frac{p^2}{2m} + \frac{1}{2}m\omega^2(t)x^2 - F(t)x, \tag{2.53}$$

where the frequency term $\omega(t)$ and force term $F(t)$ may be obtained from a second-order Taylor expansion of the pseudopotential given in Eq. (2.11).

This Hamiltonian possesses the invariant [155]

$$\mathcal{I}(t) = \frac{1}{2m}\left(\rho(\hat{p} - m\dot{\alpha}) - m\dot{\rho}(\hat{x} - \alpha)\right)^2 + \frac{1}{2}m\left(\frac{x-\alpha}{\rho}\right)^2, \tag{2.54}$$

where

$$\ddot{\rho} + \omega^2(t)\rho = \frac{1}{\rho^3} \tag{2.55}$$

and

$$\ddot{\alpha} + \omega^2(t)\alpha = \frac{F(t)}{m} \tag{2.56}$$

must be satisfied.

Eq (2.55) is the Ermakov equation in Eq. (2.30). Eq. (2.56) is usually referred to as the Newton equation.

This invariant may be used in the context of invariant based inverse engineering. Following the example of Sec. 2.5.2, one designs an invariant $\mathcal{I}$ by choosing scalar functions $\alpha(t)$ and $\rho(t)$ that parametrise an invariant via Eq. (2.54). By rearranging Eqs. (2.55) and (2.56), one can derive the frequency term $\omega(t)$ and the force term $F(t)$ in terms of the scalar functions α and ρ. As in the example of Sec. 2.5.2, this is sufficient to realise ground state to ground state shuttling.

This technique has been used to control the transportation of ions and cold atoms in a linear trap [127, 153, 150], with extensions to deal with optimal shuttling in the presence of noise [156, 157, 158]. By expanding in terms of dynamical normal modes, more than one ion may be controlled at the same time. Using such an approach, one can transport two ions simultaneously [159, 160], expand and compress ion chains [161] and separate two trapped ions into separate traps [162]. Such methods however are generally limited to the consideration of one spatial dimension.

Although the invariant $\mathcal{I}$ presented in Eq. (2.54) has been successfully used to control a wide range of physical systems, there exist situations in which this invariant is not applicable in more than one spatial mode. Generally speaking, the application of this invariant to systems with more than one spatial mode requires the application of an appropriate time-dependent point transformation to yield a separable Hamiltonian, upon which invariant-based inverse engineering may be applied to each part in turn [163]. In the absence of such transformations, inverse engineering must necessarily rely upon perturbative or numerical techniques. The invariant that is to be presented in this thesis allows for the control of systems in more than one spatial dimension without having to employ such techniques, and as such represents a milestone in the development of invariant-based inverse engineering.

2.6.2 Physical interpretation of the invariant

The scalar quantities α and ρ have a natural physical interpretation in terms of dynamical quantities of the underlying physical system, which can be of great help when designing them in the context of invariant-based inverse engineering.

During a physical process that is governed by a choice of invariant $\mathcal{I}$ via inverse engineering, the dynamical state of the system is guaranteed to be in the ground state of the invariant $\mathcal{I}$. Since the invariant $\mathcal{I}$ is quadratic in position and momentum, it is straightforward enough to determine this state directly.

The ground state wavefunction ψ_0 of the invariant $\mathcal{I}$ may be calculated to be [164]

$$\psi_0(x) = \frac{1}{\sqrt{\rho}} \left(\frac{m}{\pi}\right)^{\frac{1}{4}} \exp\left(im\left(\frac{\dot{\rho}x^2}{2\rho} + \frac{(\dot{\alpha}\rho - \alpha\dot{\rho})x}{\rho}\right)\right) \exp\left(-\frac{m}{2}\left(\frac{x-\alpha}{\rho}\right)^2\right). \tag{2.57}$$

This is the state of the system up to a time-dependent phase. Although the quantities α and ρ appear directly in Eq. (2.57), it is not yet clear how to interpret them physically. Since the state $\psi_0(x)$ is a Gaussian state, it is naturally characterised in terms of its phase space expectation X and covariance matrix Σ, as detailed in Sec. 2.4.1. These quantities may be calculated directly using Eq. (2.57), to obtain expressions in terms of the scalar quantities ρ and α. The expected position $\langle\hat{x}\rangle$ and uncertainty in position $\langle\Delta\hat{x}^2\rangle$ turn out to be

$$\langle\hat{x}\rangle = \alpha, \tag{2.58}$$

$$\langle\Delta\hat{x}^2\rangle = \frac{\rho^2}{2m}. \tag{2.59}$$

This leads to a simple and useful interpretation of the scalar quantities α and ρ.

The scalar quantity α is the expected position of the ion. In fact, since the Hamiltonian defined in Eq. (2.53) is quadratic, the expectations of position and momentum actually obey the classical equations of motion [165]. The scalar quantity α may furthermore be interpreted as the *classical* trajectory of the particle. In the context of manipulation of trapped ions, some ion trajectories are rendered impossible by the constraints of the trap trajectory. For example,

one would not want the ion to attempt to pass through a trap electrode during transport. The ability to design the classical trajectory of the ion α directly is therefore very useful.

The scalar quantity ρ governs the uncertainty in position of the particle. As such, it may be said to characterise the width of the wavepacket, as is apparent from Eq. (2.57). As a rule, one would prefer for the wavepacket to be localised in space, otherwise the wavepacket may vary on length scales that are comparable to those on which the potential varies, and the crucial assumption that the potential is quadratic in position would break down. The ability to choose the scalar quantity ρ therefore implies the possibility of ensuring the position uncertainty does not get too great, which may be of experimental utility.

2.7 Matrix anticommutator equation

This thesis involves many manipulations of matrix-valued quantities. In this section I will present an important technical lemma that is applied during the solution of certain matrix-valued equations that appear throughout this work.

The matrix anticommutator equation

$$\{A, X\} = B, \tag{2.60}$$

will often need to be solved for the matrix X, given that A and B are square matrices of size d.

Assuming that A is positive, one may always solve Eq. (2.60) uniquely for the matrix X [166], which I will now detail.

As A is positive, it is also Hermitian, so it admits an eigendecomposition $A = P\Lambda P^T$, where P is a unitary matrix and $\Lambda = \lambda_i \delta_{ij}$ is a real diagonal matrix consisting of the eigenvalues λ_i of A.

Substituting into Eq. (2.60) one obtains

$$P\Lambda P^T X + XP\Lambda P^T = B. \tag{2.61}$$

By manipulating this equation, an anticommutator equation involving the diagonal matrix Λ may be obtained, which will prove much easier to solve. Premultiplying by P^T and postmultiplying by P gives

$$\Lambda P^T XP + P^T XP\Lambda = P^T BP. \tag{2.62}$$

Eq. (2.62) may be simplified by writing it in terms of different quantities. Writing

$$Y = P^T XP, \tag{2.63}$$

and

$$C = P^T BP, \tag{2.64}$$

one can re-express Eq. (2.62) as

$$\Lambda Y + Y\Lambda = C, \tag{2.65}$$

which is to say that the problem has indeed been reduced to an anticommutator equation in which one of the matrices Λ is diagonal as promised.

It is possible to solve Eq. (2.65) in closed form, which leads eventually to a closed form expression for X. Writing Eq. (2.65) out in components gives, after simplification,

$$(\lambda_i + \lambda_j)Y_{ij} = C_{ij}. \tag{2.66}$$

Since A is positive, its eigenvalues λ_i are always positive, which means that the expression $\lambda_i + \lambda_j$ never vanishes.

One can therefore rearrange Eq. (2.66) to obtain

$$Y_{ij} = \frac{C_{ij}}{\lambda_i + \lambda_j}, \tag{2.67}$$

which gives Y in terms of C.

Eq. (2.63) may be rearranged to obtain X in terms of Y,

$$X = PYP^T, \tag{2.68}$$

which allows for the determination of X from Y, concluding the proof laid out in [166]. Consequently, the solution X always exists and is unique. The method of solution presented here may be implemented inexpensively on a computer for small matrix sizes d.

Henceforth, I will refer to 'solving the anticommutator equation' with the understanding that it may always be solved uniquely, under the assumption that the matrix A is positive, without reference to the technical details presented here.

Chapter 3

A multidimensional quantum invariant

3.1 Introduction

Quantum invariants have been used to control one-dimensional motional states of trapped ions, leading to theoretical implementations and experimental demonstrations of ion shuttling in linear traps. In this chapter, I outline the construction of a quantum invariant corresponding to that of a multidimensional harmonic oscillator, which may be used to control the motion of trapped ions in more exotic trap geometries, such as that of an X-junction trap.

I begin by outlining the difficulties and obstacles encountered in attempting to construct a useful quantum invariant. Proceeding in stages, I construct a series of increasingly sophisticated expressions for a quantum invariant until arriving at one which can be used to invert to obtain Hamiltonians. I examine its properties, proving that it can indeed be used to obtain Hamiltonians of the desired form, and offer physical interpretations of the various quantities involved. I conclude with a discussion of how this invariant generalises the traditional one-dimensional Ermakov-Lewis invariant discussed in Sec. 2.6.1 used previously to shuttle ions in one dimension.

This chapter is based on work published in [1].

3.2 A quadratic invariant

As detailed in Secs. 2.3.2 and 2.4, ions trapped in Paul traps typically experience potentials of the form

$$H(t) = \sum_i \frac{\hat{p}_i^2}{2m} + \frac{1}{2}m\sum_{ij} M_{ij}(t)\hat{x}_i\hat{x}_j - \sum_i \vec{F}_i(t)\hat{x}_i. \tag{3.1}$$

The aim of this chapter is to extend the techniques of invariant-based inverse engineering, as outlined in Sec. 2.5.2 to derive Hamiltonians $H(t)$ of the form given in Eq. (3.1). The matrix-valued quantity $M_{ij}(t)$, which characterises the curvature of the trap, and the vector-valued quantity $\vec{F}_i(t)$, which characterises the displacement of the trap, may be thought of as yet undetermined parameters which are to be fixed by a choice of invariant $\mathcal{I}$.

In order to do this, one must certainly have a candidate operator $\mathcal{I}(t)$ that may be an invariant for Hamiltonians of the form appearing in Eq. (3.1).

It is not immediately clear how to construct such an object. I start by noting that the Hamiltonian in Eq. (3.1) is quadratic in position and momentum operators. Indeed, this is what allows us to use Gaussian states to describe the dynamics compactly in the first place, as discussed in Sec. 2.4.1.

I begin the quest for a suitable quantum invariant by assuming as an ansatz that the invariant $\mathcal{I}(t)$ must also be quadratic in position and momentum operators, and determining necessary conditions that ensure that $\mathcal{I}(t)$ is indeed an invariant. In order to do this, the problem is first reformulated in phase space, where the quadratic operators $\mathcal{I}(t)$ and $H(t)$ have compact expressions that may be manipulated succinctly.

3.2.1 Phase space formulation

Following Sec. 2.4, the Hamiltonian introduced in Eq. (3.1) may be rewritten as

$$H = \frac{1}{2}\hat{X}^T \Omega \hat{X} + \vec{V} \cdot \hat{X}, \tag{3.2}$$

where

$$\Omega = \begin{bmatrix} mM & \mathbb{O} \\ \mathbb{O} & \frac{1}{m}\mathbb{1} \end{bmatrix}, \tag{3.3}$$

and

$$\vec{V} = \begin{bmatrix} -\vec{F} \\ 0 \end{bmatrix}. \tag{3.4}$$

As well as making the quadratic dependence of the Hamiltonian on the position and momentum operators explicit in Eq. (3.2), this formulation makes it straightforward to write down a suitable ansatz for the form of a possible quantum invariant $\mathcal{I}(t)$ that is also quadratic in position and momentum operators.

The operator $\mathcal{I}(t)$ is defined to be

$$\mathcal{I}(t) = \frac{1}{2}\hat{X}^T \Gamma(t) \hat{X} + \vec{W}(t) \cdot \hat{X} + \theta(t), \tag{3.5}$$

where the quantity $\Gamma(t)$ is a $2d$-by-$2d$ real symmetric matrix-valued function of time, the quantity $\vec{W}(t)$ is a $2d$ dimensional vector-valued function of time and the quantity $\theta(t)$ is a scalar-valued function of time. The explicit time dependence will sometimes be omitted for reasons of brevity.

In order for the operator $\mathcal{I}$ to be an invariant, it must satisfy the defining equation for a quantum invariant given in Eq. (2.28). By substituting the expressions for the Hamiltonian H and the operator $\mathcal{I}$ found in Eqs. (3.2) and (3.5), one can deduce necessary and sufficient conditions for the operator $\mathcal{I}$ to be an invariant.

A direct computation gives that the operator $\mathcal{I}(t)$ is an invariant if and only if the equations

$$\frac{d\Gamma}{dt} = \Omega\mathcal{S}\Gamma - \Gamma\mathcal{S}\Omega, \tag{3.6}$$

$$\frac{d\vec{W}}{dt} = \Omega\mathcal{S}\vec{W} - \Gamma\mathcal{S}\vec{V}, \tag{3.7}$$

$$\frac{d\theta}{dt} = \vec{V}^T\mathcal{S}\vec{W}, \tag{3.8}$$

hold.

As these are first-order differential equations, given a concrete choice for the Hamiltonian H (and hence the quantities Ω and $\vec{V}$), we can choose initial conditions for the quantities Γ, $\vec{W}$ and θ and integrate in order to find an invariant $\mathcal{I}(t)$. This suggests that, at least formally, there exist many invariants $\mathcal{I}$ that may be of use.

However, as discussed previously, from the perspective of invariant-based inverse engineering one views the Hamiltonian H as something undetermined that is deduced from a particular choice of invariant $\mathcal{I}$. I turn now to this perspective, and assume that the quantities Γ, $\vec{W}$ and θ are fixed, thus determining a choice of invariant $\mathcal{I}$, and explore how the Hamiltonian H may be obtained from the invariant $\mathcal{I}$.

The right hand side of Eqs. (3.6)-(3.8) are linear in the components of the matrix-valued quantity Ω and the vector-valued quantity $\vec{V}$, which suggests that given choices of the quantities Γ, $\vec{W}$ and θ, one may attempt to substitute those and solve the resulting linear system of equations for the components of the matrix-valued quantity Ω and the vector-valued quantity $\vec{V}$. Indeed, it is quite feasible to perform such an inversion numerically. Using standard results from linear algebra one may obtain easily expressions for the family (which may be infinite) of the matrix-valued quantity Ω and the vector-valued quantity $\vec{V}$ that solve this linear system.

There exist many drawbacks with this proposed approach. First of all, it is not clear that even one solution to this system of equations exist given an arbitrary choice of invariant $\mathcal{I}$, as a linear system of equations may have zero, one, or an infinite family of solutions. Most fatal of all, however, is that it is not clear how to choose solutions for the matrix-valued quantity Ω and the vector-valued quantity $\vec{V}$ that are compatible with Eqs. (3.3)-(3.4). More concretely, if one

is successful in deducing a Hamiltonian with this method, in general one can expect to obtain mixed terms $\hat{x}_i\hat{p}_j + \hat{p}_j\hat{x}_i$ of Lorentz type in the Hamiltonian, and terms linear in momentum p_i. This poses a very serious problem as they cannot easily be engineered in ion traps which are well-modelled by potentials quadratic in position of the form given in Eq. (3.1). A restricted form of the invariant $\mathcal{I}$ can be used to resolve these difficulties and obtain a Hamiltonian of the form given in Eq. (3.1).

3.3 Towards a realisable invariant

In this section, I will introduce further expressions for the quantities Γ, $\vec{W}$ and θ that will eventually allow one to invert to obtain a Hamiltonian of the desired form defined in Eq. (3.1). I will start with the matrix-valued quantity Γ that characterises the purely quadratic part of the invariant Γ as this poses the greatest difficulty, and will prove useful in obtaining appropriate expressions for the vector-valued quantity $\vec{W}$ and the scalar-valued quantity θ.

As discussed in the previous section, one cannot expect to choose the matrix-valued quantity Γ freely in such a way to be consistent with the desired Hamiltonian $H(t)$ given in Eq. (3.1). I will deal with this by imposing a functional form on the matrix-valued quantity Γ that will give rise to a Hamiltonian $H(t)$ of the correct form. Introducing a d-by-d $c$omplex-valued matrix quantity P, from now I impose that the matrix-valued quantity Γ is of the form

$$\Gamma = \mathrm{Re}\begin{bmatrix} m\dot{P}^\dagger\dot{P} & -\dot{P}^\dagger P \\ -P^\dagger\dot{P} & \frac{1}{m}P^\dagger P \end{bmatrix}. \tag{3.9}$$

The matrix-valued quantity Γ must satisfy Eq. (3.6) in order for the operator $\mathcal{I}$ to be an invariant. By substituting the expression for the matrix-valued quantity Γ given in Eq. (3.9) and the desired form for the quadratic part of the Hamiltonian Ω given in Eq. (3.3) into Eq. (3.6), one can obtain an equation involving the complex matrix-valued quantity P directly.

Substituting Eq. (3.9) into Eq. (3.6) gives

$$\begin{bmatrix} m\,\mathrm{Re}(\dot{P}^\dagger\mathcal{D}+\mathcal{D}^\dagger\dot{P}) & -\mathrm{Re}(\mathcal{D}^\dagger P) \\ -\mathrm{Re}(P^\dagger\mathcal{D}) & 0 \end{bmatrix} = 0, \tag{3.10}$$

where $\mathcal{D} = \ddot{P} + PM$.

I conclude that any choice of the complex matrix-valued quantity P that satisfies the differential equation

$$\ddot{P} + PM = 0 \tag{3.11}$$

gives rise to a physically appropriate choice of the matrix valued quantity Ω consistent with Eq. (3.3) and a choice of matrix valued quantity Γ that satisfy Eq. (3.6). The matrix valued quantity Γ is now defined entirely in terms of the complex matrix-valued quantity P via Eq. (3.9).

Armed with this new expression for the matrix valued quantity Γ, one can attempt to perform invariant-based inverse engineering. Naively, one can fix a choice of the complex matrix-valued quantity P. The requirement that Eq. (3.11) be satisfied can be rearranged to obtain the quadratic part of the trapping potential M

$$M = -P^{-1}\ddot{P}, \tag{3.12}$$

in terms of the complex matrix-valued quantity P. Such a procedure always results in a unique choice for M, which rectifies the issue raised in Sec. 3.2.1 that an inversion procedure ought to be able to deliver at least one solution. Unfortunately, there exists a further problem. The quadratic part of the trapping potential M must be real symmetric, as discussed in Sec. 2.4, and it is not clear that obtaining the quadratic part of the trapping potential M through Eq. (3.12) is guaranteed to be real symmetric. By imposing further conditions on the complex matrix-valued quantity P, one can obtain a physically appropriate quadratic part of the trapping potential M.

3.3.1 Matrix polar decomposition

The quadratic part of the trapping potential M is determined uniquely from the complex matrix-valued quantity P. Since an arbitrary choice of P complex matrix-valued quantity is not guaranteed to give that the quadratic part of the trapping potential M is real symmetric, it is necessary to choose the complex matrix-valued quantity P in such a way that guarantees that it is. In this section I outline how the complex matrix-valued quantity P may thusly be specified.

I introduce a matrix polar decomposition for the complex matrix-valued quantity P,

$$P = UR, \tag{3.13}$$

where the matrix U is unitary and the matrix R is positive. Substituting this decomposition into Eq. (3.11) leads eventually to a prescription in which R may be chosen freely in such a way to determine the unitary matrix U in terms of the positive matrix R, and the resulting quadratic part of the trapping potential M is both real and symmetric, which I proceed to detail.

3.3.2 Derivation of the matrix Ermakov equation

It will prove useful to introduce the matrix A defined by

$$A = U^\dagger \dot{U} \ . \tag{3.14}$$

It follows directly from the definition that the matrix A is anti-Hermitian, as it is a member of the unitary Lie algebra.

Eq. (3.11) determines the evolution of the complex matrix-valued quantity P. By substituting its matrix polar decomposition given in Eq. (3.13), the evolution of the positive matrix R that appears in its decomposition may be deduced. Substituting Eq. (3.13) into Eq. (3.11), and

premultiplying by the matrix $U^\dagger$, one obtains that the quantity K defined by

$$K = \dot{A}R + A^2R + 2A\dot{R} + \ddot{R} + RM = 0, \tag{3.15}$$

must vanish.

Although Eq. (3.15) is equivalent to Eq. (3.11), it is not immediately clear how it may be of use, as it mixes up the matrix-valued quantities A, $\dot{A}$, R, $\dot{R}$, $\ddot{R}$, and the quadratic part of the trapping potential M that I aim to deduce.

We note that the matrix-valued quantities M, R and the time derivatives of the positive matrix R are Hermitian, while the quantity A and its derivative $\dot{A}$ are anti-Hermitian matrices. As such, the Hermitian conjugate of Eq. (3.15) to find another relation

$$K^\dagger = -R\dot{A} + RA^2 - 2\dot{R}A + \ddot{R} + MR = 0. \tag{3.16}$$

I have derived two separate relations Eqs. (3.15) and (3.11) that relate the matrix-valued quantities M, A, $\dot{A}$, R, $\dot{R}$ and $\ddot{R}$, though it is still not clear how one could hope to obtain the quadratic part of the trapping potential M in terms of the positive matrix R and the anti-Hermitian matrix A. By taking appropriate combinations of these two relations, it is possible to integrate the resulting equation, resulting in a useful expression for the matrix A which will facilitate inverse engineering of the quadratic part of the trapping potential M.

Firstly, the relation $RK - K^\dagger R = 0$ holds as the matrix K vanishes. Substituting for the matrices K and $K^\dagger$ using Eqs. (3.15) and (3.16) in $RK - K^\dagger R = 0$ gives that

$$\frac{d}{dt}RAR = \frac{1}{2}\left([\ddot{R}, R] + [M, R^2]\right) . \tag{3.17}$$

The right hand side of Eq. (3.17) can be rewritten in terms of a total derivative to obtain

$$\frac{d}{dt}RAR = \frac{1}{2}\frac{d}{dt}\left([\dot{R}, R] + \mathcal{J}\right), \tag{3.18}$$

with

$$\mathcal{J} = \int_0^t d\tau \ [M(\tau), R(\tau)^2] \ . \tag{3.19}$$

This can be directly integrated, resulting in the explicit solution

$$A = R^{-1} C R^{-1} + \frac{1}{2}[R^{-1}, \dot{R}] + \frac{1}{2} R^{-1} \mathcal{J} R^{-1}, \tag{3.20}$$

for the matrix-valued quantity A.

Eq. (3.20) gives the matrix-valued quantity A entirely in terms of the positive matrix R and quadratic part of the trapping potential M. This is rather surprising, considering that the matrix A is defined in Eq. (3.14) only in terms of the unitary matrix U and its time derivative $\dot{U}$. Indeed, the unitary matrix U itself is no longer explicitly present in these equations.

The matrix C is a constant of integration that must be anti-Hermitian in order to be consistent via Eq. (3.20) with the requirement that the matrix A is anti-Hermitian. There exist many possible choices for the matrix C. I will make the simple choice $C = i\mathbb{1}$, as it will turn out that this leads one to recover in one spatial dimension the usual Ermakov-Lewis invariant [137, 143], and it is sufficient for invariant-based inverse engineering to be carried out successfully. The consequences of different choices of the matrix C are not explored here.

Substituting $C = i\mathbb{1}$ in Eq. (3.20) gives

$$A = iR^{-2} + \frac{1}{2}[R^{-1}, \dot{R}] + \frac{1}{2} R^{-1} \mathcal{J} R^{-1}. \tag{3.21}$$

Eq. (3.21) was derived by considering the identity $RK - K^\dagger R = 0$. By considering another combination of Eqs. (3.15) and (3.16), it is possible to derive an evolution equation for the positive matrix R that will allow for the specification of an inverse engineering procedure.

This may be done by eliminating the quantity $\dot{A}$ from Eqs. (3.15) and (3.16) to obtain an equation involving only the quantities A, M, R and the time derivatives of the positive matrix R may be derived. Forming the Hermitian combination $RK + K^\dagger R = 0$ and rearranging gives that

$$\{\ddot{R}, R\} + \{R^2, M\} = 2[\dot{R}, R]_A - 2RA^2R. \tag{3.22}$$

Eq. (3.22) relates the positive matrix R and its time derivatives $\dot{R}$ and $\ddot{R}$ to the quadratic part of the trapping potential M. Although the unitary matrix U enters into the analysis through the definition of the anti-Hermitian matrix A in Eq. (3.14), the anti-Hermitian matrix A itself is determined in Eq. (3.21) in terms of the positive matrix R the quadratic part of the trapping potential M without any reference to the unitary matrix U at all. Indeed, the unitary matrix U may then be determined up to an initial condition by integrating the anti-Hermitian matrix A in Eq. (3.14).

The unitary matrix U may therefore be regarded as determined by the positive matrix R and the quadratic part of the trapping potential M. By fixing a choice of positive matrix R, it is possible to deduce an expression for the quadratic part of the trapping potential M, which hence allows for the unitary matrix U to be calculated via integration. Hence, from now on I will regard the positive matrix R as the quantity that characterises the quadratic part of the invariant Γ via Eqs. (3.9) and (3.13), and proceed to describe how the quadratic part of the trapping potential M may be deduced from the positive matrix R.

It is possible to integrate Eq. (3.19) to determine the quadratic part of the trapping potential M in terms of the positive matrix R. Eq. (3.19) reads in differential form

$$\dot{\mathcal{J}}(t) = [M(t), R^2(t)] \tag{3.23}$$

Given the anti-symmetric matrix $\mathcal{J}(t)$, it is possible to calculate its time derivative $\dot{\mathcal{J}}(t)$, which allows for the numerical integration of Eq. (3.23) in such a way that will also determine the quadratic part of the trapping potential $M(t)$.

Eq. (3.21) is first used to evaluate the anti-Hermitian matrix $A(t)$ in terms of the anti-symmetric $\mathcal{J}(t)$. Since Eq. (3.22) is a matrix anticommutator equation for the quadratic part of the trapping potential M, and since the matrix $R(t)$ is positive, it is possible to solve Eq. (3.22)

uniquely for the quadratic part of the trapping potential $M(t)$ after substituting for the anti-Hermitian matrix $A(t)$, as detailed in Sec. 2.7. With the quadratic part of the trapping potential $M(t)$, one can then use Eq. (3.23) to calculate the quantity $\dot{\mathcal{J}}(t)$. One can then integrate the anti-symmetric $\mathcal{J}(t)$ numerically, obtaining all the while the quadratic part of the trapping potential $M(t)$, which completes the specification of the inverse engineering procedure.

Although this numerical integration is feasible, there remains one final problem. Deriving the quadratic part of the trapping potential M in this manner does not guarantee that it is real symmetric, only that it is Hermitian. In the next section we will demonstrate that, under some further restrictions on the positive matrix R, it is in fact possible to derive a real symmetric quadratic part of the trapping potential M from the positive matrix R without the need for numerical integration at all.

3.4 Proof of the reality of M

From now on, I will assume that the positive matrix R is real-valued, and that its time derivative at initial time vanishes,

$$\dot{R}(0) = 0, \tag{3.24}$$

as this is sufficient to prove that the quadratic part of the trapping potential M thusly obtained from the positive matrix R, as outlined in the previous section, is real symmetric.

I will proceed by deriving a number of necessary conditions for the quadratic part of the trapping potential M to be real symmetric, and work through the implications of these. I will show that these necessary conditions are in fact met in all cases.

3.4.1 Necessary conditions for the reality of the quadratic part of the trapping potential M

Under the assumption that the quadratic part of the trapping potential M is real and symmetric, the imaginary part of Eq. (3.22) may be rearranged to obtain

$$\{\mathcal{J}, R^{-2}\} = [\dot{R}, R^{-1}] + [R, R^{-2}]_{\dot{R}}, \tag{3.25}$$

having used the fact that the quadratic part of the potential M, the positive matrix R and its time derivatives are all real.

This relation allows one to obtain the antisymmetric matrix $\mathcal{J}$ in terms of the positive matrix R and its time derivative $\dot{R}$ by solving the matrix anticommutator equation as detailed in Sec. 2.7. This stands in contrast to the definition of the antisymmetric matrix $\mathcal{J}$ in Eq. (3.19), in which the antisymmetric matrix $\mathcal{J}$ is defined as an integral over the history of the positive matrix R and the quadratic part of the trapping potential M.

Although solving the matrix anticommutator equation is a matter of straightforward linear algebra, it cannot be expressed easily in closed form. It will prove advantageous to work in a basis in which it is simple to express the solution to such anticommutator equations. In particular, this will allow one to reformulate Eq. (3.25) obtaining the antisymmetric matrix $\mathcal{J}$ directly in terms of the positive matrix R and its time derivative $\dot{R}$.

In order to do this, I introduce the eigendecomposition

$$R = \sum_j \lambda_j |\Phi_j\rangle\langle\Phi_j| \tag{3.26}$$

of the positive matrix R, which certainly exists as the matrix R is real positive and hence Hermitian. Both the eigenvalues λ_j and the eigenvectors $|\Phi_j\rangle$ are real.

Eq. (3.25) can be solved in terms of the matrix elements with respect to the eigenstates $|\Phi_j\rangle$

of the positive matrix R,

$$\mathcal{J}_{jk} = \frac{(\lambda_j - \lambda_k)(\lambda_j + \lambda_k)^2}{\lambda_j^2 + \lambda_k^2} \dot{R}_{jk} \ , \tag{3.27}$$

where

$$O_{jk} = \langle \Phi_j | O | \Phi_k \rangle, \tag{3.28}$$

denotes the matrix elements of the operator O. The quantity

$$\dot{O}_{jk} = \langle \Phi_j | \dot{O} | \Phi_k \rangle \tag{3.29}$$

does *not* coincide in general with the quantity $\frac{\partial}{\partial t} O_{jk}$ owing to the time-dependence of the eigenstates $|\Phi_j\rangle$.

Working in terms of these matrix elements will allow for the derivation of expressions for the anti-Hermitian matrix A and the quadratic part of the trapping potential M that are as similarly compact as Eq. (3.27).

Expressing Eq. (3.22) in this basis leads to, after rearranging and solving for the matrix elements M_{jk},

$$M_{jk} = \frac{1}{\lambda_j^2 + \lambda_k^2} \left(2 \sum_l \left(\lambda_k \dot{R}_{jl} A_{lk} - \lambda_j A_{jl} \dot{R}_{lk} - \lambda_j \lambda_k A_{jl} A_{lk} \right) - \ddot{R}_{jk} \left(\lambda_j + \lambda_k \right) \right). \tag{3.30}$$

Eq. (3.21) expressed similarly in terms of matrix elements reads

$$A_{jk} = \frac{1}{2\lambda_j \lambda_k} \left(2i\delta_{jk} - (\lambda_j - \lambda_k) \dot{R}_{jk} + \mathcal{J}_{jk} \right). \tag{3.31}$$

Eq. (3.30) is a closed-form expression for the matrix elements M_{jk}. It is possible to derive a closed-form expression for the matrix elements M_{jk} that depends only on the positive matrix R and its time derivatives, which will be of use in proving that the quadratic part of the trapping potential M is real.

Substituting Eq. (3.27) into Eq. (3.31) yields

$$A_{jk} = \frac{i}{\lambda_j \lambda_k}\delta_{jk} + \frac{\lambda_j - \lambda_k}{\lambda_j^2 + \lambda_k^2}\dot{R}_{jk}. \tag{3.32}$$

Substituting Eq. (3.32) into Eq. (3.30) yields

$$M_{jk} = \frac{\delta_{jk}}{\lambda_j^4} - \frac{(\lambda_j + \lambda_k)}{\lambda_j^2 + \lambda_k^2}\ddot{R}_{jk} + 2\sum_l \dot{R}_{jl}\dot{R}_{lk}p(\lambda_j, \lambda_k, \lambda_l)\ , \tag{3.33}$$

with

$$p(\lambda_j, \lambda_k, \lambda_l) = \frac{\lambda_l^3(\lambda_j + \lambda_k) - \lambda_l^2\left(\lambda_j^2 + \lambda_k^2 - \lambda_j\lambda_k\right) - \lambda_j^2\lambda_k^2}{(\lambda_j^2 + \lambda_k^2)(\lambda_j^2 + \lambda_l^2)(\lambda_k^2 + \lambda_l^2)}, \tag{3.34}$$

where the matrix elements M_{jk} are determined entirely in terms of the positive matrix R and its time derivatives as promised.

The closed-form expressions for the antisymmetric matrix $\mathcal{J}$, the anti-Hermitian matrix A and ultimately the quadratic part of the trapping potential M, in terms of their matrix elements, given in Eqs. (3.27), (3.32) and (3.33), hold if the quadratic part of the trapping potential M is real symmetric.

Conversely, if Eqs. (3.27), (3.32) and (3.33) hold, then the quadratic part of the trapping potential M is guaranteed to be real symmetric since Eq. (3.33) is manifestly symmetric and defined solely using real quantities. As a consequence, the quadratic part of the trapping potential M is real symmetric if and only if these expressions hold. I will complete the proof by showing that Eqs. (3.27), (3.32) and (3.33) hold in all cases.

3.4.2 Direct proof of the reality of the quadratic part of the trapping potential M

What remains is thus to verify directly that taking Eqs. (3.27), (3.32) and (3.33) as defining relations for the antisymmetric matrix $\mathcal{J}$, the anti-Hermitian matrix A and the quadratic part of the trapping frequency M, implies that Eqs. (3.14), (3.19) and (3.22) are satisfied. Doing

this completes the proof that the quadratic part of the trapping potential M is real symmetric.

Henceforth it is assumed that Eqs. (3.27), (3.32) and (3.33) hold. As Eq. (3.32) is derived using Eq. (3.31) which is Eq. (3.14) expressed in terms of the matrix elements of the eigenstates of the positive matrix R, Eq. (3.14) holds by construction. Similarly, Eq. (3.33) is derived from Eq. (3.30), which itself is Eq. (3.22) expressed in terms of matrix elements, so Eq. (3.22) additionally holds.

It remains to show that Eq. (3.19), or its equivalent differential form

$$\mathcal{J}(0) = 0 \ , \text{ and} \tag{3.35}$$

$$\dot{\mathcal{J}} = R^2 M - M R^2 \ . \tag{3.36}$$

is satisfied. Noting that the quantity $\dot{R}(0)$ vanishes, as stated in Eq. (3.24), Eq. (3.35) follows directly from inspection of Eq. (3.27).

Eq. (3.36) reads in terms of matrix elements

$$\dot{\mathcal{J}}_{jk} = (\lambda_j^2 - \lambda_k^2) M_{jk}. \tag{3.37}$$

In order to complete the proof, it is sufficient to show that Eq. (3.37) is satisfied. As the antisymmetric matrix $\mathcal{J}$ is defined in terms of its matrix elements $\mathcal{J}_{jk}$ in Eq. (3.27), it is necessary to relate these to the time derivative of the matrix elements $\dot{\mathcal{J}}_{jk}$ that appear in Eq. (3.37).

The time-derivative of the matrix elements $\mathcal{J}_{jk}$ reads

$$\frac{d}{dt}\mathcal{J}_{jk} = \sum_l W_{jl}\mathcal{J}_{lk} - \sum_l \mathcal{J}_{jl} W_{lk} + \dot{\mathcal{J}}_{jk} \tag{3.38}$$

with

$$W_{jk} = \langle \dot{\Phi}_j | \Phi_k \rangle. \tag{3.39}$$

Substituting this expression into Eq. (3.37) gives

$$\frac{d}{dt}\mathcal{J}_{jk} = \sum_l W_{jl}\mathcal{J}_{lk} - \sum_l \mathcal{J}_{jl}W_{lk} + (\lambda_j^2 - \lambda_k^2)M_{jk}, \tag{3.40}$$

which is equivalent to Eq. (3.37).

The next step is to differentiate Eq. (3.27) and use the result to show that Eq. (3.40) is satisfied identically.

Defining, motivated by Eq. (3.40),

$$\Xi = \frac{d}{dt}\mathcal{J}_{jk} - \sum_l W_{jl}\mathcal{J}_{lk} + \sum_l \mathcal{J}_{jl}W_{lk} + (\lambda_k^2 - \lambda_j^2)M_{jk}, \tag{3.41}$$

the remaining task is to show that the quantity Ξ vanishes.

Substituting for the matrix elements $\mathcal{J}_{jk}$ and M_{jk} using Eqs. (3.27) and (3.33) in Eq. (3.41) gives

$$\begin{aligned}\Xi = &\frac{d}{dt}\left(\frac{(\lambda_j^2 - \lambda_k^2)(\lambda_j + \lambda_k)}{\lambda_j^2 + \lambda_k^2}\right)\dot{R}_{jk} + \frac{(\lambda_j^2 - \lambda_k^2)(\lambda_j + \lambda_k)}{\lambda_j^2 + \lambda_k^2}\frac{d}{dt}\left(\dot{R}_{jk}\right) \\ &- \sum_l \frac{(\lambda_l^2 - \lambda_k^2)(\lambda_l + \lambda_k)}{\lambda_l^2 + \lambda_k^2}W_{jl}\dot{R}_{lk} + \sum_l \frac{(\lambda_j^2 - \lambda_l^2)(\lambda_j + \lambda_l)}{\lambda_j^2 + \lambda_l^2}\dot{R}_{jl}W_{lk} \\ &+ \frac{(\lambda_j + \lambda_k)(\lambda_k^2 - \lambda_j^2)}{\lambda_j^2 + \lambda_k^2}\ddot{R}_{jk} - 2\left(\lambda_k^2 - \lambda_j^2\right)p(\lambda_j, \lambda_k, \lambda_l)\dot{R}_{jl}\dot{R}_{lk}\ .\end{aligned} \tag{3.42}$$

Given that the states $|\Phi_i\rangle$ are the eigenvectors of the positive matrix R, the explicit expressions for the matrix elements R_{ij}, $\dot{R}_{ij}$ and $\ddot{R}_{ij}$ read

$$R_{jk} = \lambda_j\delta_{jk}\ , \tag{3.43}$$

$$\dot{R}_{jk} = (\lambda_j - \lambda_k)W_{jk} + \dot{\lambda}_j\delta_{jk}\ , \tag{3.44}$$

$$\ddot{R}_{jk} = \sum_l(\lambda_j + \lambda_k - 2\lambda_l)W_{jl}W_{lk} + (\lambda_j - \lambda_k)\dot{W}_{jk} + 2(\dot{\lambda}_j - \dot{\lambda}_k)W_{jk} + \ddot{\lambda}_j\delta_{jk}\ . \tag{3.45}$$

Substituting Eq. (3.44) and Eq. (3.45) into Eq. (3.42) gives

$$\Xi = W_{jk} r(\lambda_j, \lambda_k, \dot{\lambda}_j, \dot{\lambda}_k) + \sum_l W_{jl} W_{lk} s(\lambda_j, \lambda_k, \lambda_l), \tag{3.46}$$

where

$$\begin{aligned} r(\lambda_j, \lambda_k, \dot{\lambda}_j, \dot{\lambda}_k) = (\lambda_j - \lambda_k) \frac{d}{dt} \left(\frac{(\lambda_j^2 - \lambda_k^2)(\lambda_j + \lambda_k)}{\lambda_j^2 + \lambda_k^2} \right) - \frac{(\lambda_j^2 - \lambda_k^2)(\lambda_j + \lambda_k)(\dot{\lambda}_j - \dot{\lambda}_k)}{\lambda_j^2 + \lambda_k^2} \\ - 2(\lambda_j - \lambda_k)(\lambda_k^2 - \lambda_j^2) \left(\dot{\lambda}_j p(\lambda_j, \lambda_k, \lambda_j) + \dot{\lambda}_k p(\lambda_j, \lambda_k, \lambda_k) \right) , \end{aligned} \tag{3.47}$$

and

$$\begin{aligned} s(\lambda_j, \lambda_k, \lambda_l) = -\frac{(\lambda_l^2 - \lambda_k^2)^2}{\lambda_l^2 + \lambda_k^2} + \frac{(\lambda_j^2 - \lambda_l^2)^2}{\lambda_j^2 + \lambda_l^2} + \frac{(\lambda_j + \lambda_k)(\lambda_k^2 - \lambda_j^2)(\lambda_j + \lambda_k - 2\lambda_l)}{\lambda_j^2 + \lambda_k^2} \\ - 2(\lambda_j - \lambda_l)(\lambda_k - \lambda_l)(\lambda_j^2 - \lambda_k^2) p(\lambda_j, \lambda_k, \lambda_l) \ . \end{aligned} \tag{3.48}$$

Both the functions r and s are rational functions of their arguments, and they are indeed identically vanishing. Therefore, the quantity Ξ vanishes which completes the proof.

3.4.3 Review

Having proved that the quadratic part of the trapping potential M is real symmetric given that R is real positive, I have in fact during the course of the proof discovered some new relations between the antisymmetric matrix $\mathcal{J}$ and the positive matrix R that simplify the inversion procedure considerably.

In Sec. 3.3.2, I outlined how to obtain the quadratic part of the trapping potential M by numerically integrating Eq. (3.19) in order to obtain the antisymmetric matrix $\mathcal{J}$. It is no longer necessary to use numerical integration. One can obtain the antisymmetric matrix $\mathcal{J}$ directly by solving the matrix anticommutator equation in Eq. (3.25). Having obtained the antisymmetric matrix $\mathcal{J}$, one can compute the anti-Hermitian matrix A using Eq. (3.14), and then the quadratic part of the trapping potential M by solving the matrix anticommutator

equation in Eq. (3.22). Such a procedure involves only linear algebraic manipulations that can be performed to very high precision on a computer. As such, not only is it likely to be faster than the previous numerical integration method, it also lacks the issue of having some numerical error associated to the integration, which can grow over time.

This completes the specification of the procedure that allows one to determine the quadratic part of the trapping potential M entirely in terms of the positive matrix R and its time derivatives. Although the positive matrix R was first considered merely as one part of the matrix polar decomposition of the complex-valued matrix P, it has now taken on a central importance, in that appropriate real symmetric quadratic parts of the trapping potential M can be obtained entirely in terms of it. As such, we will regard the positive matrix R as the quantity of interest that characterises the quadratic part of the invariant Γ through the relation given in Eq.(3.9). Indeed, as will be seen later, it is possible to express Eq.(3.9) explicitly in terms of the positive matrix R and its time derivatives using the results of this section. For now, however, we turn our attention to inverse-engineering the vector-valued quantity $\vec{W}$ and the scalar-valued quantity θ that appear in the invariant $\mathcal{I}$.

3.5 Linear and scalar parts of the invariant

I have derived a functional form of the quadratic part of the invariant Γ that is consistent with the desired form of the quadratic part of the Hamiltonian Ω given in Eq. (3.3), and ensure that Eq. (3.6), which governs the relationship between the quantities Γ and Ω, is satisfied.

It remains to deal with the vector-valued quantity $\vec{W}$ and the scalar-valued quantity θ, in order to complete the description of a useful quantum invariant $\mathcal{I}$. I present in this section expressions for the vector-valued quantity $\vec{W}$ and the scalar-valued quantity θ that will allow for the inverse engineering of the Hamiltonian H from the invariant $\mathcal{I}$, all the while ensuring that Eqs. (3.7) and (3.8) are satisfied.

Introducing an ansatz in Eq. (3.9) for the quadratic part of the invariant Γ allowed for much progress to be made in inverse engineering the quadratic part Γ of the invariant $\mathcal{I}$. Similarly, I

introduce another ansatz here for the quantity $\vec{W}$.

The quantity $\vec{W}$ takes the following form

$$\vec{W} = -\Gamma \begin{bmatrix} \vec{L} \\ m\dot{\vec{L}} \end{bmatrix}, \tag{3.49}$$

where the vector-valued quantity $\vec{L}$ is a d-dimensional vector-valued function of time.

By substituting Eq. (3.49) into Eq. (3.7), the vector-valued quantity $\vec{V}$ may be derived directly in terms of the vector-valued quantity $\vec{W}$. The substitution gives, after rearranging,

$$\vec{V} = \mathcal{S}^{-1}\Gamma^{-1}\left(\Omega\mathcal{S}\vec{W} - \dot{\vec{W}}\right). \tag{3.50}$$

This relation gives the vector-valued quantity $\vec{V}$ in terms of the matrix-valued quantity Γ, the vector-valued quantity $\vec{W}$ and the matrix-valued quantity Ω. At first sight, we have achieved the goal of inverse engineering to obtain the vector-valued quantity $\vec{V}$ in terms of the matrix-valued quantity Γ and the vector-valued quantity $\vec{W}$, as the matrix-valued quantity Ω can be obtained in terms of the matrix-valued quantity Γ using the techniques of the previous section. However, just as the matrix-valued quantity Ω is constrained to be of the form given in Eq. (3.3), so the vector-valued quantity $\vec{V}$ must be of the form given in Eq. (3.4). I will determine conditions on the vector-valued quantity $\vec{L}$ that ensure that this will be the case.

Eq. (3.50) involves the matrix-valued quantity Γ explicitly. Although Eq. (3.9) contains an expression for the matrix-valued quantity Γ, it is a rather cumbersome object to work with directly. By performing a change of variables, it is possible to eliminate the matrix-valued quantity Γ to obtain a more compact expression that will be much more illuminating.

By making the substitution $\vec{W} = -\Gamma\vec{Z}$, and noting that the matrix-valued quantity Γ satisfies Eq. (3.6), one obtains that

$$\vec{V} = \mathcal{S}^{-1}\dot{\vec{Z}} \ - \Omega\vec{Z}. \tag{3.51}$$

The matrix valued quantity Ω is required to be of the form specified in Eq. (3.3). In order to

make contact with Eq. (3.3), I note that Eq. (3.49) gives the following block vector decomposition for the vector-valued quantity $\vec{Z}$

$$\vec{Z} = \begin{bmatrix} \vec{L} \\ m\dot{\vec{L}} \end{bmatrix}. \tag{3.52}$$

The vector-valued quantity $\vec{Z}$ may be interpreted as defining a trajectory in phase space.

Substituting this decomposition into Eq. (3.51) gives that

$$\vec{V} = \begin{bmatrix} -mM\vec{L} - m\ddot{\vec{L}} \\ 0 \end{bmatrix}. \tag{3.53}$$

By comparison with Eq. (3.4), one can see that the vector-valued quantity $\vec{V}$ is of precisely of the desired form, provided that the identification

$$-\vec{F} = -mM\vec{L} - m\ddot{\vec{L}} \tag{3.54}$$

is made.

It is convenient to rearrange this into the following form

$$\ddot{\vec{L}} + M\vec{L} = \frac{\vec{F}}{m}, \tag{3.55}$$

which will sometimes be called the *vector Newton equation*, as it generalises the Newton equation Eq. (2.56) to vector-valued quantities $\vec{L}$ and $\vec{F}$.

As long as Eq. (3.55) is satisfied, then the expression for the vector-valued quantity $\vec{W}$ given in Eq. (3.49) will satisfy Eq. (3.7), with the vector-valued quantity $\vec{V}$ being of the desired form given in Eq. (3.3). We now outline how this equation may be employed in the context of inverse engineering to obtain the vector-valued quantity $\vec{F}$.

From the point of view of inverse engineering, we would like to choose the vector-valued quantity $\vec{W}$ and obtain a choice of vector-valued quantity $\vec{V}$ that is consistent with it. Using the results

of the previous section, one is able to choose the positive matrix R subject to the appropriate conditions and obtain the quadratic part of the trapping potential M from it. A choice of vector-valued quantity $\vec{L}$ is then fixed. One can then substitute for the vector valued quantity $\vec{L}$ and the quadratic part of the trapping potential M into Eq. (3.55) and rearrange to obtain a unique expression for the trap displacement term $\vec{F}$. In such a way, one is able to finally obtain the quadratic part of the trapping potential M and the trap displacement $\vec{F}$ ultimately from the quadratic part of the invariant Γ and the scalar part of the invariant $\vec{W}$, which are completely determined via the quantities $\vec{L}$ and R.

Although this procedure is enough in practice to inverse engineer the invariant $\mathcal{I}$ to obtain a Hamiltonian H, there remains the issue of the scalar term θ in the invariant $\mathcal{I}$, which we now turn to.

3.5.1 Scalar component

Although I have exhibited expressions for the quadratic part of the invariant Γ and the linear part of the invariant $\vec{W}$ that satisfy Eq. (3.6) and Eq. (3.7), it is necessary that Eq. (3.8) is also satisfied, otherwise the operator $\mathcal{I}$ cannot be said to be an invariant.

In this section I exhibit an expression for the scalar-valued quantity θ given in terms of previously defined quantities that will achieve this and complete the description of the invariant $\mathcal{I}$.

We define

$$\theta(t) = \frac{1}{2}\vec{Z}^T\Gamma\vec{Z} = -\frac{1}{2}\vec{Z}^T\vec{W} = \frac{1}{2}\vec{W}^T\Gamma^{-1}\vec{W}. \tag{3.56}$$

Using the fact that the quadratic part of the invariant Γ satisfies Eq. (3.6), and the linear part of the invariant $\vec{W}$ satisfies Eq. (3.8), it may be verified directly that Eq. (3.8) is satisfied.

3.5.2 Alternate expression for the invariant

During the construction of the invariant $\mathcal{I}$, the quadratic, linear and scalar parts Γ, $\vec{W}$ and θ were dealt with in turn. It is possible to recast the invariant $\mathcal{I}$ into a form which will prove useful in shedding physical insight into the interpretation of the quantities Γ, $\vec{W}$ and θ that characterise the invariant $\mathcal{I}$.

Eqs. (3.49) and (3.56) give expressions for the quantities $\vec{W}$ and θ in terms of the quantities Γ and $\vec{Z}$. By substituting these into Eq. (3.5), an expression for the invariant $\mathcal{I}$ that depends only on these two quantities may be obtained, and will prove amenable to simplification. The full expression for the invariant $\mathcal{I}$ reads

$$\mathcal{I} = \frac{1}{2}\hat{X}^T\Gamma\hat{X} - \Gamma\vec{Z}\cdot\hat{X} + \frac{1}{2}\vec{Z}^T\Gamma\vec{Z}. \tag{3.57}$$

Completing the square in Eq. (3.57) gives

$$\mathcal{I} = \frac{1}{2}(\hat{X} - \vec{Z})^T\Gamma(\hat{X} - \vec{Z}). \tag{3.58}$$

Since the linear term $\vec{Z}$ appears alongside the phase-space trajectory $\hat{X}$, this rather suggests that it has the form of a phase space trajectory, as suggested previously. I return to this point in the discussion of the interpretation of the quantities that characterise the invariant $\mathcal{I}$. For now, I turn to the question of imposing boundary conditions on the invariant $\mathcal{I}$, which must be addressed in order to demonstrate successful inverse engineering with this invariant.

3.6 Boundary conditions

I have exhibited a way to inverse engineer the invariant $\mathcal{I}$ to obtain a Hamiltonian H of the required form given in Eq. (3.1). In order for this to be useful, it is necessary to be able to impose that the invariant $\mathcal{I}$ and the Hamiltonian H commute at initial and final times, in accordance with the requirements of invariant-based inverse engineering as detailed in Sec. 2.5.2. In this

section I derive sufficient conditions on the quantities $\vec{L}$ and R that achieve this.

Since Eqs. (3.22) and (3.55) are satisfied by construction during the inverse engineering procedure, the operator $\mathcal{I}$ is an invariant, which is to say that

$$\frac{\mathrm{d}\mathcal{I}}{\mathrm{d}t} = i[\mathcal{I}, H]. \tag{3.59}$$

In order to impose that the quantities $[\mathcal{I}(0), H(0)]$ and $[\mathcal{I}(T), H(T)]$ both vanish, one need only additionally impose that the time derivative of the invariant $\dot{\mathcal{I}}$ vanishes at initial time $t = 0$ and final time $t = T$.

Although one can calculate the time derivative of the invariant $\dot{\mathcal{I}}$ explicitly, a much simpler argument gives conditions that, when met, guarantee that the time derivative of the invariant $\dot{\mathcal{I}}$ vanishes.

The invariant $\mathcal{I}$ may be viewed as a function of the quantities $\vec{L}$, $\dot{\vec{L}}$, R and $\dot{R}$,

$$\mathcal{I} = f(\vec{L}, \dot{\vec{L}}, R, \dot{R}). \tag{3.60}$$

Using the chain rule, one concludes that if the quantities $\dot{\vec{L}}$, $\ddot{\vec{L}}$, $\dot{R}$ and $\ddot{R}$ all vanish, then the time derivative of the invariant $\dot{\mathcal{I}}$ vanishes also. One therefore imposes that $\dot{\vec{L}}$, $\ddot{\vec{L}}$, $\dot{R}$ and $\ddot{R}$ all vanish at initial time $t = 0$ and final time $t = T$.

Although these ensure commutativity of the Hamiltonian H and invariant $\mathcal{I}$, the initial and final values of $\vec{L}$ and R remain undetermined. These can be obtained by evaluating Eqs. (3.22) and (3.55) at initial time $t = 0$ and final time $t = T$.

One obtains from Eq. (3.22), after rearranging

$$R = M^{-\frac{1}{4}}, \tag{3.61}$$

and from Eq. (3.55) that

$$\vec{L} = \frac{1}{m} M^{-1} \vec{F}, \tag{3.62}$$

at initial time $t = 0$ and final time $t = T$.

Together with requiring that the quantities $\dot{\vec{L}}$, $\ddot{\vec{L}}$, $\dot{R}$ and $\ddot{R}$ vanish, Eqs. (3.61) and (3.62) form all of the boundary conditions on the invariant $\mathcal{I}$ at initial time $t = 0$ and final time $t = T$ that ensure that the invariant $\mathcal{I}$ and the Hamiltonian H commute as required.

3.7 Inverse engineering the invariant

All of the results necessary to carry out invariant-based inverse engineering have been derived. In this section, I present for clarity's sake the full procedure that is employed to obtain a Hamiltonian $H(t)$.

First of all, a choice of initial and final Hamiltonians $H(0)$ and $H(T)$ is fixed by the problem at hand, between which the aim is to obtain a suitable interpolating Hamiltonian. These determine the values of the quadratic part of the trapping potential M and the trap displacement term $\vec{F}$ at initial time $t = 0$ and final time $t = T$. Using Eqs. (3.61) and (3.62), one can obtain the values of the matrix-valued quantity R and the trajectory $\vec{L}$ at initial time $t = 0$ and final time $t = T$.

Using the fact also that the first and second derivatives of the matrix-valued quantity R and the trajectory $\vec{L}$ must also vanish, one is free to interpolate smoothly between these initial and final values to obtain any choice of the quantities R and $\vec{L}$.

Finally, one obtains the quadratic part of the trapping potential M and the trap displacement term $\vec{F}$ as functions of time. By substituting the matrix-valued quantity R into Eq. (3.22), one can solve the matrix anticommutator equation to obtain the quadratic part of the trapping potential M, and then substitute for the trajectory $\vec{L}$ and the quadratic part of the trapping potential M in Eq. (3.55) to obtain the trap displacement term $\vec{F}$, which completes the specification of the Hamiltonian $H(t)$.

3.8 Interpretation of physical quantities

I present in this section a natural physical interpretation of the various quantities introduced in the description of the invariant $\mathcal{I}$, in terms of the dynamical quantities of the system. This will not only assign a useful physical interpretation to those quantities, but provide insight later on in how to design choices of the invariant $\mathcal{I}$ that may be employed in invariant-based inverse engineering.

In order to relate the invariant $\mathcal{I}$ to the dynamics of the system, it is necessary to calculate the dynamics of the system. Given a suitable choice of invariant $\mathcal{I}$ that satisfies the relevant boundary conditions outlined in the previous section, one can determine the Hamiltonian H, and then solve the Schrödinger equation to determine the dynamics. Since the initial state of the system is Gaussian, and the Hamiltonian H is quadratic in position and momentum, the dynamics may be characterised compactly in terms of the expected position and momentum of the state, as well as its covariance matrix.

However, there exists a much simpler way of deducing the dynamics of the system. In the framework of invariant-based inverse engineering, the dynamics of the system are always in the ground state of the invariant, provided that the invariant has a non-degenerate ground state.

I therefore proceed by calculating the ground state of the invariant $\mathcal{I}$. As this ground state is Gaussian, it is naturally expressed in terms of the expected location in phase space $\langle X \rangle$ and the covariance matrix Σ. The ground state of the invariant must minimise the expected value of the invariant

$$\langle \mathcal{I} \rangle = \left\langle \frac{1}{2} X^T \Gamma X + \vec{W} \cdot X + \theta \right\rangle. \tag{3.63}$$

In order to make a connection with Gaussian states, one can re-express this in terms of the phase space expectation $\langle X \rangle$ and covariance matrix Σ to obtain

$$\langle \mathcal{I} \rangle = \frac{1}{2} \Omega_{ij} \Gamma_{ij} + \frac{1}{2} \Gamma_{ij} \langle X \rangle_i \langle X \rangle_j + \vec{W}_i \langle X \rangle_i + \theta. \tag{3.64}$$

Since the expected value of the invariant $\langle \mathcal{I} \rangle$ must be minimised by the ground state of the

system, we can find the phase space expectation $\langle X \rangle$ and covariance matrix Σ that correspond to the ground state by finding those values of the phase space expectation $\langle X \rangle$ and covariance matrix Σ that minimise Eq. (3.64).

As the covariance matrix Σ is that of a pure Gaussian state, its determinant must be equal to 2^{-2d} [167]. This constraint may be included using a Lagrange multiplier λ,

$$\langle \mathcal{I} \rangle = \frac{1}{2}\Omega_{ij}\Gamma_{ij} + \frac{1}{2}\Gamma_{ij}\langle X \rangle_i \langle X \rangle_j + \vec{W}_i \langle X \rangle_i + \theta + \lambda \left(\det \Sigma - 2^{-2d} \right). \tag{3.65}$$

Carrying out the minimisation gives that

$$\langle X \rangle = -\Gamma^{-1}\vec{W}, \tag{3.66}$$

$$\Sigma = \frac{1}{2}\Gamma^{-1}. \tag{3.67}$$

There exists a subtlety in that the covariance matrix Σ must satisfy the uncertainty principle for covariance matrices, namely that [168, 167]

$$\Sigma + i\frac{\mathcal{S}}{2} \geq 0. \tag{3.68}$$

Rather than proving this directly, it is easier to simply prove directly that the matrix $\Sigma = \frac{1}{2}\Gamma^{-1}$ is the true covariance matrix of the system. We begin by noting that the matrix valued quantity $\frac{1}{2}\Gamma^{-1}$ is in fact a valid solution of the first order equation of motion for the covariance matrix Σ given in Eq. (2.24). Since the Hamiltonian $H(0)$ and invariant $\mathcal{I}(0)$ commute at initial time $t = 0$, they share the same ground state. One can therefore compute the ground state covariance $\Sigma(0)$ directly from the initial Hamiltonian $H(0)$ and compare with the initial invariant $\Gamma(0)$ to see that

$$\Sigma(0) = \frac{1}{2}\Gamma(0)^{-1} = \frac{1}{2}\begin{pmatrix} \frac{M^{-\frac{1}{2}}}{m} & 0 \\ 0 & mM^{\frac{1}{2}} \end{pmatrix}. \tag{3.69}$$

As the covariance matrix Σ and the quantity $\frac{1}{2}\Gamma^{-1}$ coincide at initial time $t = 0$, and they

satisfy the same first order differential equation, we conclude that

$$\Sigma = \frac{1}{2}\Gamma^{-1} \tag{3.70}$$

for all time.

Now that expressions for the dynamical quantities have been obtained, I will now relate them more directly to the quantities that appear in the invariant in order to give those quantities a physical interpretation.

Eq. (3.66) gives the expected position in phase space $\langle X \rangle$ in terms of the quadratic part of the invariant Γ and the linear part of the invariant $\vec{W}$, though a much more helpful expression is possible. By substituting in Eq. (3.49) one obtains

$$\langle X \rangle = \vec{Z} = \begin{bmatrix} \vec{L} \\ m\dot{\vec{L}} \end{bmatrix}, \tag{3.71}$$

from which it is clear that the vector-valued quantity $\vec{L}$ and its time derivative $\dot{\vec{L}}$ together define the expected phase space trajectory over time. Since, from the point of view of inverse engineering, the quantity $\vec{L}$ is a quantity that we are free to choose subject to boundary conditions, the implication is that we are free to choose the trajectory of the particle over time by designing the quantity $\vec{L}$ appropriately.

We turn now to the covariance matrix Σ. The covariance matrix Σ is given in terms of the inverse of the matrix-valued quantity Γ by Eq. (3.67). Since the matrix-valued quantity Γ is given in terms of a block matrix decomposition in Eq. (3.9), it is possible to compute the quantity Γ^{-1} directly, though this is likely to be a lengthy and complex expression. There in fact exists a compact expression for the covariance matrix Σ.

Although Eq. (3.9) gives the matrix-valued quantity Γ, it is not particularly useful in practical purposes given that the complex-matrix valued quantity P appears explicitly in it, while it would be more helpful to have an expression involving the positive matrix R. By substituting for the complex-matrix valued quantity $P = UR$ in Eq. (3.9), and using Eq. (3.21) to substitute

for the anti-Hermitian matrix A, one can derive an expression for the matrix-valued quantity Γ in terms of the positive matrix R and its time derivatives only. One obtains

$$\Gamma = \begin{bmatrix} m\left(\dot{R}^2 + \mathrm{Re}\left([\dot{R}, R]_A - RA^2R\right)\right) & \dfrac{\mathcal{J} - \{R, \dot{R}\}}{2} \\ \dfrac{-\mathcal{J} - \{R, \dot{R}\}}{2} & \dfrac{R^2}{m} \end{bmatrix}. \tag{3.72}$$

It is possible to show that the quantity Γ is a symplectic matrix, which is to say that it satisfies the relation $\Gamma^T \mathcal{S} \Gamma = \mathcal{S}$. Since symplectic matrices may be inverted using a simple algebraic procedure, this allows for the inverse of the matrix Γ to be calculated straightforwardly. I proceed to prove that Γ is symplectic before exhibiting the final expression for Σ.

Since the matrix Γ is symmetric, we may replace the matrix Γ^T with the matrix Γ to obtain that the relation $\Gamma \mathcal{S} \Gamma = \mathcal{S}$ must be satisfied for the matrix Γ to be symplectic. An equivalent condition for the matrix Γ to be symplectic is that the quantity $\Gamma^{-1} + \mathcal{S}\Gamma\mathcal{S}$ must vanish.

The quantity Γ satisfies the first order equation of motion given in Eq. (3.6). As the quantity $\Gamma^{-1} + \mathcal{S}\Gamma\mathcal{S}$ depends on the quantity Γ, a differential equation governing the evolution of the quantity $\Gamma^{-1} + \mathcal{S}\Gamma\mathcal{S}$ may be obtained using Eq. (3.6). Eq. (3.6) reads

$$\frac{d\Gamma}{dt} = \Omega \mathcal{S} \Gamma - \Gamma \mathcal{S} \Omega. \tag{3.73}$$

Noting additionally that

$$\frac{d\Gamma^{-1}}{dt} = -\Gamma^{-1} \dot{\Gamma} \Gamma^{-1}, \tag{3.74}$$

one can evaluate the derivative of the quantity $\Gamma^{-1} + \mathcal{S}\Gamma\mathcal{S}$.

One obtains via application of Eqs. (3.73) and (3.74) that

$$\frac{\mathrm{d}}{\mathrm{d}t}\left(\Gamma^{-1} + \mathcal{S}\Gamma\mathcal{S}\right) = \mathcal{S}\Omega(\Gamma^{-1} + \mathcal{S}\Gamma\mathcal{S}) - (\Gamma^{-1} + \mathcal{S}\Gamma\mathcal{S})\Omega\mathcal{S}, \tag{3.75}$$

which is to say that the quantity $\Gamma^{-1} + \mathcal{S}\Gamma\mathcal{S}$ satisfies a differential equation in Eq. (3.75).

Evaluating the quantity Γ at time $t = 0$ gives that

$$\Gamma(0) = \begin{bmatrix} mR^{-2}(0) & 0 \\ 0 & \frac{R^2(0)}{m} \end{bmatrix}. \tag{3.76}$$

The quantity $\Gamma^{-1}(0) + \mathcal{S}\Gamma(0)\mathcal{S}$ vanishes. Since the quantity $\Gamma^{-1} + \mathcal{S}\Gamma\mathcal{S}$ satisfies a linear first order equation Eq. (3.75), and it vanishes at initial time $t = 0$, one concludes that the quantity $\Gamma^{-1} + \mathcal{S}\Gamma\mathcal{S}$ vanishes for all time t, which is to say that the quantity Γ is always symplectic.

Using this fact, we may finally invert the quantity Γ to obtain

$$\begin{aligned} \Sigma &= \frac{1}{2}\Gamma^{-1} \\ &= \frac{1}{2}\begin{bmatrix} \frac{R^2}{m} & \frac{\{R,\dot{R}\} - \mathcal{J}}{2} \\ \frac{\{R,\dot{R}\} + \mathcal{J}}{2} & m\left(\dot{R}^2 + \mathrm{Re}([\dot{R},R]_A - RA^2R)\right) \end{bmatrix}, \end{aligned} \tag{3.77}$$

which determines the covariance matrix Σ explicitly in terms of the positive matrix R and its time derivative $\dot{R}$.

The uppermost left block of the covariance matrix Σ, which contains the position-position correlations, depends only on the positive matrix R. This leads to a natural interpretation of the positive matrix R as determining the value of these correlations to equal to the quantity $\frac{R^2}{2m}$.

As the positive matrix R is one of the parameters, alongside the trajectory $\vec{L}$, that is chosen up to appropriate boundary conditions, this means that one can effectively design the position-position correlations of the state throughout time.

3.9 Relation to Ermakov-Lewis invariant

I have presented an invariant $\mathcal{I}$ that can be used to obtain Hamiltonians $H(t)$ corresponding to harmonic potentials in any number of spatial dimensions d. Since the Ermakov-Lewis invariant

presented in Sec. 2.6.1 has been used to achieve this in one spatial dimension $d = 1$, it is natural to speculate on the relationship between the two invariants. In this section I prove that in the case $d = 1$, the invariant $\mathcal{I}$ that is derived in this chapter reduces to that of the Ermakov-Lewis invariant. The invariant $\mathcal{I}$ may therefore be viewed as a useful generalisation of the Ermakov-Lewis invariant to more than one spatial dimension $d > 1$.

I start by investigating the behaviour of the invariant $\mathcal{I}$ in one spatial dimension $d = 1$. In this case, many quantities become scalar and hence commute with each other, allowing for many simplifications. I write R_s and M_s for the quantities R and M, and so on, to distinguish them as scalars in the one-dimensional case.

The quantity $\mathcal{J}$ is antisymmetric, as may be seen by inspection of Eq. (3.19). It therefore vanishes in the case $d = 1$ when it is a scalar. This allows for further simplifications. In particular Eq. (3.21) simplifies considerably to

$$A_s = iR_s^{-2}. \tag{3.78}$$

Substituting Eq. (3.78) into Eq. (3.22) and exploiting the fact that all objects commute, gives that

$$\ddot{R}_s R_s + M_s R_s^2 = R_s^{-2} \ . \tag{3.79}$$

From Eq. (3.76), the scalar quantity Γ reads in terms of the scalar quantities

$$\Gamma_s = \begin{bmatrix} m\left(\dot{R}_s^2 + R_s^{-2}\right) & -R_s\dot{R}_s \\ -R_s\dot{R}_s & \frac{1}{m}R_s^2 \end{bmatrix}. \tag{3.80}$$

By writing the invariant $\mathcal{I}$ out explicitly in terms of the position operator $\hat{r}$ and the momentum operator $\hat{p}$, it will prove possible to recover the Ermakov-Lewis invariant directly. Using Eq. (3.80), one obtains that

$$\mathcal{I}_s = \frac{1}{2m}\left(R_s(\hat{p} - m\dot{L}) - m\dot{R}_s(\hat{r} - L)\right)^2 + \frac{1}{2}m\left(\frac{\hat{r} - L}{R_s}\right)^2, \tag{3.81}$$

which is the Ermakov-Lewis invariant [137] in Eq. (2.54).

Dividing both sides of Eq. (3.79) by the quantity R_s gives

$$\ddot{R}_s + R_s M_s = R_s^{-3}, \tag{3.82}$$

which is the Ermakov equation Eq. (2.30) where the symbol ρ is used instead of the symbol R_s, and the symbols ω^2 and α are used to denote the quantities M_s and L_s. It is for this reason that Eq. (3.22) is called the matrix Ermakov equation, as it is the natural generalisation of the Ermakov equation to matrix valued quantities.

Similarly, the vector Newton equation Eq. (3.55) reduces to

$$\ddot{L}_s + M_s L_s = \frac{F_s}{m}, \tag{3.83}$$

which is the Newton equation given in Eq. (2.56).

3.9.1 Degeneracy of the invariant

Since the invariant $\mathcal{I}$ derived in this chapter generalises the Ermakov-Lewis invariant, the two invariants share many properties. One area in which they differ however is the degeneracy of their eigenstates, which has some practical significance for the employment of invariant-based inverse engineering.

The Ermakov-Lewis invariant given in Eq. (3.81) takes the form of a Hamiltonian of a harmonic oscillator, albeit one with mixed position and momentum terms and terms proportional to the position and momentum operators. As a result, each eigenstate of the Ermakov-Lewis invariant is non-degenerate, just as those of the simple harmonic oscillator. Since the eigenstates are non-degenerate, the results of Sec. 2.5.2 may be applied while considering the excited states of the invariant in place of the ground state. The consequence is that, provided that the appropriate boundary conditions are satisfied and the system starts in the n-th excited state of the Hamiltonian $H(0)$ at initial time $t = 0$, then the population is transferred to the n-th

excited state of the final Hamiltonian $H(T)$, which is to say that not only the ground state is transferred by invariant-based inverse engineering, but all of the excited states are as well.

However, this result does not hold for the invariant $\mathcal{I}$ obtained in this chapter, as the eigenstates of the invariant are highly degenerate. The only non-degenerate eigenstate of the invariant is that of the ground state, which is to say that one is only guaranteed to successfully perform ground state to ground state shuttling with this invariant. If the initial state of the system is an excited state of the initial Hamiltonian $H(0)$, then the subsequent dynamics lie within a degenerate eigenspace of the invariant, and it is not guaranteed that one will end up in the desired excited state of the Hamiltonian $H(T)$.

As a result, the degeneracy of the invariant $\mathcal{I}$ presents some difficulties that must be overcome if invariant-based inverse engineering is to succeed in transferring excited state populations from the initial Hamiltonian $H(0)$ to the final Hamiltonian $H(T)$, while the Ermakov-Lewis invariant carries out this task without additional effort.

Chapter 4

Ion shuttling through an X-junction

4.1 Introduction

The problem of shuttling ions through X-junctions in a QCCD is of prime importance to proposals to carry out scalable quantum computing with trapped ions, as discussed in Sec. 2.2.2. In this chapter, I present how the invariant-based inverse engineering techniques derived in Ch. 3 can be used to perform fast ion shuttling through X-junctions by giving a worked example of the procedure. I demonstrate the shuttling of an ion around a corner in the plane, which models the transfer of an ion around a corner in an X-junction.

This chapter is based on work published in [1].

4.2 Motivation and formulation of problem

As explored in Sec. 2.6.1, previous results in invariant-based control of trapped ion motional states have usually assumed that the dynamics of the ion are confined to one dimension $d = 1$ [127, 153, 150, 156, 157, 158]. This is a valid approximation provided that the ion is confined to a linear trap. In this case, the radial modes of motion are decoupled from the axial mode, and they may be neglected under the assumption that only the axial mode undergoes non-trivial

dynamics during a linear shuttle.

However, as discussed in Sec. 2.2.2, most proposals for scalable quantum computing revolve around a QCCD which has junctions connecting many different ion traps. The ions must travel through junctions and around corners as they are routed to different parts of the architecture. In such a case, the assumption that the motional dynamics are effectively one-dimensional breaks down and in this case one expects all of the three spatial degrees of freedom to play a role in the motional dynamics of the ion. The invariant derived in Ch. 3 may then be used to inverse engineer Hamiltonians that can be realised experimentally.

I present here an employment of invariant-based inverse engineering that realises ion shuttling around a corner, in order to demonstrate this technique. I will exhibit the shuttling of a trapped ion around a corner in the plane, which is to say that only two spatial dimensions $d = 2$ will be considered instead of the more natural three $d = 3$. This is done in order to make the resulting dynamics of the ion and trap easier to visualise, though the example demonstrated here may straightforwardly be extended to three spatial dimensions $d = 3$.

In order to carry out invariant-based inverse engineering, the problem must be stated explicitly. The problem of shuttling an ion around a corner implies that one has initial and final trapping configurations that are separated in space, with respective trapping frequencies that are to be fixed. In an ion trap, the radial frequency ω_r is often greater than the transverse frequency ω_t. I therefore write down initial and final trapping potentials

$$V(0) = \frac{1}{2}m\left(\omega_t^2\hat{x}^2 + \omega_r^2(\hat{y} - r)^2\right), \tag{4.1}$$

and

$$V(T) = \frac{1}{2}m\left(\omega_r^2(\hat{x} - r)^2 + \omega_t^2\hat{y}^2\right), \tag{4.2}$$

that naturally determine an initial Hamiltonian $H(0)$ and final Hamiltonian $H(T)$,

$$\begin{aligned} H(0) &= \frac{\hat{p}_x^2 + \hat{p}_y^2}{m} + V(0), \\ &= \frac{\hat{p}_x^2 + \hat{p}_y^2}{m} + \frac{1}{2}m\left(\omega_t^2\hat{x}^2 + \omega_r^2(\hat{y} - r)^2\right), \end{aligned} \tag{4.3}$$

and

$$\begin{aligned} H(T) &= \frac{\hat{p}_x^2 + \hat{p}_y^2}{m} + V(T), \\ &= \frac{\hat{p}_x^2 + \hat{p}_y^2}{m} + \frac{1}{2} m \left(\omega_r^2 (\hat{x} - r)^2 + \omega_t^2 \hat{y}^2 \right). \end{aligned} \tag{4.4}$$

The position operators $\hat{x}$ and $\hat{y}$ index the spatial coordinates in the plane, while the operators $\hat{p}_x$ and $\hat{p}_y$ are the corresponding momentum operators.

Eq. (4.1) defines a trap centred at the position $(0, r)$, while Eq. (4.2) defines one centred at position $(r, 0)$, as over the course of a shuttling operation through a junction, one expects the ion to perform a 90 degree turn. The origin may accordingly be thought of as the centre of the junction. The roles of the radial frequency ω_r and the transverse frequency ω_t are exchanged at the conclusion of the operation at final time $t = T$, as a 90 degree rotation of the trapping potential will necessarily exchange the radial and trapping axes.

The goal is to derive Hamiltonians $H(t)$ that interpolate the initial and final Hamiltonians given in Eqs. (4.3) and Eq. (4.4) that realise fast ground state to ground state transfer.

4.3 Choosing the invariant

In this section, I will illustrate the selection of a quantum invariant that can be used to inverse engineer to obtain Hamiltonians that realise the shuttling of an ion around a corner, in accordance with the principles set out in Ch. 3.

The initial Hamiltonian $H(0)$ and final Hamiltonian $H(T)$ given in Eqs. (4.3) and (4.4) are of the form given in Eq. (3.1). By the results of Ch. 3, it is possible to choose a quantum invariant $\mathcal{I}$ that allows the Hamiltonian $H(t)$ to be inverse engineered at intermediate times.

As discussed in Sec. 3.7, the invariant $\mathcal{I}$ is parameterised in terms of the positive matrix valued quantity $R(t)$ and the trajectory $\vec{L}(t)$. By choosing these quantities appropriately, the Hamiltonian can be inverse engineered following the techniques of Sec. 3.7.

4.3.1 Boundary conditions

As detailed in Sec. 3.6, the positive matrix valued quantity $R(t)$ and the trajectory $\vec{L}(t)$ must satisfy certain boundary conditions in order for the resulting invariant $\mathcal{I}$ to be suitable for inverse engineering.

Eqs. (3.61) and (3.62) give the appropriate boundary conditions on the quantities $\vec{L}$ and R. They read

$$R(0) = M^{-\frac{1}{4}}(0), \tag{4.5}$$

$$R(T) = M^{-\frac{1}{4}}(T), \tag{4.6}$$

and

$$\vec{L}(0) = \frac{1}{m} M^{-1}(0)\vec{F}(0), \tag{4.7}$$

$$\vec{L}(T) = \frac{1}{m} M^{-1}(T)\vec{F}(T), \tag{4.8}$$

Eqs. (4.5)-(4.8) are given in terms of the initial and final quadratic parts of the trapping potential M and the initial and final trap displacements $\vec{F}$. By substituting for these quantities, explicit expressions for the boundary conditions that the real matrix valued quantity $R(t)$ and the trajectory $\vec{L}(t)$ must satisfy can be obtained.

The initial and final Hamiltonians given in Eqs. (4.3) and (4.4) determine the initial and final values of the quadratic part of the Hamiltonian

$$M(0) = \begin{bmatrix} \omega_t^2 & 0 \\ 0 & \omega_r^2 \end{bmatrix}, \tag{4.9}$$

$$M(T) = \begin{bmatrix} \omega_r^2 & 0 \\ 0 & \omega_t^2 \end{bmatrix}, \tag{4.10}$$

$$\vec{F}(0) = \begin{bmatrix} 0 \\ mr\omega_r^2 \end{bmatrix}, \tag{4.11}$$

$$\vec{F}(T) = \begin{bmatrix} mr\omega_r^2 \\ 0 \end{bmatrix}.$$

By substituting these expressions into Eqs. (4.5)-(4.8), one gets

$$R(0) = \begin{bmatrix} \frac{1}{\sqrt{\omega_t}} & 0 \\ 0 & \frac{1}{\sqrt{\omega_r}} \end{bmatrix}, \tag{4.13}$$

$$R(T) = \begin{bmatrix} \frac{1}{\sqrt{\omega_r}} & 0 \\ 0 & \frac{1}{\sqrt{\omega_t}} \end{bmatrix}, \tag{4.14}$$

$$\vec{L}(0) = \begin{bmatrix} 0 \\ r \end{bmatrix}, \tag{4.15}$$

$$\vec{L}(T) = \begin{bmatrix} r \\ 0 \end{bmatrix}. \tag{4.16}$$

As stated in Sec. 3.6, the positive matrix valued quantity $R(t)$ and the trajectory $\vec{L}(t)$ may be freely interpolated between their initial and final values given in Eqs. (4.13)-(4.16), provided that their first and second derivatives vanish at initial time $t = 0$ and final time $t = T$.

4.3.2 Expressions for the positive matrix valued quantity $R(t)$ and the trajectory $\vec{L}(t)$

Any functional form for the trajectory $\vec{L}$ and positive matrix valued quantity R that interpolates the boundary conditions derived in the previous section may be chosen. Since the boundary conditions involve only the quantities $\vec{L}$, R and their first and second derivatives at initial and final times, there are very many ways to do this. I will present here choices for the quantities

$\vec{L}$ and R that are nevertheless physically motivated and realise non-trivial quantum dynamics.

In order to write down the expressions concisely, it will prove convenient to introduce the polynomial, employed in earlier works [153, 159]

$$p(\tau) = 10\tau^3 - 15\tau^4 + 6\tau^5, \tag{4.17}$$

where

$$\tau = \frac{t}{T}. \tag{4.18}$$

The polynomial $p(\tau)$ is the monic polynomial of lowest degree that satisfies $p(0) = 0$, $p(1) = 1$, and $\dot{p}(0) = \dot{p}(1) = \ddot{p}(0) = \ddot{p}(1) = 0$.

I turn now to the choice of the trajectory $\vec{L}$. As discussed in Sec. 4.2, the ion trajectory is to turn a corner in order to model the effect of ion shuttling. A simple choice of trajectory is for the ion to trace out a quarter circle during the motion. I impose the following expression for the choice of trajectory $\vec{L}$

$$\vec{L}(t) = r \begin{bmatrix} \sin\left(\frac{\pi}{2}p(\tau)\right) \\ \cos\left(\frac{\pi}{2}p(\tau)\right) \end{bmatrix}. \tag{4.19}$$

Eq. (4.19) defines a trajectory $\vec{L}$ that satisfies the boundary conditions Eqs. (4.15) and (4.16). The presence of the polynomial $p(\tau)$ ensures that the first and second derivatives of the trajectory $\vec{L}$ vanish at initial time $t = 0$ and final time $t = T$.

The positive matrix-valued quantity $R(t)$ must be chosen as well. The quantity $R(t)$ is related to the covariance matrix Σ via Eq. (3.77). It is defined to be

$$R(t) = (1 - p(\tau))R(0) + p(\tau)R(T) + \tau^3 (1 - \tau)^3 R_c \ , \tag{4.20}$$

where

$$R_c = (\omega_t \omega_r)^{-\frac{1}{4}} \begin{bmatrix} 1 & 1 \\ 1 & 1 \end{bmatrix} . \tag{4.21}$$

Eq. (4.20) defines a positive-matrix valued quantity R that satisfies the boundary conditions laid out in Eqs. (4.13) and (4.14).

The first two terms $(1 - p(\tau))R(0) + p(\tau)R(T)$ in Eq. (4.20) perform an interpolation between the initial value of the quantity $R(0)$ and the final value $R(T)$. Again, the presence of the polynomial $p(\tau)$ ensures that the first and second derivatives of the quantity R vanish at initial time $t = 0$ and final time $t = T$.

The term R_c vanishes at initial time $t = 0$ and final time $t = T$. The effect of this term is to ensure that the principal axes of the matrix R undergo some non-trivial rotations during intermediate times $0 < t < T$. Without this, the principal axes of the matrix R, and those of the resulting trapping frequency matrix M are always aligned in the x and y directions. This has the effect of reducing the problem of ion shuttling to that of two decoupled one-dimensional problems. By choosing the term R_c according to Eq. (4.21), the ability of the invariant defined in Ch. 3 to deliver non-trivial Hamiltonians that undergo some rotation in the trapping potential is demonstrated.

The choice of the term R_c turns out to have some significant implications for the problem of the degeneracy of the invariant $\mathcal{I}$ discussed in Sec. 3.9.1. Although I do not explore the possibility here, recent work [144] indicates that it is possible to perform transfer of excited states by choosing the term R_c to have greater magnitude.

Now that the quantities $\vec{L}$ and R have been defined, one can deduce the quadratic part of the trapping potential M and the trap displacement term $\vec{F}$ using the techniques of Sec. 3.7.

4.4 Presentation of results

In this section, I will present some realisations of the invariant based inverse engineering procedure described previously, and discuss their qualitative features.

The shuttling problem described in earlier chapters is parametrised by quantities including the radius r of the path of the ion, the initial transverse frequency ω_t, the initial radial frequency ω_r

and the duration of the shuttling T. By varying these quantities, different shuttling procedures may be obtained, which are illustrated in Fig. 4.1. I will now outline the choices made for these quantities.

The ratio of the transverse and radial frequencies $\frac{\omega_r}{\omega_t}$ is rarely unity in an experimental trap, which is to say that ion traps are rarely isotropic. This quantity was set to be equal to 2 in insets (a), (c) and (e) and equal to 10 in insets (b), (d) and (f) to model the effects of differing trap anisotropies on the resulting dynamics.

The quantity $T\omega_t$ was varied to model the effect of changing the duration T of the shuttling procedure, which allows one to compare slow and fast ion shuttles. Insets (a) and (b) illustrate fast shuttling procedures with $\omega_t T = 3$. Insets (c) and (d) illustrate slower procedures with $\omega_t T = 5$, and insets (e) and (f) are slower still with $\omega_t T = 10$.

Fig. 4.1 presents the dynamics of the level sets of the trapping potential in orange, which are determined by the quadratic part of the trapping potential M and the centre of the trap $\vec{C}$, which is plotted in blue, defined by

$$\vec{C} = \frac{1}{m} M^{-1} \vec{F}. \tag{4.22}$$

The shuttling problem is also determined by the mass of the ion m and the radius r of the path of the ion. One can determine the effect of varying the mass m and the radius of the path of the ion r on the quadratic part of the trapping potential M and the centre of the trap $\vec{C}$ by carrying out the inverse engineering procedure outlined in Sec. 3.7. The resulting quadratic part of the trapping potential M has no dependence on the mass of the ion m and the radius r of its path. One can apply Eq. (4.22) to obtain the centre of the trap $\vec{C}$. As the trajectory $\vec{L}$ defined in Eq. (4.19) is proportional to the radius r, the resulting trap centre $\vec{C}$ is also proportional to the radius r, and has no dependence on the mass m. The effect of varying the radius r is only to vary the extent of the trajectory of the centre of the trap $\vec{C}$ and not its shape. Accordingly, varying the mass m and radius r does not produce examples distinct to those presented in Fig. 4.1.

In all of the insets, the trajectory of the ion traces out the same quarter circle as specified

by Eq. (4.19), plotted in purple. The faster shuttling protocols presented in insets (a) and (b) display substantial deviation between the trap centre and the ion trajectory. Despite these significant deviations, and the wild trajectory the ion takes, the shuttling procedure still delivers ground state to ground state transfer. The slower shuttling procedures presented in insets (c)-(f) display much smaller deviations, and the trap centre and ion trajectory almost coincide. This is symptomatic of the adiabatic regime, in which the state of the ion is close to the instantaneous ground state of the trap.

The trap trajectories presented in insets (a) and (c) differ from their less isotropic counterparts in insets (b) and (d), while this is much less pronounced when comparing insets (c) and (f). One concludes that changing the isotropy has only a minor effect on the trap protocols at slower times.

The orange ellipses indicate level sets of the trapping potential taken at equidistant times $t = jT/8$ with $j = 0, \ldots, 8$. The shape of the ellipses is determined by the quadratic part of the trapping potential M. Even in the faster shuttling protocols presented in insets (a) and (d), the orange ellipses perform gradual changes in shape, which lies in contrast to the exaggerated motions of the trap centres.

The ellipses tend to be aligned with the principal axes x and y. As a result, the dynamics they undergo tends to be composed mostly of stretching and squeezing, though some rotation is visible in inset (c). By increasing the magnitude of the term R_c defined in Eq. (4.20), it is possible to observe a greater degree of rotation in the trapping potential, which is to say that the dominance of the stretching and squeezing here is not a general characteristic of the invariant-based inverse engineering techniques.

4.5 Outlook

There exist very many possible choices of invariant $\mathcal{I}$ to inverse-engineer a Hamiltonian for this control task, of which only one is presented in Fig. 4.1. Nevertheless, several general conclusions can be drawn from this example.

The substantial deviation of the trap centre and the centre of the ion demonstrates that the inverse engineering procedure is capable of finding highly nontrivial Hamiltonians that realise the required control task. In particular, the paths of the trap centre trajectories, which are significantly different from those of the ions, suggest that invariant-based inverse engineering is capable of discovering experimental protocols that would not easily be guessed at otherwise. This implies that invariant-based inverse engineering is likely to be a useful guide for experimental implementations of fast ion shuttling, in which there is no obvious *a priori* choice for the path of the trapping potential.

Although relatively simple expressions for the quantities that parametrise the invariant $\mathcal{I}$ were chosen in Sec. 4.3.2, the traps display significant deformation in shape throughout the shuttling protocol, yet still ensure that the ion returns to its motional ground state at the end of the procedure. This implies that the ion undergoes non-trivial quantum dynamics during the procedure in addition to the classical motion of the centre of the ion. This indicates that invariant-based inverse engineering is capable of discovering with ease Hamiltonians that produce interesting quantum evolution from a theoretical perspective.

By choosing different forms for the real matrix valued quantity $R(t)$ and the trajectory $\vec{L}(t)$ that are consistent with the boundary conditions set out in Sec. 4.3.1, it is possible to inverse engineer many different Hamiltonians H and compare their features. This opens up the prospect of *optimising* over invariants $\mathcal{I}$ to find the Hamiltonian H that performs best with regard to some set of criteria, such as minimising the separation of ion and trap centre, or ensuring that the ion and trap centre take physically realisable paths within an experimental trap geometry. Such a possibility allows for more experimental considerations to be taken into account when designing a shuttling procedure, which demonstrates again the experimental utility of invariant-based inverse engineering.

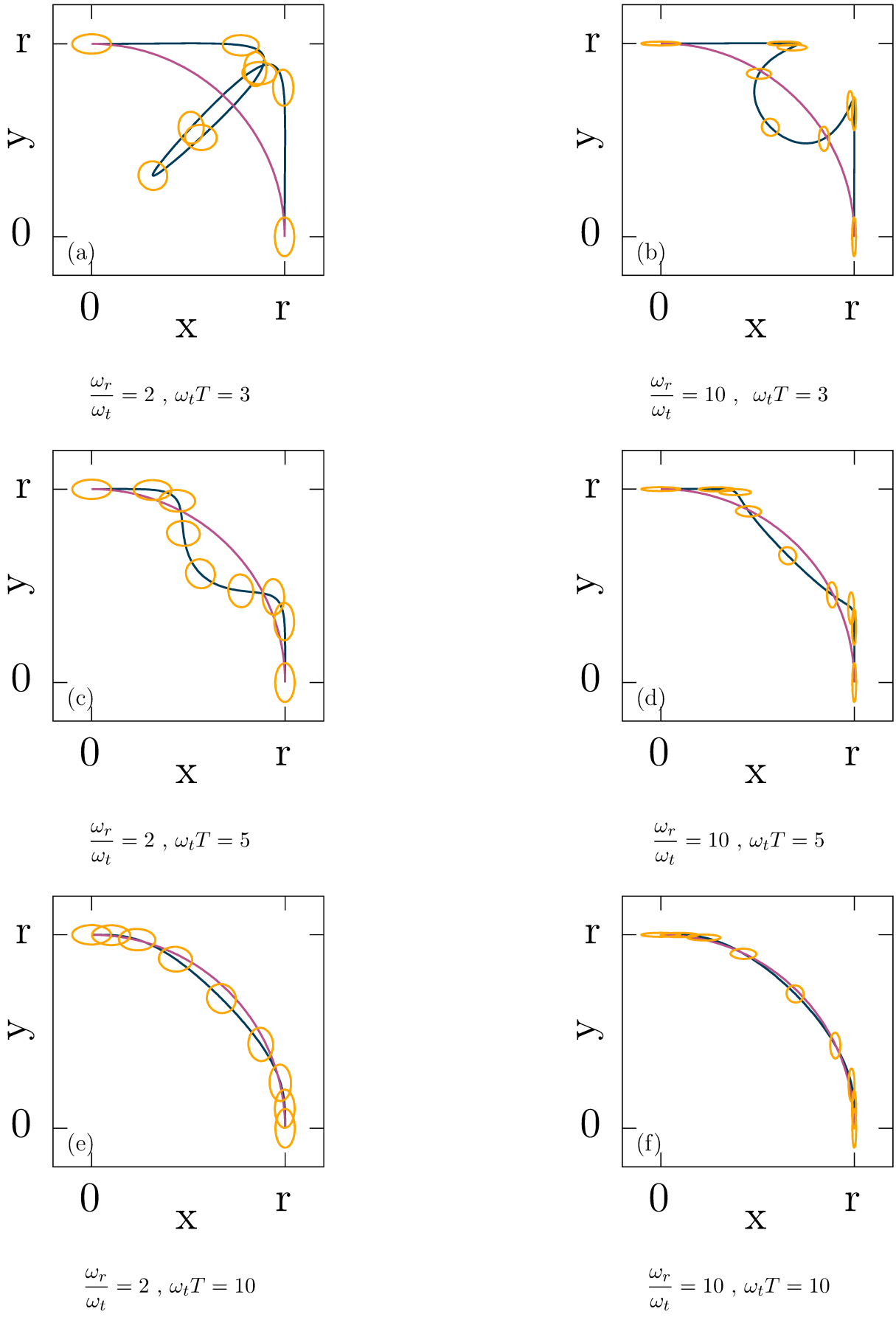

Figure 4.1: Ion shuttling around a corner. Trap centre trajectories are shown in blue, ion trajectories are shown in purple, while level sets of the trapping potential are shown as orange ellipses. The duration of the protocol increases for the lower figures. The faster protocols shown at the top of the figure display substantial deviation between trap centres and trap trajectories, and this effect is more pronounced for the more isotropic trapping potentials on the left.

Chapter 5

A many-particle quantum invariant

5.1 Introduction

The results presented in Ch. 3 allow one to control the motional state of a trapped ion in any number of spatial dimensions d. This lets one perform fast, ground state to ground state shuttling of trapped ions, as demonstrated in Ch. 4. However, these results are limited to the analysis of a single ion. In a QCCD, one is interested in controlling the motion of two or several strongly interacting ions at a time, to perform tasks such as separation of trapped ions. In this chapter, I derive another quantum invariant which corresponds to a system of any number of trapped ions strongly interacting under the Coulomb potential. I explore the possibility of inverse engineering Hamiltonians that can perform tasks such as separation of trapped ions, and discuss some of the limitations encountered. I demonstrate how the invariant may be inverse engineered to obtain Hamiltonians in a simplified regime in which there are only two ions moving in trapping potentials of equal shape.

This chapter is based on work to be published in [2].

5.2 Interacting particles: challenges

In this section, I will introduce a Hamiltonian that is used in the results of this chapter and summarise the challenges associated with controlling more than one ion at a time.

Trapped ions interact under the Coulomb potential. Although this interaction may be neglected when the ions are well-separated in space, there exist many scenarios in which it cannot. During the operation of a QCCD, ions are periodically made to interact by bringing them together in the same trap, in which they are held apart solely by the effect of their Coulomb interaction. The Coulomb potential cannot be neglected in such a situation, as without it the ions would occupy the same position in space, which is absurd.

In ion traps, the Coulomb potential between two ions tends to vary on scales that are much larger than the spatial extent of the wavepackets of the ions. As a result, the relevant quantum effects of the Coulomb potential are expected to be limited to stretching and squeezing of the quantum state, and changes in the expected displacements of the wavepackets.

As discussed in Sec. 2.4, trapped ions move in potentials that may be taken to be quadratic in position. The Hamiltonian governing n ions, trapped in potentially distinct traps in d spatial dimensions, interacting under the Coulomb potential, may be written as

$$H(t) = \sum_i^n \frac{\hat{\vec{p}}_i^{\,2}}{2m_i} + \frac{1}{2}\sum_i^n m_i \hat{\vec{x}}_i^{\,T} M_i(t) \hat{\vec{x}}_i - \sum_i^n \vec{F}_i(t) \cdot \hat{\vec{x}}_i + \sum_{1\le i<j\le n} \frac{e^2}{4\pi\epsilon_0 |\hat{\vec{x}}_i - \hat{\vec{x}}_j|}, \tag{5.1}$$

where the d-by-d matrix valued quantity M_i and the d-dimensional vector valued quantity $\vec{F}_i$ characterise the quadratic parts of the trapping potentials and the trap displacements for the i-th ion. The operators $\hat{\vec{x}}_i$ and $\hat{\vec{p}}_i$ are the position and momentum operators respectively of the i-th ion, and are both d-dimensional vector-valued operators.

The quadratic parts of the trapping potentials M_i and the trap displacement $\vec{F}_i$ are ultimately determined by local Taylor expansions of the pseudopotential, as explained in Sec. 2.3.2. They may be altered by changing the pseudopotential, which can be performed by modulating the voltages that are applied to the electrodes. As a result, the quantities M_i and $\vec{F}_i$ may be

regarded as parameters which are imposed by experimental control and are free to vary in time.

The Hamiltonian given in Eq. (5.1) reduces to that of a single ion given in Eq. (3.1) when the number of ions n is taken to be one. As such, it may be considered as a generalisation of Eq. (3.1) to higher numbers of ions. In Ch. 3, an invariant was constructed that ultimately allowed the Hamiltonian given in Eq. (3.1) to be obtained via inverse engineering of a quantum invariant, which allowed for the construction of experimentally realisable Hamiltonians that perform fast, ground state to ground state shuttling of a trapped ion.

The ability to construct a quantum invariant for the Hamiltonian given in Eq. (5.1) would similarly allow one to realise tasks involving the motional states of more than one ion such as fast ion separation, ion crystal rotation and mixed-species shuttling of several ions in a unified manner. However, there exist some challenges associated with the construction of an invariant corresponding to the Hamiltonian given in Eq. (5.1) that are not encountered in the analysis of a single ion.

In Ch. 3, the fact that the Hamiltonian was quadratic in both position and momentum operators motivated the ansatz of an invariant that was also quadratic in position and momentum in Sec. 3.2, which was crucial to progress. In contrast, the Coulomb terms that appear in Eq. (5.1) are not quadratic in position, which precludes the approach used in Ch. 3 to construct the invariant. Indeed, it is very difficult to write down, even in one spatial dimension $d = 1$, useful quantum invariants that contain a Coulomb potential term [155]. Additionally, the Coulomb terms are not experimentally controllable, so there is no prospect of mitigating their effect.

5.3 Multipole expansion of the Coulomb potential

Although it is difficult to write down a quantum invariant corresponding to a Hamiltonian containing Coulomb terms, it is possible to make progress by means of an approximation. In this section I will present an expansion of the Coulomb potential that will facilitate the construction of a quantum invariant corresponding to the Hamiltonian defined in Eq. (5.1).

The Coulomb interaction between the i-th and j-th ion is given by

$$\frac{e^2}{4\pi\epsilon_0|\hat{\vec{x}}_i - \hat{\vec{x}}_j|} = \frac{C}{|\hat{\vec{x}}_i - \hat{\vec{x}}_j|}, \tag{5.2}$$

where the prefactor $\frac{e^2}{4\pi\epsilon_0}$ has been absorbed into the constant C for notational brevity.

As discussed in Sec. 5.2, one of the obstacles to writing down an invariant associated with the Coulomb term given in Eq. (5.2) is that it is not quadratic in position. It is possible to obtain an operator quadratic in position that approximates Eq. (5.2) by performing a Taylor expansion of Eq. (5.2) to second order and discarding higher order terms.

Eq. (5.2) is a function of the operators $\hat{\vec{x}}_i$ and $\hat{\vec{x}}_j$. In the case that the Coulomb potential does not vary considerably in the region over which the wavefunction of the two ions is significant, then one can replace the Coulomb term given in Eq. (5.2) with the expected value

$$\frac{C}{|\hat{\vec{x}}_i - \hat{\vec{x}}_j|} \approx \left\langle \frac{C}{\left|\hat{\vec{x}}_i - \hat{\vec{x}}_j\right|} \right\rangle \approx \frac{C}{\left|\left\langle \hat{\vec{x}}_i \right\rangle - \left\langle \hat{\vec{x}}_j \right\rangle\right|}. \tag{5.3}$$

The right hand side of Eq. (5.3) involves no operators at all, and is simply a real number. As such, it may be regarded as a zeroth-order approximation of the Coulomb potential. Nevertheless, it is not particularly useful for present purposes, as it depends explicitly on the expected positions of the ions $\left\langle \hat{\vec{x}}_i \right\rangle$ and $\left\langle \hat{\vec{x}}_j \right\rangle$, and it is not clear whether this approximation is valid. However, it motivates an expansion of the Coulomb potential that can be employed usefully.

Performing a Taylor expansion of Eq. (5.2) around the expected positions of the ions $\left\langle \hat{\vec{x}}_i \right\rangle$ and $\left\langle \hat{\vec{x}}_j \right\rangle$ gives

$$\begin{aligned}
\frac{C}{|\hat{\vec{x}}_i - \hat{\vec{x}}_j|} &= \frac{C}{r_{ij}} + \frac{C(\Delta\hat{\vec{x}}_i - \Delta\hat{\vec{x}}_j)\cdot\vec{r}_{ij}}{r_{ij}^3} - \frac{C\Delta\hat{\vec{x}}_i\cdot\Delta\hat{\vec{x}}_i}{2r_{ij}^3} + \frac{3C(\Delta\hat{\vec{x}}_i\cdot\vec{r}_{ij})(\Delta\hat{\vec{x}}_i\cdot\vec{r}_{ij})}{2r_{ij}^5} \\
&+ \frac{C\Delta\hat{\vec{x}}_i\cdot\Delta\hat{\vec{x}}_j}{r_{ij}^3} - \frac{3C(\Delta\hat{\vec{x}}_i\cdot\vec{r}_{ij})(\Delta\hat{\vec{x}}_j\cdot\vec{r}_{ij})}{r_{ij}^5} - \frac{C\Delta\hat{\vec{x}}_j\cdot\Delta\hat{\vec{x}}_j}{2r_{ij}^3} + \frac{3C(\Delta\hat{\vec{x}}_j\cdot\vec{r}_{ij})(\Delta\hat{\vec{x}}_j\cdot\vec{r}_{ij})}{2r_{ij}^5} \\
&+ O\left(\frac{C}{r_{ij}^4}\right),
\end{aligned} \tag{5.4}$$

having defined $\vec{x}_i = \langle\hat{\vec{x}}_i\rangle$, $\vec{x}_j = \langle\hat{\vec{x}}_j\rangle$, $\Delta\hat{\vec{x}}_i = \hat{\vec{x}}_i - \vec{x}_i$, $\Delta\hat{\vec{x}}_j = \hat{\vec{x}}_j - \vec{x}_j$ and $\vec{r}_{ij} = \vec{x}_i - \vec{x}_j$.

Eq. (5.4) is an expansion of the Coulomb potential in a series of terms that are of order $\frac{1}{r^n}$, where the distance r is the expected separation of the i-th and j-th ion. It is an example of a multipole expansion. By discarding the remainder term of order $O\left(\frac{C}{r^4}\right)$, an operator quadratic in the position operators $\hat{\vec{x}}_i$ and $\hat{\vec{x}}_j$ may be obtained. However, such a truncation must be justified.

As discussed in Sec. 5.2, the Coulomb potential cannot be neglected in ion traps. However, as the Coulomb potential varies on length scales that are large compared with the spatial extents of the wavepackets, the remainder term $O\left(\frac{C}{r^4}\right)$, which contributes to non-Gaussian excitations in the quantum states, is expected to be small. From now on, this remainder term is neglected completely.

One can obtain a Hamiltonian that is quadratic in position and momentum operators, and hence more amenable to inverse engineering, by substituting for the expansion of the Coulomb potential in Eq. (5.4). Substituting Eq. (5.4) into Eq. (5.1) gives, after absorbing terms into each other and relabelling,

$$H = \sum_{i=1}^{n} \frac{\vec{p}_i^2}{2m_i} + \frac{1}{2}\sum_{i=1}^{n} m_i \vec{x}_i^T \mathcal{M}_i \vec{x}_i - \sum_{i=1}^{n} \vec{\mathcal{F}}_i \cdot \vec{x}_i + \sum_{1\leq i<j\leq n} \vec{x}_i^T D(\vec{r}_{ij}) \vec{x}_j, \tag{5.5}$$

where

$$\mathcal{M}_i = M_i + \sum_{i\neq j} \frac{3C\vec{r}_{ij}\vec{r}_{ij}^T}{m_i r_{ij}^5} - \frac{C\mathbb{1}}{m_i r_{ij}^3}, \tag{5.6}$$

$$\vec{\mathcal{F}}_i = \vec{F}_i + \sum_{i\neq j} \frac{C\vec{r}_{ij}}{r_{ij}^3}, \tag{5.7}$$

and

$$D(\vec{r}) = \frac{C\mathbb{1}}{r^3} - \frac{3C\vec{r}\vec{r}^T}{r^5}. \tag{5.8}$$

Eq. (5.5) is the Hamiltonian of n interacting time-dependent displaced d-dimensional harmonic oscillators that are coupled together via the terms $D(\vec{r}_{ij})$. The Coulomb interaction induces the couplings via the definition of the coupling constants in Eq. (5.8). Constant terms have been discarded, as they contribute only an irrelevant global time-dependent phase to the dynamics.

Eq. (5.5) bears a resemblance to Eq. (5.1) in that the quantities M_i and $\vec{F}_i$ that characterise the ion traps in Eq. (5.1) have been replaced by $\mathcal{M}_i$ and $\vec{\mathcal{F}}_i$ in Eq. (5.5). As a result, the quantities $\mathcal{M}_i$ and $\vec{\mathcal{F}}_i$ may be thought of as defining trapping potentials of their own, which are defined via Eqs. (5.6) and (5.7).

The Hamiltonian given in Eq. (5.5) is quadratic in position and momentum operators, as the Coulomb interaction has been replaced with coupling terms of the form $\hat{\vec{x}}_i^T D(\vec{r}_{ij})\hat{\vec{x}}_j$, which are quadratic in position. It is hence amenable to inverse engineering as hoped. Nevertheless, a cause for concern is that the quantities $\mathcal{M}_i$ and $\vec{\mathcal{F}}_i$ that characterise this Hamiltonian are given in terms of the as-yet-unknown expected positions of the ions via Eqs. (5.6) and (5.7). I will address this later, and turn for now to the question of deriving an invariant for the Hamiltonian given in Eq. (5.5).

5.4 Coupled harmonic oscillators

In this section, I will present a quantum invariant that corresponds to the Hamiltonian defined in Eq. (5.5).

As noted, the Hamiltonian given in Eq. (5.5) is quadratic in position and momentum operators. Following the example of Sec. 3.2, I will write down an ansatz for the proposed invariant that is also quadratic in position and momentum operators.

To facilitate this, it is helpful to specify the phase-space operator $\hat{X}$ that is used here. It is given by

$$\hat{X} = \left(\hat{\vec{x}}_1, \quad \hat{\vec{x}}_2, \quad \ldots, \quad \hat{\vec{x}}_n, \quad \hat{\vec{p}}_1, \quad \hat{\vec{p}}_2, \quad \ldots, \quad \hat{\vec{p}}_n\right). \tag{5.9}$$

Since the position operators $\hat{\vec{x}}_i$ and momentum operators $\hat{\vec{p}}_i$ are themselves d-dimensional vectors, the phase space operator $\hat{X}$ is now a $2nd$-dimensional vector.

The Hamiltonian H can now be written in terms of the phase space operator $\hat{X}$, which will motivate the explicit form of the invariant.

Following the example of Sec. 2.4, one writes the Hamiltonian as in Eq. (2.17) as a quadratic form in the phase space operator X,

$$H = \frac{1}{2} X^T \Omega X + \vec{V} \cdot X, \tag{5.10}$$

where this time the quantities Ω and $\vec{V}$ are defined to be

$$\Omega = \begin{pmatrix} m_1\mathcal{M}_1 & D(\vec{r}_{12}) & \dots & D(\vec{r}_{1n}) & 0 & 0 & \dots & 0 \\ D(\vec{r}_{12}) & m_2\mathcal{M}_2 & \dots & D(\vec{r}_{2n}) & 0 & 0 & \dots & 0 \\ \vdots & \vdots & \ddots & \vdots & \vdots & \vdots & & \vdots \\ D(\vec{r}_{1n}) & D(\vec{r}_{2n}) & \dots & m_n\mathcal{M}_n & 0 & 0 & \dots & 0 \\ 0 & 0 & \dots & 0 & \frac{\mathbb{1}}{m_1} & 0 & \dots & 0 \\ 0 & 0 & \dots & 0 & 0 & \frac{\mathbb{1}}{m_2} & \dots & 0 \\ 0 & 0 & \dots & 0 & \vdots & \vdots & \ddots & \vdots \\ 0 & 0 & \dots & 0 & 0 & 0 & \dots & \frac{\mathbb{1}}{m_n} \end{pmatrix}, \tag{5.11}$$

and

$$\vec{V} = \begin{pmatrix} -\vec{\mathcal{F}}_1, & -\vec{\mathcal{F}}_2, & \dots, & -\vec{\mathcal{F}}_n, & 0, & 0, & \dots, & 0 \end{pmatrix}. \tag{5.12}$$

The quantities Ω and $\vec{V}$ are given in terms of block matrix and vector decompositions that are consistent with the definition of $\hat{X}$ in Eq. (5.9).

It is now possible to write down a quantum invariant that is quadratic in the phase space operator $\hat{X}$. However, motivated by the analysis of the single ion invariant in Sec. 3.5.2, a slightly different form of the invariant will be chosen. The invariant $\mathcal{I}$ derived in Ch. 3 can be compactly represented by completing the square in Eq. (3.58). Doing so leads to a helpful physical interpretation of the quantity $\vec{Z}$ as the expected position of the ion in phase space. Anticipating this, I choose an ansatz in which the square is already completed, as in Eq. (3.58),

$$\mathcal{I} = \frac{1}{2} (\hat{X} - \vec{Z})^T \Gamma (X - \vec{Z}). \tag{5.13}$$

The quantity Γ is a $2nd$-by-$2nd$ square matrix valued function of time, and the quantity $\vec{Z}$ is

a vector-valued function of time of size $2nd$.

As the Hamiltonian H and invariant $\mathcal{I}$ are defined in a similar way to those in Ch. 3 through Eqs. (5.10) and (5.13), the quantities Ω, $\vec{V}$, Γ and $\vec{Z}$ satisfy similar relations to those given in Ch. 3.

The operator $\mathcal{I}$ is an invariant for the Hamiltonian H if and only if

$$\dot{\Gamma} = \Omega\mathcal{S}\Gamma - \Gamma\mathcal{S}\Omega, \tag{5.14}$$

$$\dot{\vec{Z}} = \mathcal{S}V + \mathcal{S}\Omega\vec{Z}, \tag{5.15}$$

where the symplectic matrix $\mathcal{S}$ is now a $2nd$-dimensional square matrix

$$\mathcal{S} = \begin{pmatrix} 0 & \mathbb{1} \\ -\mathbb{1} & 0 \end{pmatrix}. \tag{5.16}$$

Eq. (5.14) is identical to Eq. (3.6), and Eq. (5.15) is equivalent to Eq. (3.51) after rearranging.

Any choice of the quantities Γ and $\vec{Z}$ that satisfy equations Eqs. (5.14) and (5.15) defines a quantum invariant $\mathcal{I}$. One may attempt to inverse engineer the invariant $\mathcal{I}$ by choosing the quantities Γ and $\vec{Z}$ and attempting to deduce the quantities Ω and $\vec{V}$ via substitution of the quantities Γ and $\vec{Z}$ into Eqs. (5.14) and (5.15). However, this attempt is doomed to fail for reasons similar to those laid out in Sec. 3.2.1, namely that it is not clear how to deduce functional forms for the quantities Ω and $\vec{V}$ that are consistent with their definitions in Eqs. (5.11) and (5.12).

5.5 Restricted forms for the quantities Γ and $\vec{Z}$

In this section, I will introduce functional forms for the matrix-valued quantity Γ and the vector-valued quantity $\vec{Z}$, that will allow for the invariant $\mathcal{I}$ defined in Eq. (5.13) to be inverse engineered to obtain Hamiltonians of the form given in Eq. (5.5). I will start by choosing a

functional form for the vector-valued quantity $\vec{Z}$ before turning to the matrix-valued quantity Γ.

5.5.1 An ansatz for the quantity $\vec{Z}$

The vector-valued quantity $\vec{Z}$ obeys Eq. (5.15), which are simply Hamilton's equations written in vector form for the Hamiltonian H. This suggests that the quantity $\vec{Z}$ has the interpretation of a trajectory in phase space. Motivated by this, I choose the ansatz for $\vec{Z}$

$$\vec{Z} = \left(\vec{L}_1, \quad \vec{L}_2, \quad \ldots, \quad \vec{L}_n, \quad m_1\dot{\vec{L}}_1, \quad m_2\dot{\vec{L}}_2, \quad \ldots, \quad m_n\dot{\vec{L}}_n \right), \tag{5.17}$$

where the quantities $\vec{L}_i$ are d-dimensional vector-valued functions of time.

By substituting Eq. (5.17) into Eq. (5.15), some necessary conditions can be found involving the quantities $\vec{L}_i$ that ensure that the ansatz given in Eq. (5.17) obeys Eq. (5.15).

Introducing the shorthand notation

$$D[i,j] = D(\vec{r}_{ij}), \tag{5.18}$$

performing the substitution and rearranging gives that

$$\dot{\vec{Z}} - \mathcal{S}V + \mathcal{S}\Omega\vec{Z} = \begin{pmatrix} 0 \\ 0 \\ \vdots \\ 0 \\ m_1\ddot{\vec{L}}_1 + m_1\mathcal{M}_1\vec{L}_1 - \vec{\mathcal{F}}_1 + \sum_{j\neq 1} D[1,j]\vec{L}_j \\ m_2\dot{\vec{L}}_2 + m_2\mathcal{M}_2\vec{L}_2 - \vec{\mathcal{F}}_2 + \sum_{j\neq 2} D[2,j]\vec{L}_j \\ \vdots \\ m_n\dot{\vec{L}}_n + m_n\mathcal{M}_n\vec{L}_n - \vec{\mathcal{F}}_n + \sum_{j\neq n} D[n,j]\vec{L}_j \end{pmatrix}. \tag{5.19}$$

One concludes that if

$$\ddot{\vec{L}}_i + \mathcal{M}_i \vec{L}_i = \frac{\vec{\mathcal{F}}_i - \sum_{j \neq i} D[i,j] \vec{L}_j}{m_i} \tag{5.20}$$

for all i, then Eq. (5.15) is satisfied. Eq. (5.20) will sometimes be referred to as the *coupled vector Newton equation*, as it generalises the vector Newton equation given in Eq. (3.55) to multiple quantities $\vec{L}_i$ that are coupled together via the $D[i,j]$ that enter into the right hand side of Eq. (5.20).

Since the vector-valued quantity $\vec{Z}$ satisfies Hamilton's equations in Eq. (5.15), the quantities $\vec{L}_i$ are in fact the *classical* trajectories of the i-th ion. This not only gives a useful physical interpretation of the quantities $\vec{L}_i$, but resolves the issue raised at the end of Sec. 5.3 that the quantities $\mathcal{M}_i$ and $\vec{\mathcal{F}}_i$ that characterise the Hamiltonian through Eqs. (5.6) and (5.7) are defined in terms of the as-yet-unknown expected positions of the ions $\vec{x}_i$.

During inverse engineering, the quantities $\vec{L}_i$ are first chosen to specify, along with a choice of Γ, a choice of invariant $\mathcal{I}$ through Eq. (5.13). Since the quantities $\vec{L}_i$ are in fact the expected positions of the ions $\vec{x}_i$, the coupling terms $D(\vec{r}_{ij})$ may be calculated by substituting $\vec{r}_{ij} = \vec{L}_i - \vec{L}_j$. The quadratic parts of the trapping potential M_i and trap displacement terms $\vec{F}_i$ may be related to the quantities $\mathcal{M}_i$ and $\vec{\mathcal{F}}_i$ via substitution of $\vec{r}_{ij} = \vec{L}_i - \vec{L}_j$ in Eqs. (5.6) and (5.7).

5.5.2 An ansatz for the quantity Γ

The ansatz that will be employed for the quantity is

$$\Gamma = \mathrm{Re}\left(G^\dagger G\right) \ , \tag{5.21}$$

defined in terms of the $d \times nd$ dimensional matrix

$$G = \begin{pmatrix} m_1 \dot{Y}_1 & \dots & m_n \dot{Y}_n & -Y_1 & \dots & -Y_n \end{pmatrix}, \tag{5.22}$$

which is defined in terms of complex, d-by-d square matrices Y_i each corresponding to the i-th

ion.

Substituting Eq. (5.22) into Eq. (5.14) gives, after simplifying

$$\mathrm{Re}\left(G^\dagger\left(\dot{G}+G\mathcal{S}\Omega\right)+\left(\dot{G}+G\mathcal{S}\Omega\right)^\dagger G\right)=0, \tag{5.23}$$

from which one concludes that Eq. (5.14) is satisfied if the quantity $\dot{G}+G\mathcal{S}\Omega$ vanishes.

This quantity may be computed by substituting for the quadratic part of the Hamiltonian Ω using Eq. (5.11) and the definition of the matrix G in Eq. (5.11). One obtains

$$\dot{G}+GS\Omega=\begin{pmatrix}Q_1 & Q_2 & \dots & Q_n & \mathbb{O} & \dots & \mathbb{O}\end{pmatrix}, \tag{5.24}$$

where

$$Q_i=m_i\left(Y_i\mathcal{M}_i+\ddot{Y}_i\right)+\sum_{j\neq i}Y_jD[i,j]. \tag{5.25}$$

Eq. (5.14) is therefore satisfied if all the matrices Q_i vanish, which is equivalent to requiring that for all i,

$$\ddot{Y}_i+Y_i\mathcal{M}_i=-\sum_{j\neq i}\frac{Y_jD[i,j]}{m_i}. \tag{5.26}$$

If Eqs. (5.20) and (5.26) are satisfied, then the invariant $\mathcal{I}$ is an invariant for the Hamiltonian H of the form given in Eq. (5.5) as required. In order to apply the techniques of invariant-based inverse engineering, one would like to be able to deduce the quantities $\mathcal{M}_i$ and $\vec{\mathcal{F}}_i$ from Eqs. (5.20) and (5.26), given a choice of invariant $\mathcal{I}$. In the next section I will address how to carry this out.

5.6 Towards inverse engineering

In this section, I will outline the difficulties associated with employing the invariant characterised in Sec. 5.5 for invariant-based inverse engineering, and present a way to surpass them.

The invariant $\mathcal{I}$ defined in Eq. (5.13) is characterised in terms of matrix-valued quantities Y_i and vector-valued quantities $\vec{L}_i$ through Eqs. (5.17), (5.21) and (5.22). One can attempt to perform invariant-based inverse engineering using this invariant. Firstly, by specifying the matrix-valued quantities Y_i and vector-valued quantities $\vec{L}_i$, a choice of operator $\mathcal{I}$ may be fixed. A Hamiltonian may be deduced by requiring that Eqs. (5.26) and (5.20), which are equivalent to the requirement that the operator $\mathcal{I}$ be an invariant, are satisfied at all time.

This can be done by rearranging Eqs. (5.20) and (5.26). Rearranging Eq. (5.26) gives

$$\mathcal{M}_i = -Y_i^{-1}\left(\ddot{Y}_i + \sum_{j\neq i}\frac{Y_j D[i,j]}{m_i}\right), \tag{5.27}$$

which allows for the straightforward determination of the quadratic parts of the trapping potential $\mathcal{M}_i$ in terms of the quantities Y_i.

Having determined the quadratic parts of the trapping potential $\mathcal{M}_i$, it is possible to deduce the trap displacement terms $\vec{\mathcal{F}}_i$. Rearranging (5.20) gives

$$\vec{\mathcal{F}}_i = m_i\ddot{\vec{L}}_i + m_i\mathcal{M}_i\vec{L}_i + \sum_{j\neq i} D[i,j]\vec{L}_j, \tag{5.28}$$

which completes the derivation of the quadratic parts of the trapping potential $\mathcal{M}_i$ and the trap displacement terms $\vec{\mathcal{F}}_i$ which characterise the Hamiltonian H.

5.6.1 Matrix polar decomposition of Y_i

Unfortunately, the determination of the quadratic parts of the trapping potential $\mathcal{M}_i$ using Eq. (5.27) is not guaranteed to ensure that the quadratic parts of the trapping potential $\mathcal{M}_i$ are Hermitian, as they ought to be. A similar issue was encountered in Ch. 3 and tackled in Sec. 3.3.1 by employing a matrix polar decomposition for P. Similarly, by performing a matrix polar decomposition for the matrices Y_i, it is possible to derive equations in terms of new quantities that ensure that the resulting quadratic parts of the trapping potentials $\mathcal{M}_i$ obtained via inverse engineering are Hermitian.

The matrix polar decompositions read

$$Y_i = U_i R_i, \tag{5.29}$$

where the matrices U_i are unitary and the matrices R_i are positive.

The matrix valued quantities Y_i satisfy Eq. (5.26). Expressing Eq. (5.26) in terms of this decomposition will lead to equations involving the unitary matrices U_i and the positive matrices R_i that are amenable to inverse engineering. Substituting Eq. (5.29) into (5.26) yields

$$\ddot{U}_i R_i + 2\dot{U}_i \dot{R}_i + U_i \ddot{R}_i + U_i R_i \mathcal{M}_i = -\sum_{j \neq i} \frac{U_j R_j D[i,j]}{m_i}. \tag{5.30}$$

It will prove useful, just as in Sec. 3.3.2, to introduce the anti-Hermitian matrices

$$A_i = U_i^\dagger \dot{U}_i. \tag{5.31}$$

Eq. (5.30) may be expressed in terms of the anti-Hermitian matrices A_i. Premultiplying both sides of Eq. (5.30) by the unitary matrix $U_i^\dagger$ gives

$$U_i^\dagger \ddot{U}_i R_i + 2U_i^\dagger \dot{U}_i \dot{R}_i + \ddot{R}_i + R_i \mathcal{M}_i = -\sum_{j \neq i} \frac{U_i^\dagger U_j R_j D[i,j]}{m_i}, \tag{5.32}$$

into which the quantities A_i and $\dot{A}_i$ may be substituted. Substituting Eq. (5.31) in Eq. (5.32) gives

$$\dot{A}_i R_i + A_i^2 R_i + 2A_i \dot{R}_i + \ddot{R}_i + R_i \mathcal{M}_i = -\sum_{j \neq i} \frac{U_i^\dagger U_j R_j D[i,j]}{m_i}. \tag{5.33}$$

The left hand side of Eq. (5.33) is defined in terms of the positive matrix valued quantities R_i and their time derivatives $\dot{R}_i$ and $\ddot{R}_i$, and the anti-Hermitian matrix A_i and its time derivative $\dot{A}_i$. By taking the Hermitian conjugate of this equation, one can obtain another relation between the quantities R_i, and their derivatives that will assist in ensuring that the determination of the quadratic parts of the trapping potentials $\mathcal{M}_i$ gives that they are Hermitian.

It will prove helpful to premultiply Eq. (5.33) by R_i before taking the Hermitian conjugate. This yields

$$R_i\dot{A}_iR_i + R_iA_i^2R_i + 2R_iA_i\dot{R}_i + R_i\ddot{R}_i + R_i^2\mathcal{M}_i = -\sum_{j\neq i}\frac{R_iU_i^\dagger U_jR_jD[i,j]}{m_i}. \tag{5.34}$$

Taking the Hermitian conjugate of Eq. (5.34) gives

$$-R_i\dot{A}_iR_i + R_iA_i^2R_i - 2\dot{R}_iA_iR_i + \ddot{R}_iR_i + \mathcal{M}_iR_i^2 = -\sum_{j\neq i}\frac{D[i,j]R_jU_j^\dagger U_iR_i}{m_i}. \tag{5.35}$$

Eqs. (5.34) and (5.35) both involve the quantities A_i and $\dot{A}_i$. By forming the sum of them, one can obtain an equation involving only the anti-Hermitian matrices A_i. Taking the difference leads to a useful expression for the quantities $\dot{A}_i$, which may be integrated.

The sum yields, after rearranging,

$$\{R_i,\ddot{R}_i\}+\{R_i^2,\mathcal{M}_i\} = 2[\dot{R}_i,R_i]_{A_i} - 2R_iA_i^2R_i - \sum_{j\neq i}\frac{D[i,j]R_jU_j^\dagger U_iR_i + R_iU_i^\dagger U_jR_jD[i,j]}{m_i}, \tag{5.36}$$

and the difference gives

$$2R_i\dot{A}_iR_i + 2\{R_i,\dot{R}_i\}_{A_i} + [R_i,\ddot{R}_i] + [R_i^2,\mathcal{M}_i] = \sum_{j\neq i}\frac{D[i,j]R_jU_j^\dagger U_iR_i - R_iU_i^\dagger U_jR_jD[i,j]}{m_i}. \tag{5.37}$$

Eq. (5.36) will sometimes be referred to as the *coupled matrix Ermakov equation*, as it reduces to the matrix Ermakov equation given in Eq. (3.22) in the case of a single ion $n = 1$.

Eq. (5.36) takes the form of a matrix anticommutator equation for the quadratic parts of the trapping potentials $\mathcal{M}_i$, which is to say that it can be solved to obtain the quadratic parts of the trapping potentials $\mathcal{M}_i$ using the results of Appendix A. However, the solutions depend on the quantities A_i which evolve over time in a manner consistent with Eq. (5.37).

By rearranging Eq. (5.37), it is possible to obtain an expression for the quantities $\dot{A}_i$ that gives rise to a system of differential equations that may be integrated to obtain the quadratic parts of the trapping potentials $\mathcal{M}_i$ entirely in terms of the positive matrix valued quantities R and

its time derivatives.

5.6.2 Inversion of the invariant

Eqs. (5.36) and (5.37) define a system of first order differential equations

$$\dot{U}_i = f(U_i, A_i), \tag{5.38}$$

$$\dot{A}_i = g(U_i, A_i). \tag{5.39}$$

Such a system of equations may be integrated, thus determining the unitary matrices U_i and antisymmetric matrices A_i in terms of the positive matrices R_i. The integration also determines the quadratic parts of the trapping potential $\mathcal{M}_i$ in a way that ensures that they are Hermitian.

The function $g(U_i, A_i)$ is difficult to write in closed form. An explicit procedure will be given instead that uses Eqs. (5.36) and (5.37) to determine the quantities $\dot{U}_i$ and $\dot{A}_i$ given the quantities U_i and A_i, which is the content of Eqs. (5.38) and (5.39).

First of all, rearranging the definition of A_i in Eq. (5.31) gives that

$$\dot{U}_i = U_i A_i, \tag{5.40}$$

allowing one to determine the matrices $\dot{U}_i$ from the unitary matrices U_i and antisymmetric matrices A_i via matrix multiplication.

The problem of determining the quantities $\dot{A}_i$ remains. This may be done by rearranging Eq. (5.37) to obtain,

$$\begin{aligned} \dot{A}_i &= -\{A_i, R_i^{-1}\}_{\dot{R}_i} - \frac{1}{2}[\ddot{R}_i, R_i^{-1}] - \frac{1}{2}[R_i, R_i^{-1}]_{\mathcal{M}_i} \\ &+ \frac{1}{2}\sum_{j\neq i} \frac{R_i^{-1} D[i,j] R_j U_j^\dagger U_i - U_i^\dagger U_j R_j D[i,j] R_i^{-1}}{m_i}. \end{aligned} \tag{5.41}$$

Eq. (5.41) can be used to obtain the quantities $\dot{A}_i$. However, it involves the quadratic parts of

the trapping potential $\mathcal{M}_i$. These may be determined by solving the matrix anticommutator equation in Eq. (5.36). Substituting them into Eq. (5.41) allows one to determine the quantities $\dot{A}_i$, completing the specification of the system of differential equations contained in Eq. (5.39).

This system of equations can be integrated. In doing so, the quadratic parts of the trapping potential $\mathcal{M}_i$, the unitary matrices U_i and the anti-Hermitian matrices A_i are determined, solely in terms of positive matrix valued quantities R_i and their time derivatives. As a result, it is possible to characterise the quadratic part of the invariant Γ entirely in terms of the positive matrix valued quantities R_i instead of the complex matrix valued quantities Y_i. The quantities Y_i may be obtained from the positive matrix valued quantities R_i simply by integrating to obtain the unitary matrices U_i and evaluating the matrix polar decompositions in Eq. (5.29)

5.6.3 Numerical issues

Integrating the system of equations in Eq. (5.39) may be carried out using any standard numerical method, such as the classic Runge-Kutta method of order four [169]. There exists a subtlety in that this numerical integration is not guaranteed to determine that the matrices U_i are exactly unitary as required at every time step. Over time, the matrices U_i could drift and become highly non-unitary, which would be unlikely to lead to sensible numerical results.

There are various ways of dealing with this issue. There exist *unitary* numerical integrators [170] that ensure that numerical integration of the system

$$\dot{V}(t) = V(t)S(t), \tag{5.42}$$

where the matrix $S(t)$ is anti-Hermitian, produces solutions $V(t)$ that are unitary at every time step. The Gauss-Legendre methods [171] are unitary integrators [170].

It is plausible that using a unitary integrator [170] such as one of the Gauss-Legendre methods would preserve the unitarity of the matrices U_i at each time step, considering that Eq. (5.40) is of the form given in Eq. (5.42). However, the analysis is complicated by the fact that the

system of differential equations in Eq. (5.39) involves integrating the anti-Hermitian matrices A_i in conjunction with the unitary matrices U_i, and the computational cost of the Gauss-Legendre methods is considerably higher given that they are implicit methods that require the solution of a set of nonlinear algebraic equations at each time step [171]. Alternatively, one can use any numerical integrator and project the matrices U_i onto the space of unitary matrices after each time step in the numerical integration [170]. However, this also adds overhead to the numerical integration.

5.6.4 Further issues in inverse engineering

Although the aforementioned numerical difficulties must be addressed, they do not present in principle an insurmountable barrier to inversion of the invariant. However, there exist other issues to deal with. It is not clear that the quadratic parts of the trapping potential $\mathcal{M}_i$ obtained via this procedure are real symmetric as required, though they are guaranteed to be Hermitian due to the fact that they are obtained by solving the matrix anticommutator equation in Eq. (5.36).

Nevertheless, it is plausible that the integration does yield that the quadratic parts of the trapping potential $\mathcal{M}_i$ are real. Some preliminary numerical investigations suggest that this is the case, though no proof exists yet. The proof techniques of Sec. 3.4, which prove that the quadratic part of the trapping potential M in the single-ion case is real, could be generalised to apply here.

Of greater concern is the fact that there does not seem to be any way to impose useful boundary conditions on the invariant $\mathcal{I}$. In order for the invariant $\mathcal{I}$ to be used to perform ground state to ground state transfer, it is necessary to impose that the invariant $\mathcal{I}$ and Hamiltonian H commute at initial time $t = 0$ and final time $t = T$. As discussed in Sec. 3.6, this is achieved when the time derivative of the quantum invariant $\dot{\mathcal{I}}$ vanishes at initial time $t = 0$ and final time $t = T$.

The present quantum invariant $\mathcal{I}$ is a function not only of the positive matrix valued quantities

R_i, the vector-valued quantities $\vec{L}_i$, and their time derivatives, but also the unitary matrices U_i and the anti-Hermitian matrices A_i that are obtained by integrating the system of differential equations in Eqs. (5.38) and (5.39), which is to say that

$$\mathcal{I} = g(U_i, A_i, R_i, \dot{R}_i, \vec{L}_i, \dot{\vec{L}}_i). \tag{5.43}$$

The time derivative of the invariant $\dot{\mathcal{I}}$ vanishes if the quantities $\dot{U}_i$, $\dot{A}_i$, $\dot{R}_i$, $\ddot{R}_i$, $\dot{\vec{L}}_i$ and $\ddot{\vec{L}}_i$ all vanish, via the chain rule. Since the unitary matrices U_i are obtained via numerical integration of the system of differential equations in Eq. (5.39), it is very difficult to see how to ensure that the time derivatives of the unitaries $\dot{U}_i$ vanish at final time $t = T$.

As a result, it is not possible to ensure that the Hamiltonian H and invariant $\mathcal{I}$ commute at final time $t = T$, which means that it is not possible to establish the precepts of invariant-based inverse engineering. Unless a way can be found to surmount this obstacle, it is not possible to employ this invariant $\mathcal{I}$ to carry out invariant-based inverse engineering. However, there exists a simplified physical regime in which invariant-based inverse engineering becomes possible, which I will now outline.

5.7 Symmetric trapping potentials

Without a procedure to fix the boundary conditions of the invariant $\mathcal{I}$, it is not possible to use it to perform useful invariant-based inverse engineering. In this section, I will demonstrate that imposing the requirement that the quadratic parts of the trapping potentials $\mathcal{M}_i$ are equal results in a practical inverse engineering procedure, and discuss its limitations.

Under the assumption that the $\mathcal{M}_i$ are all equal, a much simpler inversion procedure results in which it is no longer necessary to carry out any numerical integration. Concretely, the analysis will be limited to the case of two ions $n = 2$ from now on and it is imposed that $\mathcal{M}_1 = \mathcal{M}_2$. Both $\mathcal{M}_1$ and $\mathcal{M}_2$ will be denoted as $\mathcal{M}$, and since there is only one coupling constant $D[1, 2]$, the indexing will be omitted altogether in favour of D.

These assumptions allow for considerable simplifications to be made. Eq. (5.26) now yields,

$$\ddot{Y}_1 + Y_1\mathcal{M} = -\frac{Y_2 D}{m_1}, \tag{5.44}$$

$$\ddot{Y}_2 + Y_2\mathcal{M} = -\frac{Y_1 D}{m_2}. \tag{5.45}$$

Eqs. (5.44) and (5.45) are similar in form. By choosing the matrix valued quantities Y_1 and Y_2 appropriately, Eqs. (5.44) and (5.45) reduce to a single equation which will prove much easier to manipulate. The choice is made that

$$Y = \sqrt{m_1}Y_1 = \sqrt{m_2}Y_2. \tag{5.46}$$

Eqs. (5.44) and (5.45) then both reduce to

$$\ddot{Y} + Y\left(\mathcal{M} + \frac{D}{\sqrt{m_1 m_2}}\right) = 0. \tag{5.47}$$

For convenience, the scaled coupling term will be introduced

$$\mathcal{D} = \frac{D}{\sqrt{m_1 m_2}}. \tag{5.48}$$

The invariant $\mathcal{I}$ is characterised by the quantities U_1, U_2, R_1 and R_2 that form the matrix polar decompositions of the matrix valued quantities Y_1 and Y_2, as discussed in Sec. 5.6. As the quantities Y_1 and Y_2 are related to the quantity Y via Eq. (5.46), it is possible to express the quantities U_1, U_2, R_1 and R_2 in terms of the matrix polar decomposition of Y, which allows for further simplifications to be made. Writing

$$Y = UR, \tag{5.49}$$

for the matrix polar decomposition of the quantity Y, one gets by comparing decompositions that

$$R = \sqrt{m_1}R_1 = \sqrt{m_2}R_2, \tag{5.50}$$

and

$$U = U_1 = U_2. \tag{5.51}$$

Eqs. (5.36) and (5.37) govern the evolution of the quantities U_1, U_2, R_1 and R_2. They may be written in terms of the unitary matrix U and positive matrix R by substituting Eqs. (5.50) and (5.51), which yields, after simplification,

$$\{\ddot{R}, R\} + \{R^2, \mathcal{M} + \mathcal{D}\} = 2[\dot{R}, R]_A - 2RA^2R. \tag{5.52}$$

and

$$\frac{d}{dt}RAR = \frac{1}{2}\left([\ddot{R}, R] + [\mathcal{M} + \mathcal{D}, R^2]\right) \ . \tag{5.53}$$

These equations have already been encountered during the derivation of the single ion invariant in Ch. 3. Eq. (5.52) is the matrix Ermakov equation defined in Eq. (3.22) identifying the quadratic part of the trapping potential M with the term $\mathcal{M} + \mathcal{D}$, and Eq. (5.53) is Eq. (3.17) again having made the identification of the quadratic part of the trapping potential M with the term $\mathcal{M} + \mathcal{D}$.

As a result, from this point on, the analysis of Secs. 3.3 and 3.4 may be applied here, identifying the quadratic part of the trapping potential M with the term $\mathcal{M} + \mathcal{D}$ throughout. The term $\mathcal{M} + \mathcal{D}$ is guaranteed to be real symmetric by the results of Sec. 3.4. Both Eqs. (3.21) and (3.25) hold, which allows for the deduction of the term $\mathcal{M}+\mathcal{D}$ by substituting for the quantities R, $\dot{R}$ and $\ddot{R}$ in Eq. (5.52), and solving the matrix anticommutator equation to obtain the term $\mathcal{M} + \mathcal{D}$. One can then subtract off the coupling term $\mathcal{D}$ to finally obtain the quadratic part of the trapping potential $\mathcal{M}$ as required, which is guaranteed to be real symmetric. The trap displacement terms $\vec{\mathcal{F}}_1$ and $\vec{\mathcal{F}}_2$ may then be determined via substitution in Eq. (5.27), which completes the specification of the Hamiltonian.

5.7.1 Boundary conditions

Now that the invariant $\mathcal{I}$ can be inverse engineered to obtain Hamiltonians, it is necessary to address the boundary conditions that the invariant must satisfy.

In order for the ions to be transferred from their motional ground state at initial time $t = 0$ to their motional state $t = T$ at final time, the invariant $\mathcal{I}$ must commute with the Hamiltonian H at initial time $t = 0$ and final time $t = T$, as discussed in Sec. 2.5.2. As the invariant $\mathcal{I}$ satisfies the defining relation for a quantum invariant

$$\frac{\mathrm{d}\mathcal{I}(t)}{\mathrm{d}t} = i[\mathcal{I}(t), H(t)], \tag{5.54}$$

the Hamiltonian H and invariant $\mathcal{I}$ commute when the derivative of the invariant $\dot{\mathcal{I}}$ vanishes. As pointed out in Sec. 5.6.2, this is not straightforward to arrange in general. However, it is possible in the present case, as the invariant $\mathcal{I}$ can be written as a regular function of the quantities R_i and $\vec{L}_i$.

The invariant is characterised by the matrix-valued quantity Γ and the vector-valued quantity $\vec{Z}$. The quantity $\vec{Z}$ may already be written as a function of the trajectories $\vec{L}_i$ via Eq. (5.17). The quantity Γ may be evaluated by substituting the matrix polar decompositions $Y_1 = \sqrt{m_1}UR$ and $Y_2 = \sqrt{m_2}UR$ into Eqs. (5.21) and (5.22) to obtain

$$\Gamma = \begin{pmatrix} m_1\left(\dot{R}^2 + \mathcal{K}\right) & \sqrt{m_1 m_2}\left(\dot{R}^2 + \mathcal{K}\right) & \frac{\mathcal{J}-\{R,\dot{R}\}}{2} & \frac{\sqrt{m_1}\left(-\mathcal{J}-\{R,\dot{R}\}\right)}{2\sqrt{m_2}} \\ \sqrt{m_1 m_2}\left(\dot{R}^2 + \mathcal{K}\right) & m_2\left(\dot{R}^2 + \mathcal{K}\right) & \frac{\sqrt{m_2}\left(-\mathcal{J}-\{R,\dot{R}\}\right)}{2\sqrt{m_1}} & \frac{\mathcal{J}-\{R,\dot{R}\}}{2} \\ \frac{-\mathcal{J}-\{R,\dot{R}\}}{2} & \frac{\sqrt{m_2}\left(-\mathcal{J}-\{R,\dot{R}\}\right)}{2\sqrt{m_1}} & \frac{R^2}{m_1} & \frac{R^2}{\sqrt{m_1 m_2}} \\ \frac{\sqrt{m_1}\left(-\mathcal{J}-\{R,\dot{R}\}\right)}{2\sqrt{m_2}} & \frac{-\mathcal{J}-\{R,\dot{R}\}}{2} & \frac{R^2}{\sqrt{m_1 m_2}} & \frac{R^2}{m_2} \end{pmatrix}, \tag{5.55}$$

where

$$\mathcal{K} = \mathrm{Re}\left([\dot{R}, R]_A - RA^2R\right). \tag{5.56}$$

The unitary matrix U does not enter at all into Eq. (5.55), which expresses Γ entirely in terms of R and its time derivatives. Since the invariant may be thus be written in terms of the

quantities R and $\vec{L}_i$, and their time derivatives,

$$\mathcal{I} = f(R, \dot{R}, \vec{L}_i, \dot{\vec{L}}_i), \tag{5.57}$$

the derivative of the invariant vanishes when $\dot{R}$, $\ddot{R}$, $\dot{\vec{L}}_i$ and $\ddot{\vec{L}}_i$ all vanish by the chain rule. As a result, it is required that $\dot{R}$,$\ddot{R}$, $\dot{\vec{L}}_i$ and $\ddot{\vec{L}}_i$ all vanish at initial time $t = 0$ and final time $t = T$.

The initial and final Hamiltonians $H(0)$ and $H(T)$ are fixed by the choice of problem at hand, which is to say that the quantities $\mathcal{M}(0)$, $\mathcal{M}(T)$, $\vec{\mathcal{F}}_i(0)$ and $\vec{\mathcal{F}}_i(T)$ are fixed.

Eqs. (5.20) and (5.52) must be satisfied at all times, including initial time $t = 0$ and $t = T$. By evaluating them at initial time $t = 0$ and final time $t = T$, an initial set of boundary conditions can be determined which involve the quantities R, $\vec{L}_1$ and $\vec{L}_2$.

Substituting into Eq. (5.20) gives that

$$\mathcal{M}\vec{L}_2 = \vec{\mathcal{F}}_2 - D\vec{L}_1. \tag{5.58}$$

and

$$\mathcal{M}\vec{L}_1 = \vec{\mathcal{F}}_1 - D\vec{L}_2. \tag{5.59}$$

Substituting into Eq. (5.52) gives that

$$R = (\mathcal{M} + \mathcal{D})^{-\frac{1}{4}}. \tag{5.60}$$

Eqs. (5.58)-(5.60) must be satisfied at initial time $t = 0$ and final time $t = T$.

Interpolating the quantities R and $\vec{L}_i$ between these boundary conditions at initial and final times gives a valid choice of invariant for inverse engineering.

5.7.2 Degeneracy of the invariant

Although this scheme for inverse engineering satisfies the necessary boundary conditions, it does not perform true ground-state to ground state transfer. As discussed in Sec. 2.5.2, a requirement of any invariant used to perform ground state to ground state transfer is that it has a non-degenerate ground state.

Unfortunately, the expression given for Γ in Eq. (5.55) is not invertible, as the columns of the matrix Γ are not linearly independent. For example, the second column of the matrix Γ is proportional to the first column. This means that the ground state of the invariant is degenerate. As a result, the Hamiltonians derived via inverse engineering of this invariant are not guaranteed to achieve full ground state to ground state transfer. However, as will be seen in the next chapter, it is possible to quantify their performance numerically.

Chapter 6

Ion separation

6.1 Introduction

Separating trapped ions is a key challenge to be overcome in scalable trapped ion quantum computing, as discussed in Sec. 2.2.2. In this chapter, I will demonstrate how the invariant derived in Ch. 5 may be used to separate trapped ions, by means of an explicit demonstration with experimental relevance. Two trapped ions are separated in the plane to model the separation of ions in a X-junction trap.

This chapter is based on work to be published in [2].

6.2 Motivation and formulation of problem

As discussed in Sec. 2.2.2, the separation of trapped ions is an important task that must be implemented during the operation of a QCCD. Most theoretical [81] and experimental [106] investigations have to date focused on the separation of ions in a linear trap, in which only one motional mode is considered.

Using the results of Ch. 5, it is possible to construct ion separation protocols that work in more than one spatial dimension. I present here a demonstration of ion shuttling in the plane. As

in Ch. 4, the choice of $d = 2$ dimensions is made to illustrate the ability to control the ions in more than one spatial dimension, while making it easy to visualise the dynamics at hand.

The problem of ion separation involves the determination of Hamiltonians $H(t)$ that interpolate an initial Hamiltonian $H(0)$, corresponding to two ions trapped together, and a final Hamiltonian $H(T)$, corresponding to two ions that are well-separated in space. In order to do this, one must certainly specify the initial Hamiltonian $H(0)$ and final Hamiltonian $H(T)$.

The ions are initially trapped together at the origin. Concretely,

$$H(0) = \sum_{i=1}^{2} \frac{\hat{\vec{p}}_i^{\,2}}{2m_i} + \frac{1}{2}\sum_{i=1}^{2} m_i \hat{\vec{x}}_i^{\,T} M_i(0) \hat{\vec{x}}_i + \frac{e^2}{4\pi\epsilon_0 |\hat{\vec{x}}_2 - \hat{\vec{x}}_1|}, \tag{6.1}$$

where

$$M_1(0) = M_2(0) = \begin{pmatrix} \omega_t^2 & 0 \\ 0 & \omega_r^2 \end{pmatrix}. \tag{6.2}$$

The transverse frequency ω_t and the radial frequency ω_r determine the shape of the initial trapping potential. The trap displacement terms $\vec{F}_i(0)$ all vanish to reflect the fact that the ions are trapped at the origin.

The final Hamiltonian $H(T)$ must correspond to ions that are well-separated in space, if the ions are indeed to be separated. The final Hamiltonian is

$$H(T) = \sum_{i=1}^{2} \frac{\hat{\vec{p}}_i^{\,2}}{2m_i} + \frac{1}{2}\sum_{i=1}^{2} m_i \hat{\vec{x}}_i^{\,T} M_i(T) \hat{\vec{x}}_i - \sum_{i=1}^{2} \vec{F}_i(T) \cdot \hat{\vec{x}}_i + \frac{e^2}{4\pi\epsilon_0 |\hat{\vec{x}}_2 - \hat{\vec{x}}_1|}, \tag{6.3}$$

where

$$M_1(T) = M_2(T) = \begin{pmatrix} \omega_r^2 & 0 \\ 0 & \omega_t^2 \end{pmatrix}, \tag{6.4}$$

$$\vec{F}_1(T) = \begin{pmatrix} \frac{r\omega_r^2}{m_1} \\ \frac{r\omega_t^2}{m_1} \end{pmatrix}, \tag{6.5}$$

and

$$\vec{F}_2(T) = \begin{pmatrix} -\frac{r\omega_r^2}{m_2} \\ \frac{r\omega_t^2}{m_2} \end{pmatrix}. \tag{6.6}$$

The roles of the transverse frequency ω_t and radial frequency ω_r are interchanged in the final quadratic parts of the trapping potentials $M_1(T)$ and $M_2(T)$, compared to the initial quadratic parts of the trapping potentials $M_1(0)$ and $M_2(0)$ in Eq. (6.2). This is to model the effect of a rotation of the trap by 90 degrees, in order to demonstrate the ability of the inverse engineering procedure to deliver trapping potentials that rotate non-trivially over time. The trap displacement terms $\vec{F}_1(T)$ and $\vec{F}_2(T)$ are chosen to ensure that the centres of the traps $C_i(T)$, which are given by

$$C_i(T) = \frac{1}{m_i} M_i(T)^{-1} \vec{F}_i(T), \tag{6.7}$$

are equal to

$$C_1(T) = \begin{pmatrix} r \\ r \end{pmatrix}, \tag{6.8}$$

and

$$C_2(T) = \begin{pmatrix} -r \\ r \end{pmatrix}, \tag{6.9}$$

which is to say that the ions are separated into distinct traps with a separation of $d = 2r$.

6.3 Choice of invariant

In this section, I will illustrate how to use the invariant-based inverse engineering scheme of 5.7 to inverse engineer Hamiltonians that carry out separation of trapped ions.

In order to use the invariant-based inverse engineering scheme of Sec. 5.7, it is imposed that $\mathcal{M}_1 = \mathcal{M}_2 = \mathcal{M}$ at all times. As detailed in Sec. 5.7, a Hamiltonian of the form may be inverse-engineered using an invariant $\mathcal{I}$ that is determined in terms of quantities R, $\vec{L}_1$ and $\vec{L}_2$ via Eqs. (5.13), (5.17) and (5.55).

The quantities $\vec{L}_1$, $\vec{L}_2$ and R that characterise the invariant $\mathcal{I}$ may be chosen freely as long as they satisfy the boundary conditions laid out in Sec. 5.7.1, namely that

$$R = (\mathcal{M} + \mathcal{D})^{-\frac{1}{4}}, \tag{6.10}$$

$$\mathcal{M}\vec{L}_1 = \vec{\mathcal{F}}_1 - D\vec{L}_2, \tag{6.11}$$

and

$$\mathcal{M}\vec{L}_2 = \vec{\mathcal{F}}_2 - D\vec{L}_1, \tag{6.12}$$

at initial time $t = 0$ and final time $t = T$, and that the first and second derivatives of the quantities $\vec{L}_1$, $\vec{L}_2$ and R all vanish.

Eqs. (6.10)-(6.12) relate the quantities $\vec{L}_1$, $\vec{L}_2$ and R that characterise the invariant $\mathcal{I}$ at initial and final time to the quantities $\mathcal{M}$, $\vec{\mathcal{F}}_1$ and $\vec{\mathcal{F}}_2$ that characterise the Hamiltonian H at initial and final time. The quantities $\mathcal{M}$, $\vec{\mathcal{F}}_1$ and $\vec{\mathcal{F}}_2$ are ultimately determined by the choices of initial and final Hamiltonian made in Sec. 6.2.

In order to interpolate the quantities $\vec{L}_1$, $\vec{L}_2$ and R, one must certainly needs to solve Eqs. (6.10)-(6.12) in order to determine their initial and final values. As the coupling constant D depends on $\vec{L}_1$ and $\vec{L}_2$ via Eq. (5.8), Eqs. (6.10)-(6.12) are non-linear.

Additionally, the first and second time derivatives of these quantities $\dot{R}$, $\ddot{R}$, $\dot{\vec{L}}_i$ and $\ddot{\vec{L}}_i$ must all vanish.

The quantities $\mathcal{M}$, $\vec{\mathcal{F}}_1$ and $\vec{\mathcal{F}}_2$ are determined at initial time $t = 0$ and final time $t = T$ by the initial and final Hamiltonians laid out in Sec. 6.2. Eqs. (6.10)-(6.12) may be solved numerically using a nonlinear solver such as differential evolution [172] to obtain values of $\vec{L}_1$, $\vec{L}_2$ and R that satisfy Eqs. (6.10)-(6.12).

The quantities $\vec{L}_1$, $\vec{L}_2$ and R must be interpolated between their initial and final values in such a way that their first and second derivatives vanish at initial time $t = 0$ and final time $t = T$ in order to complete the specification of the invariant $\mathcal{I}$.

Using again the polynomial introduced in Sec. 4.3.2,

$$p(\tau) = 10\tau^3 - 15\tau^4 + 6\tau^5, \tag{6.13}$$

where

$$\tau = \frac{t}{T}. \tag{6.14}$$

it is possible to construct simple expressions for the quantities $\vec{L}_1$, $\vec{L}_2$ and R that interpolate their initial and final values appropriately. I choose

$$R(t) = (1 - p(\tau))R(0) + p(\tau)R(T), \tag{6.15}$$

$$\vec{L}_1(t) = (1 - p(\tau))\vec{L}_1(0) + p(\tau)\vec{L}_1(T), \tag{6.16}$$

and

$$\vec{L}_2(t) = (1 - p(\tau))\vec{L}_2(0) + p(\tau)\vec{L}_2(T), \tag{6.17}$$

which completes the specification of the invariant $\mathcal{I}$.

Now that the invariant $\mathcal{I}$ has been chosen, the Hamiltonian H may be inverse engineered using the procedures outlined in Sec. 5.7, to obtain the quantities $\mathcal{M}$, $\vec{\mathcal{F}}_1$ and $\vec{\mathcal{F}}_2$. The quantities M_i and $\vec{F}_i$ that characterise the Hamiltonian may be determined via substitution into Eqs. (5.6) and (5.7).

6.4 Presentation of results

In this section, I will present some numerical demonstrations of the inverse engineering procedure set out in Secs. 6.3.

The numerical examples presented use the explicit choices

$$\omega_r = 10\omega_t, \tag{6.18}$$

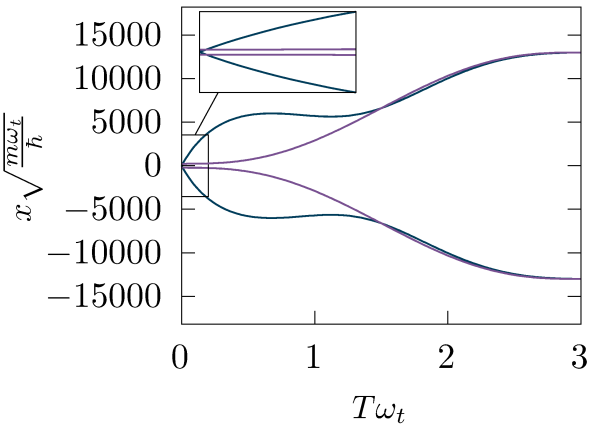

(a) $T = 3\omega_t^{-1}$

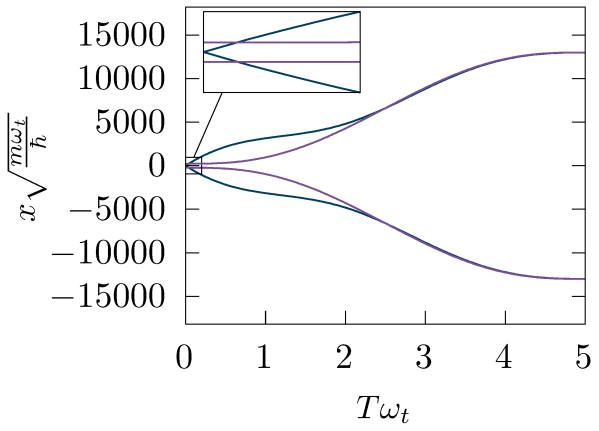

(b) $T = 5\omega_t^{-1}$

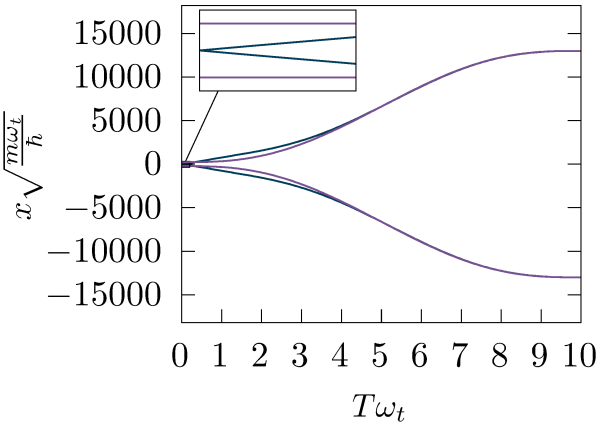

(c) $T = 10\omega_t^{-1}$

Figure 6.1: Separation of two ions in a T-junction. Inset (a) depicts a fast shuttling protocol, while inset (b) contains a slower shuttling protocol, and (c) contains a protocol that is slower still. The dynamics of the trap centres are depicted in blue, and the dynamics of the ions are in purple. The trap centres and ions deviate from each other, particularly for the faster protocols. Due to the Coulomb interaction, the ions start separated from each other and their positions do not coincide with the centre of the trap.

and

$$\omega_t = 2\pi \times 1\text{MHz}, \tag{6.19}$$

as these are typical values one would expect to encounter in an experimental ion trap.

The ions are separated into traps that lie a distance $d = 200\mu\text{m}$ from each other, at which point the Coulomb potential is negligible.

Fig. 6.1 illustrates some examples of the dynamics obtained for different values of the duration of the separation T. Inset (a) contains a fast separation protocol of duration $T = 3\omega_t^{-1}$, while

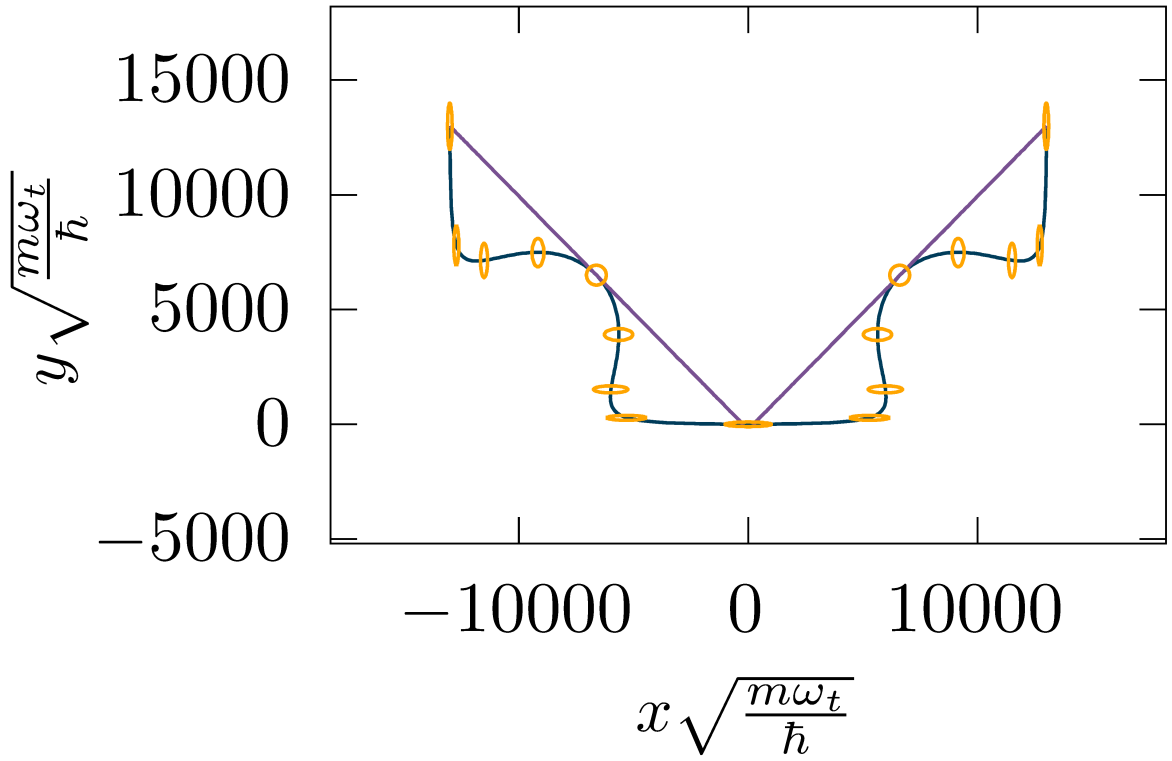

Figure 6.2: Two ions, initially trapped together in a T-junction, are separated into two distinct trapping locations at an angle of 90 degrees, over a duration $T = 3\omega_t^{-1}$. The trap centre trajectories, plotted here in purple and orange, have superimposed on them level sets of the trapping frequencies in light blue and dark blue. The ions themselves travel on straight line trajectories shown in green and purple.

the protocol in inset (b) is slower with duration $T = 5\omega_t^{-1}$ and that of inset (c) is slower still with duration $T = 10\omega_t^{-1}$. The trajectories of the ions are shown in purple, while the trajectories of the trap centres are shown in blue, each projected onto the x-axis. The protocol shown in inset (a) demonstrates significant deviation between the trajectories of the ions and the trap centres, which is symptomatic of diabatic dynamics. Accordingly, as the duration T is increased in insets (b) and (c), the trajectories of the ions and trap centres coincide more. However, they do not converge exactly, even in the limit of long times. Since the Coulomb interaction is significant at early times t while the ions are still close to each other, they are effectively held apart by their mutual Coulomb interaction and do not lie at the centre of their respective traps. This effect is not noticeable at the end of the separation procedure, as the Coulomb interaction is negligible when the ions are well-separated.

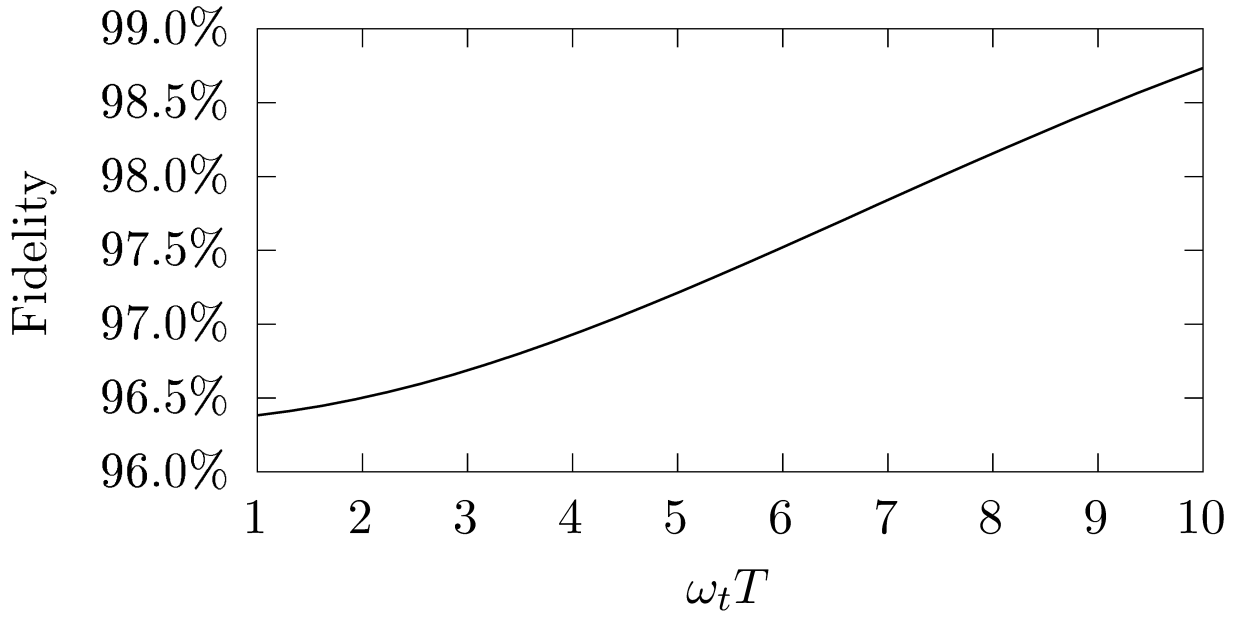

Figure 6.3: Fidelity of the ion separation protocol as a function of the duration T. High fidelities are obtained even for fast protocols with short durations T, in which ground state to ground state state transfer is not guaranteed.

Fig. 6.2 contains the dynamics of the ion and trap centre in the plane when the duration $T = 3\omega_t^{-1}$. The ion trajectories are shown in purple, while the trajectories of the trap centres are shown in blue. Level sets of the trapping potentials are depicted in orange, and characterise the shape of the trapping potential at equidistant times $t = jT/8$ with $j = 0, \ldots, 8$. As can be seen, the trapping potentials undergo some significant squeezing during the motion. The trajectory of the trap centre diverges from the trajectories of the ions which trace out straight lines in the plane.

As alluded to in Sec. 5.7.2, since the invariant $\mathcal{I}$ is degenerate, the Hamiltonian H is not guaranteed to achieve ground state to ground state transfer. Nevertheless, it is possible to quantify the efficacy of the Hamiltonian obtained via invariant-based inverse engineering by solving for the dynamics numerically. The Hamiltonian H obtained via inverse engineering is quadratic in position and momentum. As a result, the ground state of the initial Hamiltonian $H(0)$ is a Gaussian state. Since the Hamiltonian H is quadratic in position and momentum operators, the subsequent dynamics of the system remain Gaussian, and can be obtained by a relativly inexpensive numerical integration, as detailed in Sec. 2.4.1. Fig. 6.3 depicts the resulting fidelities between the motional state of the system at final time $t = T$ obtained

numerically and the ground state of the final Hamiltonian $H(T)$. The resulting fidelities exceed 96% for a wide range of durations T, including those in the diabatic regime, and increase as the duration T increases. In the limit of large times T, it is expected that the fidelity approaches 100%, as any slowly changing Hamiltonian $H(t)$ will transfer the ground state population of the initial Hamiltonian $H(0)$ to that of the final Hamiltonian $H(T)$ by the adiabatic theorem.

As the dynamics of the motional state of the ions are Gaussian, they are characterised by the covariance matrix Σ and the phase space expectation X. The covariance matrix Σ is visualised in Fig. 6.4, in the case that the duration T is equal to $3\omega_t^{-1}$. The initial covariance at time $t = 0$ is shown in inset (a), the covariance matrix halfway through the dynamics in inset (b), and at the end of the dynamics in inset (c). Inset (d) shows the covariance matrix of the true ground state of the Hamiltonian $H(T)$ at final time $t = T$.

The elements of the covariance matrices of the initial and final states of the system are determined by the shape of the initial trapping potential. In particular, the spatial uncertainty in the x-direction is larger than that in the y-direction for the initial covariance matrix, and reversed for the final covariance matrix. The initial covariance matrix in inset (a) has significant x_1-x_2 and p_{x_1}-p_{x_2} covariances owing to the presence of the Coulomb potential. The desired ground state of the final Hamiltonian $H(T)$ is diagonal as the ions are sufficiently well-separated for the Coulomb potential to be neglected.

The position-momentum correlations are non-negligible in inset (b), which is indicative of the fact that the ion is not at rest. The covariance matrices in insets (c) and (d) differ in some places, which accounts for the observed infidelities of the final motional state of the ions.

Fig. 6.5 shows the behaviour of some of the individual covariances of the dynamics. Inset (a) depicts the time-dependence of the p_{x_1}-p_{x_1} correlation. This correlation is non-vanishing at both the start and the end of the protocol. Over time, it develops some oscillations, and eventually settles on a much higher value than it had at the start of the protocol. Nevertheless, some deviation with the expected value is observed at the end of the protocol. Inset (b) depicts the time-dependence of the p_{x_1}-p_{x_2}-covariance. This value is expected to become negligible at the end of the separation procedure, as may be seen by inspecting Fig. 6.4. Physically, this is

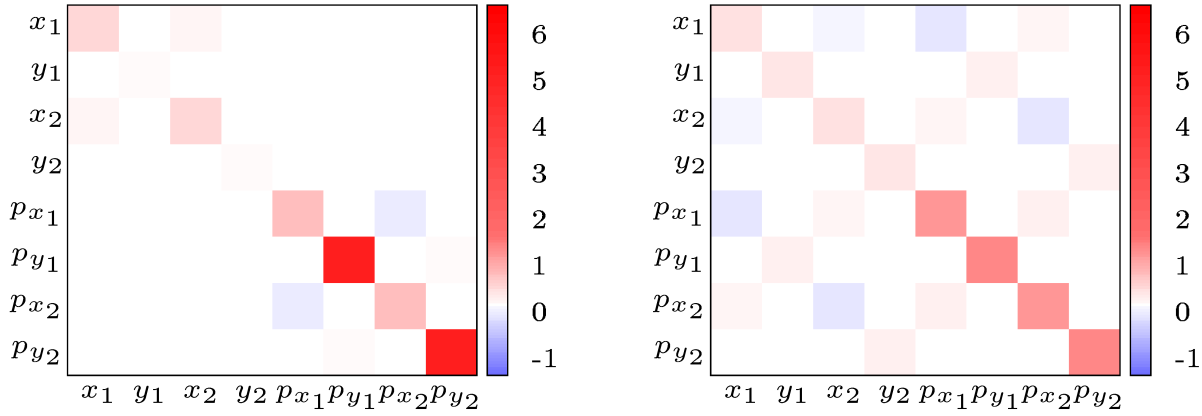

(a) $t = 0$

(b) $t = \frac{1}{2}T$

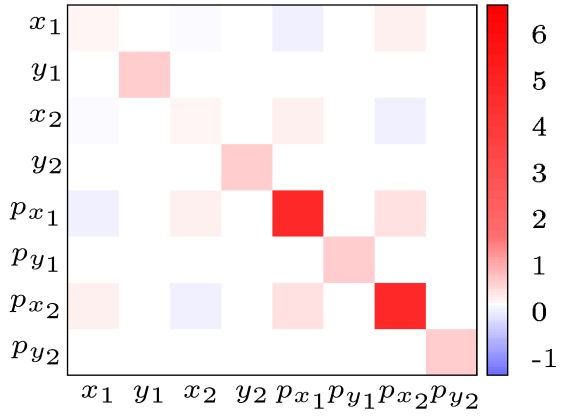

(c) $t = T$

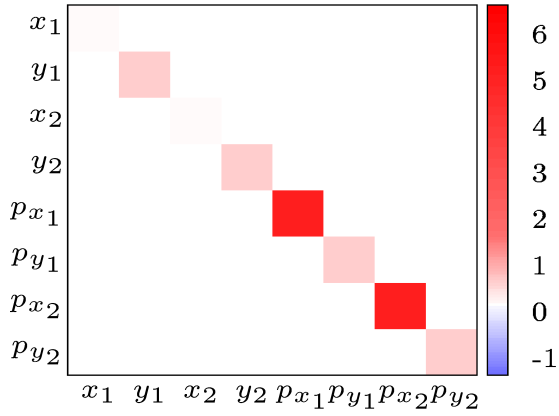

(d) Ground state at $t = T$

Figure 6.4: Covariance matrices Σ of the state of the system at different times of the fast shuttling protocol of duration $T = 3\omega_t^{-1}$. The individual matrix elements are displayed in harmonic oscillator units; the position-position correlations have the unit $m\hbar\omega_t$, the position-position correlations have the unit $\hbar/(m\omega_t)$, and the position-momentum correlations have the unit $\hbar$.

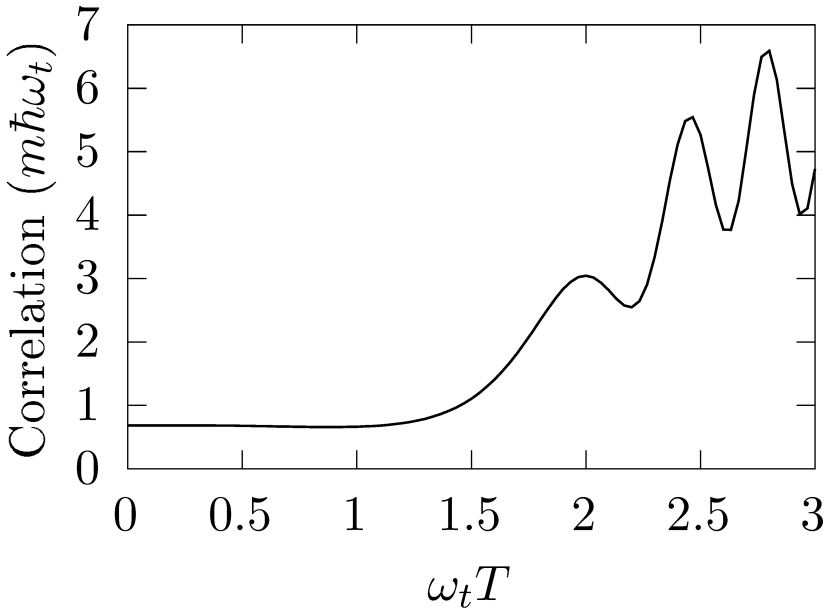

(a) $\Sigma_{p_{x_1}p_{x_1}}$

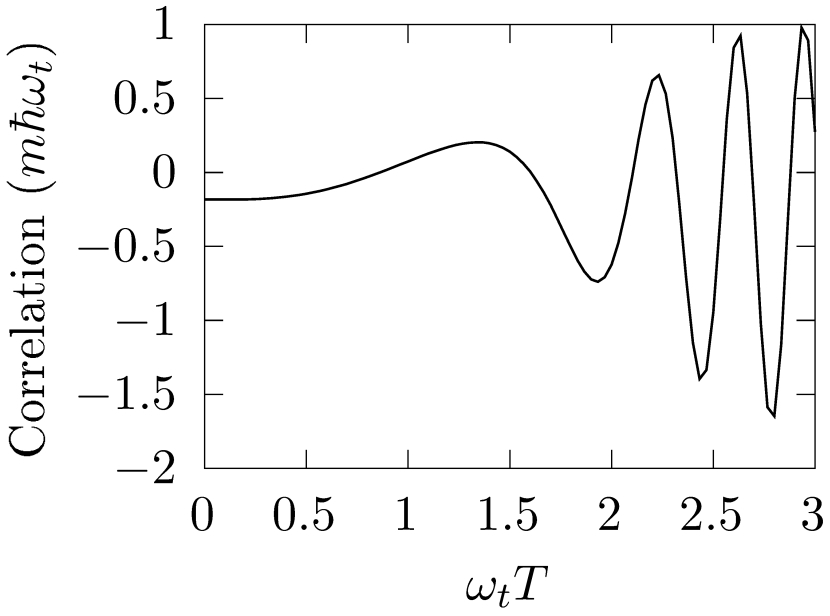

(b) $\Sigma_{p_{x_1}p_{x_2}}$

Figure 6.5: The p_{x_1}-p_{x_1} correlation (inset a) and the p_{x_1}-p_{x_2} correlation (inset b) for the fast shuttling protocol of duration $T = 3\omega_t^{-1}$. Both correlations undergo some oscillatory dynamics. Due to the degeneracy of the invariant, the p_{x_1}-p_{x_2} correlation does not vanish at final time T.

due to the fact at large ion separations the Coulomb potential is negligible and one may expect there to be no correlations between the two ions in their ground state. Nevertheless, as one can see from inset (b), some oscillations build up over time and at the end of the protocol, the covariance does not attain a value close to 0 as it should.

6.5 Outlook

The ion separation procedure presented here allows one to conclude several things about the efficacy of invariant-based inverse engineering to deal with more than one ion. Although the invariant $\mathcal{I}$ was constructed using simple functional forms for the quantities $\vec{L}_1$, $\vec{L}_2$ and R in Sec. 6.3, it still delivered high transfer fidelities in excess of 96%, even at fast times. Accordingly, one can conclude that the degeneracy of the ground state of the invariant used here need not pose a significant obstacle in general.

As in Ch. 4, the Hamiltonian presented here gives trap centre trajectories that are significantly different from the trajectories of the trapped ions. This suggests that invariant-based inverse engineering leads to non-obvious ion separation protocols that are not what one would take as a starting guess for Hamiltonians that realise ion separation. As a result, invariant-based inverse engineering is likely to be of use in designing experimental protocols.

As the covariance matrix of the motional state of the ions undergoes significant changes throughout the procedure, one concludes that invariant-based inverse engineering is capable of producing Hamiltonians that realise inherently quantum dynamics, which is of interest from a theoretical point of view, just as in Ch. 4.

Chapter 7

Beyond the harmonic approximation

7.1 Overview

The harmonic approximation, in which ion traps are assumed to be perfectly quadratic in position, has been essential in deriving invariant-based control techniques for trapped ions in Chs. 3 and 5. Although this approximation is often assumed to hold to a very high degree, there exist situations in which it may not. For example, as ion traps become smaller, anharmonic terms in the trapping potential are expected to become significant [173]. In such a situation, the anharmonic contributions to the trapping potential must be taken into account in designing ion shuttling and separation procedures.

A further assumption that has been made so far is that one has perfect control of the experimental apparatus. More concretely, I have assumed that it is possible to apply any desired trapping potential. Of course, this is not always a valid assumption in real-world experimental conditions. One is limited in the possible potentials that can be constructed by the finite precision of the voltages that end up being applied to the electrodes, and applied voltages in any case may always experience some fluctuating noise, or undergo some static drift over time. The effect of these phenomena is ultimately to introduce noise and imperfections into the trapping potential that an ion experiences. These can potentially destroy the efficacy of any invariant-based shuttling protocol that one constructs, so they must be considered when designing an

experimental implementation.

In this chapter, I outline a method that may be used to model the dynamical effects of noise and anharmonic contributions, using time-dependent perturbation theory. I explore its advantages and list further work that needs to be done in order to successfully implement it.

7.2 Statement of problem

As detailed in Sec. 7.1, I aim to work beyond the harmonic approximation. In this section, I explain how the invariants derived so far may be used to deal with dynamics beyond the harmonic approximation for a single ion using time-dependent perturbation theory.

There exist very many different anharmonic potentials and sources of noise that a trapped ion may experience. In order to deal with them in a general way, I write down the Hamiltonian

$$H = H_0 + V(\vec{x}, t) \tag{7.1}$$

where the Hamiltonian H_0 is quadratic and of the form given in Eq. (3.1). The potential term V contains terms that are higher than quadratic in the position term $\vec{x}$, and any noise terms that are due to imperfection of implementation of the experimental controls.

As the Hamiltonian H_0 is quadratic, it may be determined using the invariant-based engineering as detailed in Ch. 3. Given a choice of initial and final Hamiltonian $H_0(0)$ and $H_0(T)$, that correspond to idealised quadratic trapping potentials, I assume that a choice of appropriate invariant $\mathcal{I}$, as specified in Ch. 3 has been selected and the Hamiltonian $H_0(t)$ obtained for all values of t between 0 and T.

In the case that the potential term V vanishes, one recovers the results of Ch. 3, in which the ion is transferred to the ground state of the final Hamiltonian $H(T)$ at the end of the motion. In the case that the potential term V does not vanish, this no longer holds. The dynamics must be obtained by simulating the true dynamics under the time evolution of H.

I assume further that the magnitude of the potential term V is small compared to the quadratic part of the trapping potential H_0. This certainly holds in the limit of weak noise, and assuming that any anharmonicities are not too large. Such a condition is the quantitative justification for the validity of a perturbative treatment, in which the dynamics under the full Hamiltonian H are derived in terms of those under H_0, treating the potential term V as a perturbation.

In order to carry out a perturbative treatment, it is usually required that the eigenstates and eigenvalues of the unperturbed Hamiltonian H_0 are known. However, as in this case H_0 is free to vary in time, the requirements are somewhat more stringent. The perturbative solution of the dynamics under the full Hamiltonian H requires the solutions of the Schrödinger equation for H_0. These are in general difficult to determine for a time-dependent system. However, one is greatly aided by the fact that one has access to a quantum invariant $\mathcal{I}$ that corresponds to H_0. As the eigenstates of the invariant $\mathcal{I}$ may be chosen to be solutions of the Schrödinger equation for H_0, as detailed in Sec. 2.5.1, the perturbative treatment may be carried out in terms of the eigenstates of the invariant $\mathcal{I}$.

7.3 Time-dependent perturbation theory

In this section I will detail how to employ time-dependent perturbation theory to determine the dynamics of the full Hamiltonian H, and illustrate how they relate to the invariant $\mathcal{I}$.

First of all, it is necessary to derive the dynamics under the Hamiltonian H_0. As detailed in Sec. 2.5.1, the eigenstates of the invariant $\mathcal{I}$ may be chosen to satisfy the Schrödinger equation for H_0. One writes

$$\mathcal{I}(t)\,|\chi_i\rangle = \lambda_i\,|\chi_i\rangle \tag{7.2}$$

for the eigenstates $|\chi_i\rangle$ of the invariant $\mathcal{I}$, and they satisfy the Schrödinger equation for H_0

$$i\frac{\mathrm{d}}{\mathrm{d}t}\,|\chi_i\rangle = H_0\,|\chi_i\rangle\,. \tag{7.3}$$

As is typical of time-dependent perturbation theory, I choose as an ansatz for the solution of

the dynamics under the full Hamiltonian H,

$$|\psi\rangle = \sum_i c_i(t)\,|\chi_i\rangle \tag{7.4}$$

where the coefficients c_i vary in time. Since the states $|\chi_i\rangle$ form an eigenbasis of the invariant $\mathcal{I}$, they are complete. As a result, the right hand side of Eq. (7.4) can express any desired state $|\psi\rangle$, which is to say that one has lost no generality in taking Eq. (7.4) as an expression for the true dynamics of the system $|\psi\rangle$.

The state $|\psi\rangle$ must satisfy the time-dependent Schrödinger equation for H,

$$i\frac{\mathrm{d}}{\mathrm{d}t}\,|\psi\rangle = H_0\,|\psi\rangle + V\,|\psi\rangle\,. \tag{7.5}$$

By substituting Eq. (7.4) into Eq. (7.5), one can obtain conditions on the coefficients c_i that ensure that Eq. (7.5) is satisfied. One gets that

$$\sum_i ic_i(t)\frac{\mathrm{d}}{\mathrm{d}t}\,|\chi_i\rangle + i\dot{c}_i(t)\,|\chi_i\rangle = \sum_i c_i(t)H_0(t)\,|\chi_i\rangle + c_i(t)V\,|\chi_i\rangle\,. \tag{7.6}$$

As the eigenstates $|\chi_i\rangle$ satisfy Eq. (7.3), a great simplification may be made. Both sides of Eq. (7.3) may be eliminated from Eq. (7.6) to obtain

$$\sum_i i\dot{c}_i(t)\,|\chi_i\rangle = \sum_i c_i(t)V\,|\chi_i\rangle\,. \tag{7.7}$$

By taking the inner product of Eq. (7.7) with the state $\langle\chi_j|$, one may obtain a set of first-order differential equations for the coefficients c_i,

$$i\dot{c}_j(t) = \sum_i c_i(t)\,\langle\chi_j|V|\chi_i\rangle\,. \tag{7.8}$$

Up until this point, no approximations have been made, which is to say that any solution of Eq. (7.8) gives rise to an exact solution of Eq. (7.5). Eq. (7.8) may be integrated numerically

by truncating the sum at a suitably large cutoff. In such a way, one can obtain a numerical solution to Eq. (7.5) simply by integrating Eq. (7.8) to obtain the coefficients c_i. This presents much less difficulty than solving the time-dependent Schrödinger equation numerically directly, as it is a partial differential equation.

7.4 Eigenstates of the quantum invariant

In order to perform the integration of Eq. (7.8), one must calculate the matrix elements $\langle\chi_j|V|\chi_i\rangle$. Such a calculation requires the determination of the eigenstates $|\chi_j\rangle$ of the invariant $\mathcal{I}$. In this section, I will present a method by which the eigenstates $|\chi_j\rangle$ may be obtained.

The invariant $\mathcal{I}$ defined in Eq. (3.5) reads

$$\mathcal{I} = \frac{1}{2}X^T\Gamma X + \vec{W}\cdot X + \theta. \tag{7.9}$$

The invariant $\mathcal{I}$ contains many terms of Lorentz form $\hat{x}_i\hat{p}_i+\hat{p}_i\hat{x}_i$, and terms linear in momentum p_i. As such, it is not clear how to diagonalise it to obtain the eigenstates $|\chi_j\rangle$, despite the fact that it is quadratic in position and momentum operators.

In contrast to the invariant $\mathcal{I}$, the Hamiltonian of the isotropic harmonic oscillator

$$\frac{1}{2}X^TX = \sum_{i=1}^{d}\frac{\hat{x}_i^2+\hat{p}_i^2}{2}, \tag{7.10}$$

being a sum of d independent one-dimensional harmonic oscillators, has a well-known basis [174] in terms of Fock states,

$$\frac{1}{2}X^TX\,|n_1,...,n_d\rangle = \left(n_1+...+n_d+\frac{d}{2}\right)|n_1,...,n_d\rangle\,. \tag{7.11}$$

There exists a way to relate the invariant $\mathcal{I}$ to the Hamiltonian of the isotropic harmonic oscillator $\frac{1}{2}X^TX$ that allows for the determination of the eigenstates $|\chi_j\rangle$ of the invariant $\mathcal{I}$ in terms of those of the isotropic harmonic oscillator.

Concretely, there exists a unitary operator T such that

$$T\mathcal{I}T^{\dagger} = \frac{1}{2}X^{T}X. \tag{7.12}$$

The unitary transformation in Eq. (7.12) defined using the unitary operator T has the effect of removing terms of Lorentz form such as $\hat{x}_i\hat{p}_i + \hat{p}_i\hat{x}_i$ and terms linear in momentum p_i from the invariant $\mathcal{I}$ to yield the isotropic harmonic oscillator $\frac{1}{2}X^{T}X$. As the eigenstates of the isotropic harmonic oscillator are given in Eq. (7.11), it is possible to obtain the eigenstates $|\chi_j\rangle$ of the invariant $\mathcal{I}$ also by means of a unitary transformation.

Operating on both sides of Eq. (7.11) with the operator $T^{\dagger}$ gives

$$\frac{1}{2}T^{\dagger}X^{T}X\left|n_1,...,n_d\right\rangle = \left(n_1 + ... + n_d + \frac{d}{2}\right)T^{\dagger}\left|n_1,...,n_d\right\rangle, \tag{7.13}$$

while operating on both sides of Eq. (7.12) with the operator $T^{\dagger}$ yields

$$\mathcal{I}T^{\dagger} = \frac{1}{2}T^{\dagger}X^{T}X. \tag{7.14}$$

Substituting for the term $\frac{1}{2}T^{\dagger}X^{T}X$ in Eq. (7.13) using Eq. (7.14) gives

$$\mathcal{I}T^{\dagger}\left|n_1,...,n_d\right\rangle = \left(n_1 + ... + n_d + \frac{d}{2}\right)T^{\dagger}\left|n_1,...,n_d\right\rangle, \tag{7.15}$$

which is to say that the eigenstates $|\chi_j\rangle$ of the invariant $\mathcal{I}$ are given precisely by the expression $T^{\dagger}\left|n_1,...,n_d\right\rangle$.

7.5 Proof of validity of the unitary transformation

In this section, I will present the form of the unitary operator T, and prove that it satisfies Eq. (7.12).

The unitary operator T is given by

$$T = U_3 U_2 U_1, \tag{7.16}$$

where

$$U_3 = \exp\left(\frac{i}{2} \hat{X}^T \begin{bmatrix} 0 & \log \frac{R}{\sqrt{m}} \\ \log \frac{R}{\sqrt{m}} & 0 \end{bmatrix} \hat{X} \right), \tag{7.17}$$

$$U_2 = \exp\left(-\frac{im}{4} \vec{\hat{x}}^T (R^{-2}\mathcal{J} + R^{-1}\dot{R} + R^{-2}\dot{R}R)\vec{\hat{x}} \right), \tag{7.18}$$

and

$$U_1 = \exp\left(i\vec{L} \cdot \vec{\hat{p}} - im\dot{\vec{L}} \cdot \vec{\hat{x}} \right). \tag{7.19}$$

In order to show that the unitary operator T satisfies Eq. (7.12), it is necessary to evaluate the quantity $T\mathcal{I}T^\dagger$ that appears on the left hand side of Eq. (7.12).

This quantity reads, in terms of the U_i,

$$T\mathcal{I}T^\dagger = U_3 U_2 U_1 \mathcal{I} U_1^\dagger U_2^\dagger U_3^\dagger. \tag{7.20}$$

The right hand side of Eq. (7.20) may be evaluated more easily by introducing additional quantities. Defining

$$\mathcal{I}_1 = U_1 \mathcal{I} U_1^\dagger, \tag{7.21}$$

$$\mathcal{I}_2 = U_2 \mathcal{I}_1 U_2^\dagger, \tag{7.22}$$

$$\mathcal{I}_3 = U_3 \mathcal{I}_2 U_3^\dagger, \tag{7.23}$$

one obtains that $T\mathcal{I}T^\dagger = \mathcal{I}_3$. In order to show that Eq. (7.12) is satisfied, it is necessary to show that

$$\mathcal{I}_3 = \frac{1}{2} X^T X. \tag{7.24}$$

7.5.1 Matrix lemmas

In order to show that Eq. (7.12) is satisfied, some useful lemmas must be first introduced.

The identities

$$e^{A}Be^{-A} = B + [A,B] + \frac{1}{2!}[A,[A,B]] + ..., \tag{7.25}$$

$$e^{A}Be^{A} = B + \{A,B\} + \frac{1}{2!}\{A,\{A,B\}\} + ..., \tag{7.26}$$

hold [175], which may be shown by performing series expansions of the exponentials that appear in the left hand sides of Eqs. (7.25) and (7.26) and comparing the results with the right hand sides of Eqs. (7.25) and (7.26).

In the case that the operators A and B are quadratic forms in X, Eq. (7.25) may be reduced to a useful form in terms of an infinite sum. One obtains

$$e^{-\frac{i}{2}X^{T}CX}X^{T}DXe^{\frac{i}{2}X^{T}CX} = X^{T}\left(\sum_{n=0}^{\infty}\frac{M_n}{n!}\right)X, \tag{7.27}$$

where the matrices M_n are defined inductively as

$$M_0 = D, \tag{7.28}$$

$$M_n = CSM_{n-1} - M_{n-1}SC. \tag{7.29}$$

7.5.2 Computation of the transformed invariant $\mathcal{I}_1$

I start by using the form of the invariant given in Eq. (3.58),

$$\mathcal{I} = \frac{1}{2}(X-\vec{Z})^{T}\Gamma(X-\vec{Z}). \tag{7.30}$$

In order to bring the invariant to the form of an isotropic harmonic oscillator, in accordance with Eq. (7.12), the linear and scalar terms in $\mathcal{I}$ must certainly be removed. This can be done using a displacement operator.

The operator U_1 takes the form

$$U_1 = \exp\Big(iQ \cdot \hat{X}\Big). \tag{7.31}$$

By choosing the vector Q appropriately, it is possible to ensure that the transformed invariant $\mathcal{I}_1 = U_1 \mathcal{I} U_1^\dagger$ has no scalar or linear terms.

In order to compute the transformed invariant $\mathcal{I}_1$, it is simplest to compute the effect of the unitary operator U_1 on the phase space operator $\hat{X}$. This can be done by applying Eq. (7.25), with $A = iQ \cdot \hat{X}$ and $B = \hat{X}$ to give that

$$U_1 \hat{X} U_1^\dagger = \hat{X} + \mathcal{S}Q, \tag{7.32}$$

as all higher order terms in the expansion given in Eq. (7.25) vanish.

The transformed invariant $\mathcal{I}_1$ may now be computed to get

$$\mathcal{I}_1 = \frac{1}{2}(X - \vec{Z} + \mathcal{S}Q)^T \Gamma (X - \vec{Z} + \mathcal{S}Q). \tag{7.33}$$

It may be seen directly that if $\vec{Z} = \mathcal{S}Q$, then $\mathcal{I}_1$ will contain no linear or scalar terms as desired. Rearranging gives that $Q = -\mathcal{S}\vec{Z}$, which is to say that

$$Q = \begin{pmatrix} -m\dot{\vec{L}} \\ \vec{L} \end{pmatrix}, \tag{7.34}$$

giving finally that

$$U_1 = \exp\Big(i\vec{L} \cdot \hat{p} - im\dot{\vec{L}} \cdot \hat{x}\Big), \tag{7.35}$$

which is of the form given in Eq. (7.19) as required. One now obtains for the transformed invariant $\mathcal{I}_1$

$$\mathcal{I}_1 = \frac{1}{2} X^T \Gamma X. \tag{7.36}$$

Eq. (7.36) gives that $\mathcal{I}_1$ contains no linear or scalar terms as desired.

7.5.3 Computation of the transformed invariant $\mathcal{I}_2$

Although the linear and scalar terms have been removed, the transformed operator $\mathcal{I}_1$ given in Eq. (7.36) still contains terms of Lorentz type proportional to $\hat{x}_i\hat{p}_i + \hat{p}_i\hat{x}_i$. In this section, I will derive an expression for the unitary transformation U_2 that ensures that these are removed in the transformed operator $\mathcal{I}_2 = U_2\mathcal{I}_1U_2\dagger$.

Concretely, the goal is to take the transformed invariant $\mathcal{I}_1$ to a new transformed invariant $\mathcal{I}_2$

$$\mathcal{I}_2 = U_2\mathcal{I}_1U_2^\dagger = \frac{1}{2}\hat{X}\Gamma'\hat{X} \tag{7.37}$$

where Γ' is in block diagonal form,

$$\Gamma' = \begin{pmatrix} \bullet & 0 \\ 0 & \bullet \end{pmatrix}. \tag{7.38}$$

This block diagonal form ensures that the transformed invariant $\mathcal{I}_2$ possesses no terms of Lorentz type $\hat{x}_i\hat{p}_i + \hat{p}_i\hat{x}_i$.

In order to affect such a transformation, the unitary matrix U_2 must take the form of a squeezing operator, which is quadratic in position and momentum operators. I write down the ansatz for the unitary matrix U_2

$$U_2 = \exp\big(iX^TAX\big), \tag{7.39}$$

where the matrix A is a Hermitian matrix. The transformed invariant $\mathcal{I}_2 = U_2\mathcal{I}_1U_2^\dagger$ may be computed by applying the matrix lemma in Eq. (7.27). However, a source of great difficulty results from the fact that the series in Eq. (7.27), given in terms of the series M_n, is infinite in general, making it difficult to calculate a closed form expression for $\mathcal{I}_2$.

This may be dealt with by considering a restricted form for U_2 that will ensure that the series

eventually terminates. I make the choice

$$\begin{aligned} U_2 &= \exp\left(-\frac{i}{2}\hat{X}^T \begin{pmatrix} G & 0 \\ 0 & 0 \end{pmatrix} X\right) \\ &= \exp\left(-\frac{i}{2}\hat{x}^T G \hat{x}\right), \end{aligned} \tag{7.40}$$

where G is a d by d square real symmetric matrix.

The transformed invariant $\mathcal{I}_2$ may be calculated using Eq. (7.27). Setting

$$C = \begin{pmatrix} G & 0 \\ 0 & 0 \end{pmatrix}, \tag{7.41}$$

and

$$D = \Gamma, \tag{7.42}$$

in Eq. (7.27), one gets that

$$\mathcal{I}_2 = \frac{1}{2}\hat{X}^T \sum_{n=0}^{\infty} \frac{M_n}{n!}\hat{X}, \tag{7.43}$$

where

$$M_0 = \begin{bmatrix} m\left(\dot{R}^2 + \mathrm{Re}\left([\dot{R}, R]_A - RA^2R\right)\right) & \frac{\mathcal{J}-\{R,\dot{R}\}}{2} \\ \frac{-\mathcal{J}-\{R,\dot{R}\}}{2} & \frac{R^2}{m} \end{bmatrix}, \tag{7.44}$$

$$M_1 = \begin{bmatrix} \frac{[\mathcal{J},G]-\{G,\{R,\dot{R}\}\}}{2} & \frac{GR^2}{m} \\ \frac{R^2G}{m} & 0 \end{bmatrix}, \tag{7.45}$$

$$M_2 = \begin{bmatrix} \frac{2GR^2G}{m} & 0 \\ 0 & 0 \end{bmatrix}, \tag{7.46}$$

$$M_3 = 0. \tag{7.47}$$

Since the matrix M_3 vanishes, it follows that all other M_i for $i > 3$ vanish as a result of the recurrence relation given in Eq. (7.29). As a result, the infinite sum given in Eq. (7.43) terminates. The transformed invariant $\mathcal{I}_2$ may be obtained by evaluating the sum in Eq. (7.43)

to obtain

$$\mathcal{I}_2 = \frac{1}{2}\hat{X}^T \begin{bmatrix} m\left(\dot{R}^2 + \mathrm{Re}\left([\dot{R},R]_A - RA^2R\right)\right) + \frac{[\mathcal{J},G]-\{G,\{R,\dot{R}\}\}}{2} + \frac{GR^2G}{m} & \frac{\mathcal{J}-\{R,\dot{R}\}}{2} + \frac{GR^2}{m} \\ \frac{-\mathcal{J}-\{R,\dot{R}\}}{2} + \frac{R^2G}{m} & \frac{R^2}{m} \end{bmatrix} \hat{X}. \tag{7.48}$$

The goal is to ensure that $\mathcal{I}_2$ possesses no terms of Lorentz type. As may be seen by inspection of Eq. (7.48), this is obtained if

$$G = \frac{mR^{-2}}{2}\left(\mathcal{J} + \{R,\dot{R}\}\right) = \frac{m}{2}\left(R^{-2}\mathcal{J} + R^{-1}\dot{R} + R^{-2}\dot{R}R\right). \tag{7.49}$$

One concern is that it is required that the matrix G be real symmetric. Yet it is not clear that the right hand side of Eq. (7.49) defines a real symmetric matrix.

Taking Eq. (7.49) to define the matrix G, it follows that

$$G - G^T = \frac{m}{2}\left(\{R^{-2},\mathcal{J}\} + [R^{-1},\dot{R}] + [R^{-2},R]_{\dot{R}}\right). \tag{7.50}$$

However, it may be seen readily by substituting Eq. (3.25) that the right hand side of Eq. (7.50) vanishes. It follows that G is a real symmetric matrix as required, and so it defines a valid choice of U_2 through Eq. (7.40).

Eq. (7.40) yields, after substituting for the matrix G using Eq. (7.50),

$$U_2 = \exp\left(-\frac{im}{4}\hat{x}^T\left(R^{-2}\mathcal{J} + R^{-1}\dot{R} + R^{-2}\dot{R}R\right)\hat{x}\right), \tag{7.51}$$

which is the desired expression for the unitary operator U_2 given in Eq. (7.18).

Although this choice of unitary operator U_2 guarantees that the transformed invariant $\mathcal{I}_2$ given in Eq. (7.48) possesses no terms of Lorentz type, it remains to determine what the transformed invariant $\mathcal{I}_2$ actually is. As the matrix G is specified in Eq. (7.49), the transformed invariant $\mathcal{I}_2$ can be determined by substituting for the matrix G in Eq. (7.48). One eventually obtains,

after much simplification, that

$$\Gamma' = \begin{bmatrix} mR^{-2} & 0 \\ 0 & \frac{R^2}{m} \end{bmatrix}, \tag{7.52}$$

and so

$$\mathcal{I}_2 = \frac{1}{2}\hat{X} \begin{bmatrix} mR^{-2} & 0 \\ 0 & \frac{R^2}{m} \end{bmatrix} \hat{X}. \tag{7.53}$$

7.5.4 Computation of the transformed invariant $\mathcal{I}_3$

The transformed invariant $\mathcal{I}_2$, given in Eq. (7.53) contains no terms of Lorentz type as desired. By introducing an additional squeezing transformation determined by the unitary operator U_3, it is possible to ensure that the transformed invariant $\mathcal{I}_3$ takes the form of the isotropic harmonic oscillator $\frac{1}{2}\hat{X}^T\hat{X}$.

Choosing the matrix in Eq. (7.40) to have non-zero support in the upper left block led to the elimination of terms of Lorentz type in $\mathcal{I}_2$. Since these terms have already been eliminated, it makes little sense to choose a similar functional form for the unitary operator U_3. I instead choose the form

$$U_3 = \exp\left(-\frac{i}{2}\hat{X}^T \begin{bmatrix} 0 & H \\ H & 0 \end{bmatrix} \hat{X} \right), \tag{7.54}$$

where H is a real symmetric matrix of size d. Choosing the matrix H appropriately will achieve the desired transformation that $\mathcal{I}_3 = \frac{1}{2}\hat{X}^T\hat{X}$.

The transformed invariant $\mathcal{I}_3$ may be calculated by applying the matrix lemma in Eq. (7.27). One sets

$$C = \begin{bmatrix} 0 & H \\ H & 0 \end{bmatrix}, \tag{7.55}$$

and

$$D = \begin{bmatrix} mR^{-2} & 0 \\ 0 & \frac{R^2}{m} \end{bmatrix}. \tag{7.56}$$

The stem of the lemma in Eq. (7.27) may be applied to obtain the M_i. One may calculate the

first few to obtain

$$M_1 = \begin{bmatrix} -\{H, mR^{-2}\} & 0 \\ 0 & \{H, \frac{R^2}{m}\} \end{bmatrix} \tag{7.57}$$

$$M_2 = \begin{bmatrix} \{H, \{H, mR^{-2}\}\} & 0 \\ 0 & \{H, \{H, \frac{R^2}{m}\}\} \end{bmatrix} \tag{7.58}$$

$$M_3 = \begin{bmatrix} -\{H, \{H, \{H, mR^{-2}\}\}\} & 0 \\ 0 & \{H, \{H, \{H, \frac{R^2}{m}\}\}\} \end{bmatrix} \tag{7.59}$$

and so on.

Inspection of M_1, M_2 and M_3 suggests a general form for the M_i in terms of nested anticommutators. Indeed, it is straightforward to prove inductively that

$$M_i = \begin{bmatrix} \underbrace{\{-H, \{-H, \ldots, \{-H}_{i \text{ times}}, mR^{-2}\} \ldots\}\} & 0 \\ 0 & \underbrace{\{H, \{H, \ldots, \{H}_{i \text{ times}}, \frac{R^2}{m}\} \ldots\}\} \end{bmatrix}. \tag{7.60}$$

In order to compute the transformed invariant $\mathcal{I}_3$, the sum $\sum_{n=0}^{\infty} \frac{M_n}{n!}$ must be formed in accordance with Eq. (7.27). One obtains that

$$\sum_{n=0}^{\infty} \frac{M_n}{n!} = \begin{bmatrix} mR^{-2} - \{H, mR^{-2}\} + \frac{1}{2}\{H, \{H, mR^{-2}\}\} + \ldots & 0 \\ 0 & \frac{R^2}{m} + \{H, \frac{R^2}{m}\} + \frac{1}{2}\{H, \{H, \frac{R^2}{m}\}\} + \ldots \end{bmatrix}. \tag{7.61}$$

Although Eq. (7.61) can be used to evaluate the transformed invariant $\mathcal{I}_3$, it is given in terms of an infinite series. In particular, it is not clear how to choose the matrix H in such a way that ensures that the transformed invariant $\mathcal{I}_3$ is of the form of an isotropic harmonic oscillator. However, one can obtain a closed form for these infinite series to yield a more tractable expression. The infinite series take the form of those appearing on the right hand side of the matrix lemma given in Eq. (7.26). By equating them with the left hand side of the

lemma in Eq. (7.26), one obtains that

$$\sum_{n=0}^{\infty} \frac{M_n}{n!} = \begin{bmatrix} me^{-H}R^{-2}e^{-H} & 0 \\ 0 & e^{H}\frac{R^2}{m}e^{H} \end{bmatrix}, \tag{7.62}$$

giving finally that

$$\mathcal{I}_3 = \frac{1}{2}\hat{X}^T \begin{bmatrix} me^{-H}R^{-2}e^{-H} & 0 \\ 0 & e^{H}\frac{R^2}{m}e^{H} \end{bmatrix} \hat{X}. \tag{7.63}$$

By choosing the matrix D appropriately, one can ensure that $\mathcal{I}_3 = \frac{1}{2}\hat{X}^T\hat{X}$. This is the case if

$$me^{-H}R^{-2}e^{-H} = \mathbb{1}, \tag{7.64}$$

and

$$e^{H}\frac{R^2}{m}e^{H} = \mathbb{1}. \tag{7.65}$$

Both conditions are met if

$$e^{2H} = mR^{-2}. \tag{7.66}$$

Taking the principal matrix logarithm and dividing by two gives that

$$H = \frac{1}{2}\log mR^{-2} = -\log\frac{R}{\sqrt{m}}. \tag{7.67}$$

Taking Eq. (7.67) to define H, one gets finally that

$$U_3 = \exp\left(\frac{i}{2}\hat{X}^T \begin{bmatrix} 0 & \log\frac{R}{\sqrt{m}} \\ \log\frac{R}{\sqrt{m}} & 0 \end{bmatrix} \hat{X}\right), \tag{7.68}$$

and

$$\mathcal{I}_3 = \frac{1}{2}\hat{X}^T\hat{X}, \tag{7.69}$$

which completes the proof of Eq. (7.12).

It follows that the eigenstates of the invariant $\mathcal{I}$ are given by the expression $T^\dagger|n_1, ..., n_d\rangle$,

as discussed in Sec. 7.4. As the eigenstates have now been determined, the time-dependent perturbation theory outlined in Sec. 7.3 may be implemented.

7.6 Outlook

In this section, I will outline some future technical directions that must be pursued in order for the perturbation theory approach outlined in Sec. 7.3 to be implemented, and future potential applications.

The determination of the eigenstates of the invariant $\mathcal{I}$ given so far is only a first step in the implementation of the perturbation theory outlined in Sec. 7.3. There exists a subtlety in that the eigenstates $T^\dagger |n_1, n_2, ..., n_d\rangle$ of the invariant $\mathcal{I}$ do not necessarily satisfy the Schrödinger equation. The results of Sec. 2.5.1.2 show only that the eigenstates of the invariant $\mathcal{I}$ may be chosen in such a way that they satisfy the Schrödinger equation, with attention paid in particular to the determination of the correct phases of the eigenstates. The eigenbasis of the invariant in which the Schrödinger equation is solved must hence be determined in accordance with the technique outlined in Sec. 2.5.1.2, using the eigenbasis $T^\dagger |n_1, n_2, ..., n_d\rangle$ of the invariant $\mathcal{I}$ as a starting point.

If the numerical use of time-dependent perturbation theory is to be of practical use, then one must evaluate the computational requirements with respect to some experimental problem, which would likely be an in-depth investigation itself. One is encouraged, however, by the fact that in one spatial dimension, similar numerical methods have proven orders of magnitude more robust and efficient than the alternatives [136]. It is also plausible that the results of this chapter, pertaining as they do to systems that are approximately harmonic, have applicability outside of the realm of quantum control of trapped ions. In particular, such nearly harmonic potentials are found in the field of intramolecular dynamics, in which electronic wavepackets move in potentials that, as in the case of trapped ion dynamics, often vary on length scales much larger than those of the electronic wavepackets. The results of this chapter could be used to simulate dynamics beyond the Gaussian approximation in complicated molecules that are

not limited to a linear structure, as in the one-dimensional case [136].

Chapter 8

Conclusion

In this thesis, I derived and presented work relating to invariant-based inverse engineering of quantum systems, applied principally to the control of motional states of trapped ions, in a number of contexts. I will present here some of the implications of this work, outlining in particular future lines of research and potential experimental implementations of the results presented in this thesis.

In Ch. 2, the notions of quantum invariants and invariant-based inverse engineering were introduced, as well as a review of the field of ion shuttling and separation.

In Ch. 3, I derived a quantum invariant corresponding to a Hamiltonian that controls the dynamics of a trapped ion in any number of spatial dimensions. To the best of my knowledge, this is the first quantum invariant to be derived that corresponds to a physical system in any number of spatial dimensions, and as such represents a significant addition to the library of quantum invariants. From a theoretical point of view, this opens up a new field of investigation into the possibility of deriving other invariants that correspond to physical systems that exist in more than one spatial dimension. A procedure to inverse engineer Hamiltonians using this invariant was presented in this chapter, which shows that the invariant presented in this chapter is not only of theoretical interest, but a useful addition to the toolkit of invariant-based inverse engineering that promises to be of use in designing experimental procedures to control the motion of single trapped ions in more than one spatial dimension.

In Ch. 4, I demonstrated the ability of the invariant derived in Ch. 3 to carry out shuttling of trapped ions within a X-junction trap. The resulting dynamics contain many interesting features, and show that inverse engineering Hamiltonians using the invariant of Ch. 3 leads to dynamics which are non-trivial from a theoretical point of view and carry out a physically relevant task in quantum control. The successful numerical demonstration of ion shuttling raises the possibility of experimental implementation in a X-junction trap. This is the subject of an active collaboration with the University of Sussex, which hopefully should deliver fruitful results in the near future. A realisation of fast ground-state to ground-state ion shuttling in a X-junction trap would be an experimental first, in which the invariant of Ch. 3 promises to play a key role.

In Ch. 5, I tackled the problem of generalising the invariant derived in Ch. 3 to control more than one ion. Although much progress was made in deriving an invariant corresponding to more than one ion, there remain several unanswered theoretical questions relating to the invariant which may form a productive line of enquiry in the future. An open question is whether the quadratic parts of the trapping potential $\mathcal{M}_i$ obtained via inverse engineering are all real and symmetric, which must certainly be settled in the affirmative if invariant-based inverse engineering is to succeed. It is also not yet clear how to ensure that the invariant and Hamiltonian commute at final time. If these problems are settled successfully, then it may be possible to carry out inverse engineering of more than one ion. Since this would allow one to carry out shuttling of more than one ion at a time, as well as ion separation and ion crystal rotation, there exists the possibility of one day carrying out all of these tasks within a single coherent picture, which is an exciting prospect both theoretically and experimentally.

In Ch. 6, I demonstrated how one can use the invariant derived in Ch. 5 to carry out separation of trapped ions in a T-junction trap. Despite the limitations of using this invariant for quantum control, transfer fidelities of above 96% were observed in all cases, showing that the degeneracy of the invariant does not pose a problem in practice when separating trapped ions. This numerical demonstration also raises the possibility of separating trapped ions using invariant-based inverse engineering in experiment.

In Ch. 7, I addressed the problem of working with noise and anharmonic potentials, which are typically encountered in experimental conditions. I proposed a variant of time-dependent perturbation theory that is tightly integrated with the quantum invariant proposed in Ch. 3, that allows one to deal with these phenomena in a general manner numerically. I derived an expression for the eigenstates of the invariant by means of a unitary transformation that relates the invariant to the Hamiltonian of the isotropic harmonic oscillator. There remain theoretical issues to be resolved, but it seems likely that the techniques proposed in Ch. 7 will in fact permit the use of time-dependent perturbation theory to investigate noise and anharmonicities. Although similar techniques have been used to investigate dynamics beyond the harmonic approximation before [136], they are generally limited to one spatial dimension. The use of a quantum invariant here to facilitate time-dependent perturbation theory is to the best of my knowledge a novel application of quantum invariants, that may lead to investigations of dynamics beyond the harmonic approximation in multidimensional systems. This may be of use in studying the dynamics not only of trapped ions but also of electronic wavepackets in complicated molecules.

Finally, it is to be remembered that the field of trapped ion quantum computing continues to demonstrate significant experimental advances and remains one of the premier platforms for the implementation of a scalable quantum computer. The use of invariant-based inverse engineering, still in its relative infancy, promises to facilitate many important tasks that must be carried out in the construction of such a device. It is to be hoped that future progress in invariant-based engineering drives forward the capabilities of trapped ion quantum processing, pushing forward experimental frontiers to new heights that until recently lay in the domain of pure theoretical speculation.

Appendix A

Numerical methods

This thesis contains not only theoretical results, but numerical investigations that demonstrate how one may employ the theory usefully in experiment. In this section I will detail how such investigations were carried out.

Most of the numerical work done during my studies, and all of the work presented here, was developed in Common Lisp [176]. I made use of a large number of open source libraries for tasks such as linear algebra [177], numerical integration [178] and array manipulation [179]. In order to carry out the invariant inversion outlined in Chs. 4 and 6, I developed a computer algebra system in order to perform the necessary manipulation of matrix and vector-valued functions and their time derivatives. The graphs presented in this thesis were all generated using gnuplot [180], an open-source plotting library. Integration of systems of ODEs was performed with the Runge-Kutta family of numerical integrators.

The numerics and graphics presented here were produced on my personal computer, though at times during my studies I made use of the Imperial HPC facility [181].

Mathematica was used to carry out some of the algebraic manipulations in Sec. 3.4.2.

Bibliography

[1] Selwyn Simsek and Florian Mintert. Quantum control with a multi-dimensional Gaussian quantum invariant. *Quantum*, 5:409, March 2021.

[2] Selwyn Simsek and Florian Mintert. Quantum invariant-based control of interacting trapped ions. *arXiv:2112.13905*, December 2021.

[3] Richard P. Feynman. Simulating physics with computers. *International Journal of Theoretical Physics*, 21(6):467–488, June 1982.

[4] Richard P. Feynman. Quantum mechanical computers. *Foundations of Physics*, 16(6):507–531, June 1986.

[5] D. Deutsch. Quantum Computational Networks. *Proceedings of the Royal Society of London. Series A, Mathematical and Physical Sciences*, 425(1868):73–90, 1989.

[6] Adriano Barenco, Charles H. Bennett, Richard Cleve, David P. DiVincenzo, Norman Margolus, Peter Shor, Tycho Sleator, John A. Smolin, and Harald Weinfurter. Elementary gates for quantum computation. *Physical Review A*, 52(5):3457–3467, November 1995.

[7] Richard Jozsa and Benjamin Schumacher. A New Proof of the Quantum Noiseless Coding Theorem. *Journal of Modern Optics*, 41(12):2343–2349, December 1994.

[8] Benjamin Schumacher. Quantum coding. *Physical Review A*, 51(4):2738–2747, April 1995.

[9] David Deutsch and Richard Jozsa. Rapid solution of problems by quantum computation. *Proceedings of the Royal Society of London. Series A: Mathematical and Physical Sciences*, 439(1907):553–558, December 1992.

[10] Daniel R. Simon. On the Power of Quantum Computation. *SIAM Journal on Computing*, 26(5):1474–1483, October 1997.

[11] P.W. Shor. Algorithms for quantum computation: Discrete logarithms and factoring. In *Proceedings 35th Annual Symposium on Foundations of Computer Science*, pages 124–134, November 1994.

[12] Lov K. Grover. A fast quantum mechanical algorithm for database search. In *Proceedings of the Twenty-Eighth Annual ACM Symposium on Theory of Computing*, STOC '96, pages 212–219, New York, NY, USA, July 1996. Association for Computing Machinery.

[13] Mark Ettinger, Peter Høyer, and Emanuel Knill. The quantum query complexity of the hidden subgroup problem is polynomial. *Information Processing Letters*, 91(1):43–48, July 2004.

[14] Daniel S. Abrams and Seth Lloyd. Quantum Algorithm Providing Exponential Speed Increase for Finding Eigenvalues and Eigenvectors. *Physical Review Letters*, 83(24):5162–5165, December 1999.

[15] Abhinav Kandala, Antonio Mezzacapo, Kristan Temme, Maika Takita, Markus Brink, Jerry M. Chow, and Jay M. Gambetta. Hardware-efficient variational quantum eigensolver for small molecules and quantum magnets. *Nature*, 549(7671):242–246, September 2017.

[16] William Zeng and Bob Coecke. Quantum Algorithms for Compositional Natural Language Processing. *Electronic Proceedings in Theoretical Computer Science*, 221:67–75, August 2016.

[17] Bob Coecke, Giovanni de Felice, Konstantinos Meichanetzidis, and Alexis Toumi. Foundations for Near-Term Quantum Natural Language Processing. *arXiv:2012.03755*, December 2020.

[18] Konstantinos Meichanetzidis, Alexis Toumi, Giovanni de Felice, and Bob Coecke. Grammar-Aware Question-Answering on Quantum Computers. *arXiv:2012.03756*, December 2020.

[19] Aram W. Harrow, Avinatan Hassidim, and Seth Lloyd. Quantum Algorithm for Linear Systems of Equations. *Physical Review Letters*, 103(15):150502, October 2009.

[20] Patrick Rebentrost, Masoud Mohseni, and Seth Lloyd. Quantum Support Vector Machine for Big Data Classification. *Physical Review Letters*, 113(13):130503, September 2014.

[21] Seth Lloyd and Christian Weedbrook. Quantum Generative Adversarial Learning. *Physical Review Letters*, 121(4):040502, July 2018.

[22] Sonika Johri, Shantanu Debnath, Avinash Mocherla, Alexandros Singk, Anupam Prakash, Jungsang Kim, and Iordanis Kerenidis. Nearest centroid classification on a trapped ion quantum computer. *npj Quantum Information*, 7(1):1–11, August 2021.

[23] Rolf Landauer. Is Quantum Mechanics Useful? *Philosophical Transactions: Physical Sciences and Engineering*, 353(1703):367–376, 1995.

[24] Asher Peres. Reversible logic and quantum computers. *Physical Review A*, 32(6):3266–3276, December 1985.

[25] Peter W. Shor. Scheme for reducing decoherence in quantum computer memory. *Physical Review A*, 52(4):R2493–R2496, October 1995.

[26] E. Knill, R. Laflamme, R. Martinez, and C. Negrevergne. Benchmarking Quantum Computers: The Five-Qubit Error Correcting Code. *Physical Review Letters*, 86(25):5811–5814, June 2001.

[27] P.W. Shor. Fault-tolerant quantum computation. In *Proceedings of 37th Conference on Foundations of Computer Science*, pages 56–65, October 1996.

[28] Dorit Aharonov and Michael Ben-Or. Fault-Tolerant Quantum Computation with Constant Error Rate. *SIAM Journal on Computing*, 38(4):1207–1282, January 2008.

[29] Michael Freedman and David Meyer. Projective Plane And Planar Quantum Codes. *Foundations of Computational Mathematics*, 1, February 1999.

[30] S. B. Bravyi and A. Yu Kitaev. Quantum codes on a lattice with boundary. *arXiv:quant-ph/9811052*, November 1998.

[31] Oscar Higgott and Nikolas P. Breuckmann. Subsystem Codes with High Thresholds by Gauge Fixing and Reduced Qubit Overhead. *Physical Review X*, 11(3):031039, August 2021.

[32] Jingfu Zhang, Raymond Laflamme, and Dieter Suter. Experimental Implementation of Encoded Logical Qubit Operations in a Perfect Quantum Error Correcting Code. *Physical Review Letters*, 109(10):100503, September 2012.

[33] J. Eli Bourassa, Rafael N. Alexander, Michael Vasmer, Ashlesha Patil, Ilan Tzitrin, Takaya Matsuura, Daiqin Su, Ben Q. Baragiola, Saikat Guha, Guillaume Dauphinais, Krishna K. Sabapathy, Nicolas C. Menicucci, and Ish Dhand. Blueprint for a Scalable Photonic Fault-Tolerant Quantum Computer. *Quantum*, 5:392, February 2021.

[34] C. Ryan-Anderson, J. G. Bohnet, K. Lee, D. Gresh, A. Hankin, J. P. Gaebler, D. Francois, A. Chernoguzov, D. Lucchetti, N. C. Brown, T. M. Gatterman, S. K. Halit, K. Gilmore, J. A. Gerber, B. Neyenhuis, D. Hayes, and R. P. Stutz. Realization of Real-Time Fault-Tolerant Quantum Error Correction. *Physical Review X*, 11(4):041058, December 2021.

[35] Austin G. Fowler, Ashley M. Stephens, and Peter Groszkowski. High-threshold universal quantum computation on the surface code. *Physical Review A*, 80(5):052312, November 2009.

[36] David S. Wang, Austin G. Fowler, and Lloyd C. L. Hollenberg. Surface code quantum computing with error rates over 1%. *Physical Review A*, 83(2):020302, February 2011.

[37] David K. Tuckett, Stephen D. Bartlett, Steven T. Flammia, and Benjamin J. Brown. Fault-Tolerant Thresholds for the Surface Code in Excess of 5% under Biased Noise. *Physical Review Letters*, 124(13):130501, March 2020.

[38] David P. DiVincenzo. The Physical Implementation of Quantum Computation. *Fortschritte der Physik*, 48(9-11):771–783, 2000.

[39] Alexander Shnirman, Gerd Schön, and Ziv Hermon. Quantum Manipulations of Small Josephson Junctions. *Physical Review Letters*, 79(12):2371–2374, September 1997.

[40] Yuriy Makhlin, Gerd Scöhn, and Alexander Shnirman. Josephson-junction qubits with controlled couplings. *Nature*, 398(6725):305–307, March 1999.

[41] Y. Nakamura, Yu A. Pashkin, and J. S. Tsai. Coherent control of macroscopic quantum states in a single-Cooper-pair box. *Nature*, 398(6730):786–788, April 1999.

[42] E. Knill, R. Laflamme, and G. J. Milburn. A scheme for efficient quantum computation with linear optics. *Nature*, 409(6816):46–52, January 2001.

[43] J. L. O'Brien, G. J. Pryde, A. G. White, T. C. Ralph, and D. Branning. Demonstration of an all-optical quantum controlled-NOT gate. *Nature*, 426(6964):264–267, November 2003.

[44] Mercedes Gimeno-Segovia, Pete Shadbolt, Dan E. Browne, and Terry Rudolph. From Three-Photon Greenberger-Horne-Zeilinger States to Ballistic Universal Quantum Computation. *Physical Review Letters*, 115(2):020502, July 2015.

[45] Ivan H. Deutsch, Gavin K. Brennen, and Poul S. Jessen. Quantum Computing with Neutral Atoms in an Optical Lattice. *Fortschritte der Physik*, 48(9-11):925–943, 2000.

[46] Loïc Henriet, Lucas Beguin, Adrien Signoles, Thierry Lahaye, Antoine Browaeys, Georges-Olivier Reymond, and Christophe Jurczak. Quantum computing with neutral atoms. *Quantum*, 4:327, September 2020.

[47] Frank Arute, Kunal Arya, Ryan Babbush, Dave Bacon, Joseph C. Bardin, Rami Barends, Rupak Biswas, Sergio Boixo, Fernando G. S. L. Brandao, David A. Buell, Brian Burkett, Yu Chen, Zijun Chen, Ben Chiaro, Roberto Collins, William Courtney, Andrew Dunsworth, Edward Farhi, Brooks Foxen, Austin Fowler, Craig Gidney, Marissa Giustina, Rob Graff, Keith Guerin, Steve Habegger, Matthew P. Harrigan, Michael J. Hartmann,

Alan Ho, Markus Hoffmann, Trent Huang, Travis S. Humble, Sergei V. Isakov, Evan Jeffrey, Zhang Jiang, Dvir Kafri, Kostyantyn Kechedzhi, Julian Kelly, Paul V. Klimov, Sergey Knysh, Alexander Korotkov, Fedor Kostritsa, David Landhuis, Mike Lindmark, Erik Lucero, Dmitry Lyakh, Salvatore Mandrà, Jarrod R. McClean, Matthew McEwen, Anthony Megrant, Xiao Mi, Kristel Michielsen, Masoud Mohseni, Josh Mutus, Ofer Naaman, Matthew Neeley, Charles Neill, Murphy Yuezhen Niu, Eric Ostby, Andre Petukhov, John C. Platt, Chris Quintana, Eleanor G. Rieffel, Pedram Roushan, Nicholas C. Rubin, Daniel Sank, Kevin J. Satzinger, Vadim Smelyanskiy, Kevin J. Sung, Matthew D. Trevithick, Amit Vainsencher, Benjamin Villalonga, Theodore White, Z. Jamie Yao, Ping Yeh, Adam Zalcman, Hartmut Neven, and John M. Martinis. Quantum supremacy using a programmable superconducting processor. *Nature*, 574(7779):505–510, October 2019.

[48] Peter J. Karalekas, Nikolas A. Tezak, Eric C. Peterson, Colm A. Ryan, Marcus P. da Silva, and Robert S. Smith. A quantum-classical cloud platform optimized for variational hybrid algorithms. *Quantum Science and Technology*, 5(2):024003, April 2020.

[49] Han-Sen Zhong, Hui Wang, Yu-Hao Deng, Ming-Cheng Chen, Li-Chao Peng, Yi-Han Luo, Jian Qin, Dian Wu, Xing Ding, Yi Hu, Peng Hu, Xiao-Yan Yang, Wei-Jun Zhang, Hao Li, Yuxuan Li, Xiao Jiang, Lin Gan, Guangwen Yang, Lixing You, Zhen Wang, Li Li, Nai-Le Liu, Chao-Yang Lu, and Jian-Wei Pan. Quantum computational advantage using photons. *Science*, December 2020.

[50] Wolfgang Paul and Helmut Steinwedel. Ein neues Massenspektrometer ohne Magnetfeld. *Zeitschrift fur Naturforschung - Section A Journal of Physical Sciences*, 8(7):448–450, January 1953.

[51] W. Neuhauser, M. Hohenstatt, P. E. Toschek, and H. Dehmelt. Localized visible Ba^+ mono-ion oscillator. *Physical Review A*, 22(3):1137–1140, September 1980.

[52] V. Letokhov, V. Minogin, and B. Pavlik. Cooling and capture of atoms and molecules by a resonant light field. *Soviet Journal of Experimental and Theoretical Physics*, 45:698, March 1977.

[53] D. J. Wineland, R. E. Drullinger, and F. L. Walls. Radiation-Pressure Cooling of Bound Resonant Absorbers. *Physical Review Letters*, 40(25):1639–1642, June 1978.

[54] W. Neuhauser, M. Hohenstatt, P. E. Toschek, and H. G. Dehmelt. Visual observation and optical cooling of electrodynamically contained ions. *Applied Physics*, 17(2):123–129, October 1978.

[55] F. Diedrich, J. C. Bergquist, Wayne M. Itano, and D. J. Wineland. Laser Cooling to the Zero-Point Energy of Motion. *Physical Review Letters*, 62(4):403–406, January 1989.

[56] Ye Wang, Mark Um, Junhua Zhang, Shuoming An, Ming Lyu, Jing-Ning Zhang, L.-M. Duan, Dahyun Yum, and Kihwan Kim. Single-qubit quantum memory exceeding ten-minute coherence time. *Nature Photonics*, 11(10):646–650, October 2017.

[57] N. Huntemann, C. Sanner, B. Lipphardt, Chr Tamm, and E. Peik. Single-Ion Atomic Clock with 3×10^{-18} Systematic Uncertainty. *Physical Review Letters*, 116(6), February 2016.

[58] Philip S H Wong. Ion Trap Mass Spectrometry. *Current Separations*, 16(3):8, December 1997.

[59] Jan Benhelm, Gerhard Kirchmair, Christian F. Roos, and Rainer Blatt. Towards fault-tolerant quantum computing with trapped ions. *Nature Physics*, 4(6):463–466, June 2008.

[60] Alice Heather Burrell. *High Fidelity Readout of Trapped Ion Qubits*. PhD thesis, Oxford University, UK, 2010.

[61] D. T. C. Allcock, W. C. Campbell, J. Chiaverini, I. L. Chuang, E. R. Hudson, I. D. Moore, A. Ransford, C. Roman, J. M. Sage, and D. J. Wineland. Omg blueprint for trapped ion quantum computing with metastable states. *Applied Physics Letters*, 119(21):214002, November 2021.

[62] C. Monroe, D. M. Meekhof, B. E. King, W. M. Itano, and D. J. Wineland. Demonstration of a Fundamental Quantum Logic Gate. *Physical Review Letters*, 75(25):4714–4717, December 1995.

[63] Florian Mintert and Christof Wunderlich. Ion-Trap Quantum Logic Using Long-Wavelength Radiation. *Physical Review Letters*, 87(25):257904, November 2001.

[64] U. Warring, C. Ospelkaus, Y. Colombe, R. Jördens, D. Leibfried, and D. J. Wineland. Individual-Ion Addressing with Microwave Field Gradients. *Physical Review Letters*, 110(17):173002, April 2013.

[65] T. P. Harty, D. T. C. Allcock, C. J. Ballance, L. Guidoni, H. A. Janacek, N. M. Linke, D. N. Stacey, and D. M. Lucas. High-Fidelity Preparation, Gates, Memory, and Readout of a Trapped-Ion Quantum Bit. *Physical Review Letters*, 113(22):220501, November 2014.

[66] W. C. Campbell, J. Mizrahi, Q. Quraishi, C. Senko, D. Hayes, D. Hucul, D. N. Matsukevich, P. Maunz, and C. Monroe. Ultrafast Gates for Single Atomic Qubits. *Physical Review Letters*, 105(9):090502, August 2010.

[67] K. R. Brown, A. C. Wilson, Y. Colombe, C. Ospelkaus, A. M. Meier, E. Knill, D. Leibfried, and D. J. Wineland. Single-qubit-gate error below 10^{-4} in a trapped ion. *Physical Review A*, 84(3):030303, September 2011.

[68] Warren Nagourney, Jon Sandberg, and Hans Dehmelt. Shelved optical electron amplifier: Observation of quantum jumps. *Physical Review Letters*, 56(26):2797–2799, June 1986.

[69] J. C. Bergquist, Randall G. Hulet, Wayne M. Itano, and D. J. Wineland. Observation of Quantum Jumps in a Single Atom. *Physical Review Letters*, 57(14):1699–1702, October 1986.

[70] Th. Sauter, W. Neuhauser, R. Blatt, and P. E. Toschek. Observation of Quantum Jumps. *Physical Review Letters*, 57(14):1696–1698, October 1986.

[71] J. I. Cirac and P. Zoller. Quantum Computations with Cold Trapped Ions. *Physical Review Letters*, 74(20):4091–4094, May 1995.

[72] Ferdinand Schmidt-Kaler, Hartmut Häffner, Mark Riebe, Stephan Gulde, Gavin P. T. Lancaster, Thomas Deuschle, Christoph Becher, Christian F. Roos, Jürgen Eschner, and

Rainer Blatt. Realization of the Cirac–Zoller controlled-NOT quantum gate. *Nature*, 422(6930):408–411, March 2003.

[73] Klaus Molmer and Anders Sorensen. Multi-particle entanglement of hot trapped ions. *Physical Review Letters*, 82(9):1835–1838, March 1999.

[74] C. A. Sackett, D. Kielpinski, B. E. King, C. Langer, V. Meyer, C. J. Myatt, M. Rowe, Q. A. Turchette, W. M. Itano, D. J. Wineland, and C. Monroe. Experimental entanglement of four particles. *Nature*, 404(6775):256–259, March 2000.

[75] V. M. Schäfer, C. J. Ballance, K. Thirumalai, L. J. Stephenson, T. G. Ballance, A. M. Steane, and D. M. Lucas. Fast quantum logic gates with trapped-ion qubits. *Nature*, 555(7694):75–78, March 2018.

[76] Jake Lishman and Florian Mintert. Trapped-ion entangling gates robust against qubit frequency errors. *Physical Review Research*, 2(3):033117, July 2020.

[77] Farhang Haddadfarshi and Florian Mintert. High fidelity quantum gates of trapped ions in the presence of motional heating. *New Journal of Physics*, 18(12):123007, December 2016.

[78] A. E. Webb, S. C. Webster, S. Collingbourne, D. Bretaud, A. M. Lawrence, S. Weidt, F. Mintert, and W. K. Hensinger. Resilient Entangling Gates for Trapped Ions. *Physical Review Letters*, 121(18), November 2018.

[79] Norbert M. Linke, Dmitri Maslov, Martin Roetteler, Shantanu Debnath, Caroline Figgatt, Kevin A. Landsman, Kenneth Wright, and Christopher Monroe. Experimental comparison of two quantum computing architectures. *Proceedings of the National Academy of Sciences*, 114(13):3305–3310, March 2017.

[80] K. Wright, K. M. Beck, S. Debnath, J. M. Amini, Y. Nam, N. Grzesiak, J.-S. Chen, N. C. Pisenti, M. Chmielewski, C. Collins, K. M. Hudek, J. Mizrahi, J. D. Wong-Campos, S. Allen, J. Apisdorf, P. Solomon, M. Williams, A. M. Ducore, A. Blinov, S. M. Kreikemeier, V. Chaplin, M. Keesan, C. Monroe, and J. Kim. Benchmarking an 11-qubit quantum computer. *Nature Communications*, 10(1):5464, November 2019.

[81] J. M. Pino, J. M. Dreiling, C. Figgatt, J. P. Gaebler, S. A. Moses, M. S. Allman, C. H. Baldwin, M. Foss-Feig, D. Hayes, K. Mayer, C. Ryan-Anderson, and B. Neyenhuis. Demonstration of the trapped-ion quantum CCD computer architecture. *Nature*, 592(7853):209–213, April 2021.

[82] John Preskill. Quantum Computing in the NISQ era and beyond. *Quantum*, 2:79, August 2018.

[83] Markus Reiher, Nathan Wiebe, Krysta M. Svore, Dave Wecker, and Matthias Troyer. Elucidating reaction mechanisms on quantum computers. *Proceedings of the National Academy of Sciences*, 114(29):7555–7560, July 2017.

[84] Dominic W. Berry, Craig Gidney, Mario Motta, Jarrod R. McClean, and Ryan Babbush. Qubitization of Arbitrary Basis Quantum Chemistry Leveraging Sparsity and Low Rank Factorization. *Quantum*, 3:208, December 2019.

[85] Ian D. Kivlichan, Craig Gidney, Dominic W. Berry, Nathan Wiebe, Jarrod McClean, Wei Sun, Zhang Jiang, Nicholas Rubin, Austin Fowler, Alán Aspuru-Guzik, Hartmut Neven, and Ryan Babbush. Improved Fault-Tolerant Quantum Simulation of Condensed-Phase Correlated Electrons via Trotterization. *Quantum*, 4:296, July 2020.

[86] G. Pagano, P. W. Hess, H. B. Kaplan, W. L. Tan, P. Richerme, P. Becker, A. Kyprianidis, J. Zhang, E. Birckelbaw, M. R. Hernandez, Y. Wu, and C. Monroe. Cryogenic trapped-ion system for large scale quantum simulation. *Quantum Science and Technology*, 4(1):014004, October 2018.

[87] I. Pogorelov, T. Feldker, Ch. D. Marciniak, L. Postler, G. Jacob, O. Krieglsteiner, V. Podlesnic, M. Meth, V. Negnevitsky, M. Stadler, B. Höfer, C. Wächter, K. Lakhmanskiy, R. Blatt, P. Schindler, and T. Monz. Compact Ion-Trap Quantum Computing Demonstrator. *PRX Quantum*, 2(2):020343, June 2021.

[88] H. C. Nägerl, D. Leibfried, H. Rohde, G. Thalhammer, J. Eschner, F. Schmidt-Kaler, and R. Blatt. Laser addressing of individual ions in a linear ion trap. *Physical Review A*, 60(1):145–148, July 1999.

[89] Peter Staanum and Michael Drewsen. Trapped-ion quantum logic utilizing position-dependent ac Stark shifts. *Physical Review A*, 66(4):040302, October 2002.

[90] Shannon X. Wang, Jaroslaw Labaziewicz, Yufei Ge, Ruth Shewmon, and Isaac L. Chuang. Individual addressing of ions using magnetic field gradients in a surface-electrode ion trap. *Applied Physics Letters*, 94(9):094103, March 2009.

[91] D.F.V. James. Quantum dynamics of cold trapped ions with application to quantum computation. *Applied Physics B*, 66(2):181–190, February 1998.

[92] D.J. Wineland, C. Monroe, W.M. Itano, D. Leibfried, B.E. King, and D.M. Meekhof. Experimental issues in coherent quantum-state manipulation of trapped atomic ions. *Journal of Research of the National Institute of Standards and Technology*, 103(3):259, May 1998.

[93] D. Kielpinski, C. Monroe, and D. J. Wineland. Architecture for a large-scale ion-trap quantum computer. *Nature*, 417(6890):709–711, June 2002.

[94] Bjoern Lekitsch, Sebastian Weidt, Austin G. Fowler, Klaus Mølmer, Simon J. Devitt, Christof Wunderlich, and Winfried K. Hensinger. Blueprint for a microwave trapped ion quantum computer. *Science Advances*, 3(2):e1601540, 2017.

[95] Mark Webber, Steven Herbert, Sebastian Weidt, and Winfried K. Hensinger. Efficient Qubit Routing for a Globally Connected Trapped Ion Quantum Computer. *Advanced Quantum Technologies*, 3(8):2000027, 2020.

[96] R. C. Sterling, H. Rattanasonti, S. Weidt, K. Lake, P. Srinivasan, S. C. Webster, M. Kraft, and W. K. Hensinger. Fabrication and operation of a two-dimensional ion-trap lattice on a high-voltage microchip. *Nature Communications*, 5, April 2014.

[97] Joe Britton. Microfabrication techniques for trapped ion quantum information processing. *arXiv:1008.2222*, August 2010.

[98] B. B. Blinov, D. L. Moehring, L.-M. Duan, and C. Monroe. Observation of entanglement between a single trapped atom and a single photon. *Nature*, 428(6979):153–157, March 2004.

[99] D. L. Moehring, P. Maunz, S. Olmschenk, K. C. Younge, D. N. Matsukevich, L.-M. Duan, and C. Monroe. Entanglement of single-atom quantum bits at a distance. *Nature*, 449(7158):68–71, September 2007.

[100] C. Monroe, R. Raussendorf, A. Ruthven, K. R. Brown, P. Maunz, L.-M. Duan, and J. Kim. Large-scale modular quantum-computer architecture with atomic memory and photonic interconnects. *Physical Review A*, 89(2):022317, February 2014.

[101] L. J. Stephenson, D. P. Nadlinger, B. C. Nichol, S. An, P. Drmota, T. G. Ballance, K. Thirumalai, J. F. Goodwin, D. M. Lucas, and C. J. Ballance. High-Rate, High-Fidelity Entanglement of Qubits Across an Elementary Quantum Network. *Physical Review Letters*, 124(11):110501, March 2020.

[102] D. Hucul, I. V. Inlek, G. Vittorini, C. Crocker, S. Debnath, S. M. Clark, and C. Monroe. Modular entanglement of atomic qubits using photons and phonons. *Nature Physics*, 11(1):37–42, January 2015.

[103] R. B. Blakestad, C. Ospelkaus, A. P. VanDevender, J. M. Amini, J. Britton, D. Leibfried, and D. J. Wineland. High fidelity transport of trapped-ion qubits through an X-junction trap array. *Physical Review Letters*, 102(15):153002, April 2009.

[104] Kenneth Wright, Jason M. Amini, Daniel L. Faircloth, Curtis Volin, S. Charles Doret, Harley Hayden, C.-S. Pai, David W. Landgren, Douglas Denison, Tyler Killian, Richart E. Slusher, and Alexa W. Harter. Reliable transport through a microfabricated X-junction surface-electrode ion trap. *New Journal of Physics*, 15(3):033004, March 2013.

[105] Chao-Yang Lu, Wei-Bo Gao, Jin Zhang, Xiao-Qi Zhou, Tao Yang, and Jian-Wei Pan. Experimental quantum coding against qubit loss error. *Proceedings of the National Academy of Sciences of the United States of America*, 105(32):11050–11054, August 2008.

[106] M. A. Rowe, A. Ben-Kish, B. Demarco, D. Leibfried, V. Meyer, J. Beall, J. Britton, J. Hughes, W. M. Itano, B. Jelenković, C. Langer, T. Rosenband, and D. J. Wineland. Transport of quantum states and separation of ions in a dual RF ion trap. *Quantum Information & Computation*, 2(4):257–271, May 2002.

[107] Andreas Walther, Frank Ziesel, Thomas Ruster, Sam T Dawkins, Konstantin Ott, Max Hettrich, Kilian Singer, Ferdinand Schmidt-Kaler, and Ulrich Poschinger. Controlling Fast Transport of Cold Trapped Ions. *Physical Review Letters*, 109(8):080501, August 2012.

[108] V. Kaushal, B. Lekitsch, A. Stahl, J. Hilder, D. Pijn, C. Schmiegelow, A. Bermudez, M. Müller, F. Schmidt-Kaler, and U. Poschinger. Shuttling-based trapped-ion quantum information processing. *AVS Quantum Science*, 2(1):014101, March 2020.

[109] B. B. Blinov, L. Deslauriers, P. Lee, M. J. Madsen, R. Miller, and C. Monroe. Sympathetic cooling of trapped Cd^+ isotopes. *Physical Review A*, 65(4):040304, April 2002.

[110] W. K. Hensinger, S. Olmschenk, D. Stick, D. Hucul, M. Yeo, M. Acton, L. Deslauriers, C. Monroe, and J. Rabchuk. T-junction ion trap array for two-dimensional ion shuttling, storage, and manipulation. *Applied Physics Letters*, 88(3):034101, January 2006.

[111] D. L. Moehring, C. Highstrete, D. Stick, K. M. Fortier, R. Haltli, C. Tigges, and M. G. Blain. Design, fabrication and experimental demonstration of junction surface ion traps. *New Journal of Physics*, 13(7):075018, July 2011.

[112] T. Ruster, C. Warschburger, H. Kaufmann, C. T. Schmiegelow, A. Walther, M. Hettrich, A. Pfister, V. Kaushal, F. Schmidt-Kaler, and U. G. Poschinger. Experimental realization of fast ion separation in segmented Paul traps. *Physical Review A*, 90(3):033410, September 2014.

[113] J. P. Home and A. M. Steane. Electrode Configurations for Fast Separation of Trapped Ions. *Quantum Information & Computation*, 6(4):289–325, November 2006.

[114] A. H. Nizamani and W. K. Hensinger. Optimum electrode configurations for fast ion separation in microfabricated surface ion traps. *Applied Physics B*, 106(2):327–338, February 2012.

[115] Samuel Earnshaw. On the Nature of the Molecular Forces which Regulate the Constitution of the Luminiferous Ether. *Transactions of the Cambridge Philosophical Society*, 7:97–114, 1842.

[116] H. G. Dehmelt. Radiofrequency Spectroscopy of Stored Ions I: Storage. In D. R. Bates and Immanuel Estermann, editors, *Advances in Atomic and Molecular Physics*, volume 3, pages 53–72. Academic Press, January 1968.

[117] Joseph W. Britton, Brian C. Sawyer, Adam C. Keith, C.-C. Joseph Wang, James K. Freericks, Hermann Uys, Michael J. Biercuk, and John J. Bollinger. Engineered two-dimensional Ising interactions in a trapped-ion quantum simulator with hundreds of spins. *Nature*, 484(7395):489–492, April 2012.

[118] G. Graff, F. G. Major, R. W. H. Roeder, and G. Werth. Method for Measuring the Cyclotron and Spin Resonance of Free Electrons. *Physical Review Letters*, 21(6):340–342, August 1968.

[119] Sascha Rau, Fabian Heiße, Florian Köhler-Langes, Sangeetha Sasidharan, Raphael Haas, Dennis Renisch, Christoph E. Düllmann, Wolfgang Quint, Sven Sturm, and Klaus Blaum. Penning trap mass measurements of the deuteron and the HD^+ molecular ion. *Nature*, 585(7823):43–47, September 2020.

[120] G. Gabrielse, X. Fei, L. A. Orozco, R. L. Tjoelker, J. Haas, H. Kalinowsky, T. A. Trainor, and W. Kells. Thousandfold improvement in the measured antiproton mass. *Physical Review Letters*, 65(11):1317–1320, September 1990.

[121] S. Jain, J. Alonso, M. Grau, and J. P. Home. Scalable Arrays of Micro-Penning Traps for Quantum Computing and Simulation. *Physical Review X*, 10(3):031027, August 2020.

[122] S. Seidelin, J. Chiaverini, R. Reichle, J. J. Bollinger, D. Leibfried, J. Britton, J. H. Wesenberg, R. B. Blakestad, R. J. Epstein, D. B. Hume, W. M. Itano, J. D. Jost, C. Langer,

R. Ozeri, N. Shiga, and D. J. Wineland. Microfabricated Surface-Electrode Ion Trap for Scalable Quantum Information Processing. *Physical Review Letters*, 96(25):253003, June 2006.

[123] Karan Kartik Mehta, Amira M. Eltony, Colin D. Bruzewicz, Isaak Chuang, Rajeev J. Ram, Jeremy M. Sage, and John Chiaverini. Ion traps fabricated in a CMOS foundry. *Applied Physics Letters*, 105, June 2014.

[124] A. H. Myerson, D. J. Szwer, S. C. Webster, D. T. C. Allcock, M. J. Curtis, G. Imreh, J. A. Sherman, D. N. Stacey, A. M. Steane, and D. M. Lucas. High-Fidelity Readout of Trapped-Ion Qubits. *Physical Review Letters*, 100(20):200502, May 2008.

[125] Gebhard Littich. Electrostatic Control and Transport of Ions on a Planar Trap for Quantum Information Processing. Master's thesis, ETH Zürich.

[126] D. J. Berkeland, J. D. Miller, J. C. Bergquist, W. M. Itano, and D. J. Wineland. Minimization of ion micromotion in a Paul trap. *Journal of Applied Physics*, 83(10):5025–5033, May 1998.

[127] Xi Chen, E. Torrontegui, Dionisis Stefanatos, Jr-Shin Li, and J. G. Muga. Optimal trajectories for efficient atomic transport without final excitation. *Physical Review A*, 84(4):043415, October 2011.

[128] Eric Heller. Time-dependent approach to semiclassical dynamics. *The Journal of Chemical Physics*, 62, February 1975.

[129] Eric J. Heller. Wavepacket path integral formulation of semiclassical dynamics. *Chemical Physics Letters*, 34(2):321–325, July 1975.

[130] Eric J. Heller. Time dependent variational approach to semiclassical dynamics. *The Journal of Chemical Physics*, 64(1):63–73, January 1976.

[131] Eric J. Heller. Classical S-matrix limit of wave packet dynamics. *The Journal of Chemical Physics*, 65(11):4979–4989, December 1976.

[132] Eric J. Heller. Generalized theory of semiclassical amplitudes. *The Journal of Chemical Physics*, 66(12):5777–5785, June 1977.

[133] Eric J. Heller. Frozen Gaussians: A very simple semiclassical approximation. *The Journal of Chemical Physics*, 75(6):2923–2931, September 1981.

[134] Soo-Y. Lee. Theory of multidimensional wavepacket propagation. *Chemical Physics*, 108(3):451–459, October 1986.

[135] Florian Mintert and Eric J. Heller. Simulation of open quantum systems. *EPL (Europhysics Letters)*, 86(5):50006, June 2009.

[136] B M Garraway. Extended Gaussian wavepacket dynamics. *Journal of Physics B: Atomic, Molecular and Optical Physics*, 33(20):4447, August 2000.

[137] H. R. Lewis. Classical and Quantum Systems with Time-Dependent Harmonic-Oscillator-Type Hamiltonians. *Physical Review Letters*, 18(13):510–512, March 1967.

[138] H. R. Lewis. Motion of a Time-Dependent Harmonic Oscillator, and of a Charged Particle in a Class of Time-Dependent, Axially Symmetric Electromagnetic Fields. *Physical Review*, 172(5):1313–1315, August 1968.

[139] M. Devaud, V. Leroy, J.-C. Bacri, and T. Hocquet. The adiabatic invariant of the n - degree-of-freedom harmonic oscillator. *European Journal of Physics*, 29(4):831–843, June 2008.

[140] J. R. Mohallem. Two helpful developments towards better understanding of adiabatic invariance in classical mechanics. *Revista Brasileira de Ensino de Física*, 41, September 2018.

[141] Martin Kruskal. Asymptotic Theory of Hamiltonian and other Systems with all Solutions Nearly Periodic. *Journal of Mathematical Physics*, 3(4):806–828, July 1962.

[142] H. R. Lewis. Class of Exact Invariants for Classical and Quantum Time-Dependent Harmonic Oscillators. *Journal of Mathematical Physics*, 9(11):1976–1986, November 1968.

[143] P.G.L. Leach and S.K. Andriopoulos. The Ermakov equation: A commentary. *Applicable Analysis and Discrete Mathematics*, 2(2):146–157, 2008.

[144] Xiao-Jing Lu, Ion Lizuain, and J. G. Muga. Inverse engineering of fast state transfer among coupled oscillators. *Manuscript accepted by Quantum*, June 2022.

[145] H. R. Lewis and W. B. Riesenfeld. An Exact Quantum Theory of the Time-Dependent Harmonic Oscillator and of a Charged Particle in a Time-Dependent Electromagnetic Field. *Journal of Mathematical Physics*, 10(8):1458–1473, August 1969.

[146] H. C. Rosu and J. L. Romero. Ermakov approach for the one-dimensional Helmholtz Hamiltonian. *arXiv:quant-ph/9707044*, June 1999.

[147] Pedro B. Espinoza. Ermakov-Lewis dynamic invariants with some applications. *arXiv:math-ph/0002005*, February 2000.

[148] A. M. Goncharenko, Yu. A. Logvin, A. M. Samson, P. S. Shapovalov, and S. I. Turovets. Ermakov Hamiltonian systems in nonlinear optics of elliptic Gaussian beams. *Physics Letters A*, 160(2):138–142, November 1991.

[149] J.-Q. Shen, H.-Y. Zhu, and P. Chen. Exact solutions and geometric phase factor of time-dependent three-generator quantum systems. *The European Physical Journal D - Atomic, Molecular, Optical and Plasma Physics*, 23(2):305–313, May 2003.

[150] Erik Torrontegui, Sara Ibáñez, Sofia Martínez-Garaot, Michele Modugno, Adolfo del Campo, David Guéry-Odelin, Andreas Ruschhaupt, Xi Chen, and Juan Gonzalo Muga. Chapter 2 - Shortcuts to Adiabaticity. In Ennio Arimondo, Paul R. Berman, and Chun C. Lin, editors, *Advances In Atomic, Molecular, and Optical Physics*, volume 62, pages 117–169. Academic Press, January 2013.

[151] Utkan Güngördü, Yidun Wan, Mohammad Ali Fasihi, and Mikio Nakahara. Dynamical invariants for quantum control of four-level systems. *Physical Review A*, 86(6):062312, December 2012.

[152] Xi Chen, A. Ruschhaupt, S. Schmidt, A. del Campo, D. Guéry-Odelin, and J. G. Muga. Fast Optimal Frictionless Atom Cooling in Harmonic Traps: Shortcut to Adiabaticity. *Physical Review Letters*, 104(6):063002, February 2010.

[153] E. Torrontegui, S. Ibáñez, Xi Chen, A. Ruschhaupt, D. Guéry-Odelin, and J. G. Muga. Fast atomic transport without vibrational heating. *Physical Review A*, 83(1):013415, January 2011.

[154] D. Guéry-Odelin, A. Ruschhaupt, A. Kiely, E. Torrontegui, S. Martínez-Garaot, and J. G. Muga. Shortcuts to adiabaticity: Concepts, methods, and applications. *Reviews of Modern Physics*, 91(4):045001, October 2019.

[155] H. Ralph Lewis and P. G. L. Leach. A direct approach to finding exact invariants for one-dimensional time-dependent classical Hamiltonians. *Journal of Mathematical Physics*, 23(12):2371–2374, December 1982.

[156] Xiao-Jing Lu, J. G. Muga, Xi Chen, U. G. Poschinger, F. Schmidt-Kaler, and A. Ruschhaupt. Fast shuttling of a trapped ion in the presence of noise. *Physical Review A*, 89(6):063414, June 2014.

[157] Amikam Levy, A Kiely, J G Muga, R Kosloff, and E Torrontegui. Noise resistant quantum control using dynamical invariants. *New Journal of Physics*, 20(2):025006, February 2018.

[158] Xiao-Jing Lu, A. Ruschhaupt, and J. G. Muga. Fast shuttling of a particle under weak spring-constant noise of the moving trap. *Physical Review A*, 97(5):053402, May 2018.

[159] M. Palmero, E. Torrontegui, D. Guéry-Odelin, and J. G. Muga. Fast transport of two ions in an anharmonic trap. *Physical Review A*, 88(5):053423, November 2013.

[160] Xiao-Jing Lu, Mikel Palmero, Andreas Ruschhaupt, Xi Chen, and Juan Gonzalo Muga. Optimal transport of two ions under slow spring-constant drifts. *Physica Scripta*, 90(7):074038, June 2015.

[161] M. Palmero, S. Martínez-Garaot, J. Alonso, J. P. Home, and J. G. Muga. Fast expansions and compressions of trapped-ion chains. *Physical Review A*, 91(5):053411, May 2015.

[162] M Palmero, S Martínez-Garaot, U G Poschinger, A Ruschhaupt, and J G Muga. Fast separation of two trapped ions. *New Journal of Physics*, 17(9):093031, September 2015.

[163] I. Lizuain, M. Palmero, and J. G. Muga. Dynamical normal modes for time-dependent Hamiltonians in two dimensions. *Physical Review A*, 95(2):022130, February 2017.

[164] A. Tobalina, M. Palmero, S. Martínez-Garaot, and J. G. Muga. Fast atom transport and launching in a nonrigid trap. *Scientific Reports*, 7(1):5753, December 2017.

[165] Brian C. Hall. A First Approach to Quantum Mechanics. In Brian C. Hall, editor, *Quantum Theory for Mathematicians*, Graduate Texts in Mathematics, page 78. Springer, New York, NY, 2013.

[166] Robert Lewis (https://math.stackexchange.com/users/67071/robert-lewis). Solutions to the anticommutator matrix equation. Mathematics Stack Exchange.

[167] Gerardo Adesso, Sammy Ragy, and Antony R. Lee. Continuous Variable Quantum Information: Gaussian States and Beyond. *Open Systems & Information Dynamics*, 21(01n02):1440001, June 2014.

[168] R. Simon, N. Mukunda, and Biswadeb Dutta. Quantum-noise matrix for multimode systems: U(n) invariance, squeezing, and normal forms. *Physical Review A*, 49(3):1567–1583, March 1994.

[169] David F. Mayers and Endre Süli. Initial value problems for ODEs. In *An Introduction to Numerical Analysis*, pages 325–328. Cambridge University Press, Cambridge, 2003.

[170] Luca Dieci, Robert D. Russell, and Erik S. Van Vleck. Unitary Integrators and Applications to Continuous Orthonormalization Techniques. *SIAM Journal on Numerical Analysis*, 31(1):261–281, February 1994.

[171] Arieh Iserles. Runge–Kutta methods. In *A First Course in the Numerical Analysis of Differential Equations*, Cambridge Texts in Applied Mathematics, page 47. Cambridge University Press, Cambridge, second edition, 2008.

[172] Rainer Storn and Kenneth Price. Differential Evolution – A Simple and Efficient Heuristic for Global Optimization over Continuous Spaces. *Journal of Global Optimization*, 11(4):341–359, December 1997.

[173] J. P. Home, D. Hanneke, J. D. Jost, D. Leibfried, and D. J. Wineland. Normal modes of trapped ions in the presence of anharmonic trap potentials. *New Journal of Physics*, 13(7):073026, July 2011.

[174] P. A. M. Dirac. In *The Principles of Quantum Mechanics*, page 136. Clarendon Press, 1930.

[175] Brian Hall. Lie Algebras. In *Lie Groups, Lie Algebras, and Representations: An Elementary Introduction*, Graduate Texts in Mathematics, page 64. Springer International Publishing, Cham, 2015.

[176] Guy Steele. *Common LISP: The Language*. Digital Press, 2nd edition edition, March 1991.

[177] An updated set of basic linear algebra subprograms (BLAS). *ACM Transactions on Mathematical Software*, 28(2):135–151, June 2002.

[178] Ben Diedrich. Bld-ode <https://github.com/bld/bld-ode>, January 2021.

[179] Ben Dudson. Array-operations <https://github.com/bendudson/array-operations>, January 2022.

[180] Thomas Williams and Colin Kelley. Gnuplot, April 2013.

[181] Matthew Harvey. Imperial College Research Computing Service, 2017.